Features of Rashba-coupled Fermi gases, master equations and memory effects

Daniel Maldonado-Mundo, M.Sc. Physics

Submitted for the degree of Doctor of Philosophy

Heriot-Watt University

EPS / IPaQS

January 2015

Abstract

The first part of this thesis studies interactions in Rashba-coupled Fermi gases. The main objective of this part of the thesis consists of proposing a model to describe dilute Fermi gases. Recent theoretical works propose to use Rashba spin-orbit-coupled systems by means to enhance superconductivity, topologically protected insulators, or quantum computing. The richness and potential of Rashba-coupled Fermi systems has been proved with currently ongoing experiments with cold atoms and synthetic gauge fields, which allow to simulate neutral particles using laser fields. In this part of the thesis, we conclude that it is possible to describe dilute Rashba-coupled Fermi gases with a model that has meaningful predictive power. In the second part of the thesis we analyse the validity of the master equation approach to describe open quantum systems. Using a Jaynes-Cummings Hamiltonian we show that under certain circumstances, the master equation approach does not fully describe the effect of the environment onto the system, hence additional tools are needed.

Acknowledgments

This thesis is not a one-person job at all. Might seem so, since there is only one author, but at the end of the day is the result of a collaborative work among different people.

First of all, I am deeply indebted to my supervisors Erika Andersson and Patrik Öhberg. Their help and support has been invaluable. They have always been accessible, with time to discuss and comment different issues during the last four years. Additionally, they helped on everything related to my injury and rehab process. Regarding this issue, I would like to thank IPaQS and Prof. Gerard Buller for providing me with additional funding.

Manuel Valiente is definitely the person I have annoyed, bothered, bored and disappointed most during the last years. Unfortunately for him I am looking forward to keep doing that. Lucky me, his patience is unlimited.

I would like to thank the CM-DTC and all the people involved in it. Christine Edwards and Julie Massey deserve special attention for making our – at least mine – life easier. At Heriot-Watt, the help of Ian Galbraith has been profoundly appreciated.

During the last years I have met really remarkable people at Heriot-Watt. I am really thankful to Jack Wildman, Yvan Buggy, Lawrence Phillips, Carole Addis, Guillem Ballesteros, Adetunmise Dada, Vedran Dunjko, Ryan Amiri (nobody ever encountered so many problems to submit a thesis), JC, Oliver Brown, Artur Kaczmarczyk, Aurora Maccarone, Matthew Edmonds, Christian Redondo, Silvia Butera, Nathan Gemmell, Electra Eleftheriadou and Ross Donaldson. Although for a short time, having lunch with Airán Ródenas, Andrés García, Juan Moreno, Diego Alonso, Laura Martínez and Diego Rodríguez was an experience. I am really thankful to Elena Muñoz, Pablo Smith, David Polo and Alberto Díaz for showing me the other side of research. I also learned a lot, in every aspect, from Michael Hartmann. Additional warm thanks go to Bogna Bylicka, Massimo Borrelli, Elsi Laine, Giuseppe Intermite, Francesca Calarco and Chaitanya Joshi, probably I cannot thank you enough for everything.

I would also like to thank Prof. Göran Johansson for hosting me at Chalmers Univer-

sity in Gothenburg.

My stay in Edinburgh would not be as good as it is without people like Raúl Martínez, Alvaro Aldeguer, Teba González, Estefanía Garzón (coffee never tasted so good), Jorge Sanz, Marta Argemí, Ana Llabrés, Koya Bejay, Julian Schmehr, Alberto de Arriba, Clara Molina, María Maralli, Rocío Iglesias, Marc Pino and Manuel Tejera.

Marco del Rey, Oscar Viyuela and Emilio Alba made Glasgow a place to remember. Special mentioning is of Alejandro Bermúdez, Valle Martos, Borja Peropadre and Elena Herránz, pointing out just one thing I learnt from them would be unfair.

There is a lot of people who do not appear here and I apologise to all of them since all deserve to be mentioned (unfortunately space is limited), but thanks to all of you.

Last but certainly not least, I would like to thank my parents and my brother for everything.

In a few words, thanks to everyone.

Contents

List of Figures

Glossary

T-matrix Transfer matrix

BCS Bardeen-Cooper-Schrieffer

BEC Bose-Einstein condensate

CM Centre of Mass

CPTP Completely positive trace-preserving

GB Galilean boost

RHS Right hand side

RWA Rotating wave approximation

SO Spin-orbit

UV Ultraviolet

List of publications

The work in this thesis is based in the following publications:

- D. Maldonado-Mundo, P. Öhberg, B. Lovett, and E. Andersson. Investigating the generality of time-local master equations. *Physical Review A* **86**(4), 042107 (2012).
- D. Maldonado-Mundo, P. Öhberg ,and M. Valiente. Single-branch theory of ultracold Fermi gases with artificial Rashba spinorbit coupling. *Journal of Physics B: Atomic, Molecular and Optical Physics* **46**(13), 134002 (2013).
- D. Maldonado-Mundo,L. He,P. Öhberg, and M. Valiente. Non-Galilean response of Rashba-coupled Fermi gases. *Physical Review A* **88**(5), 053609(11 2013).

Chapter 1

Introduction

This thesis comprises of two different and sometimes related topics, condensed matter physics and open quantum systems. The first part of the thesis is devoted to the introduction and description of Rashba spin-orbit coupling in Fermi gases and to a review of scattering theory, Chapter 2 and Chapter 3, respectively. In the second part, Chapter 4 and Chapter 5, new features of Rashba-coupled Fermi gases are described. The third and last part of the thesis, Chapter 6, sheds some light on the validity of the master equation approach when quantum systems interact with their surroundings.

The first experimental observation of optically trapped cold sodium atoms, by S. Chu *et al.* in 1986 [1], led the way to a new experimental platform that allows to manipulate single particles [2, 3] and to simulate many-body physics [4, 5]. It was not until nearly a decade later, when the longtime predicted Bose-Einstein condensate (BEC) was observed by E. Cornell and C. Wieman [6], and W. Ketterle [7]. A BEC is a macroscopic quantum state of matter where a large fraction of bosons — particles with integer spin — occupy the same quantum state. If the constitutive particles of the gas are fermions — particles with half-integer spin —, one obtains a degenerate Fermi gas governed by the Pauli exclusion principle. By tuning the interaction strength between particles, the system changes from the BEC phase, a short-distance bound state, to the Bardeen-Cooper-Schrieffer (BCS) phase, where the characteristic size of the bound state is much larger than the interparticle spacing [8].

In Chapter 2 we will introduce the spin of a quantum particle, an intrinsic angular momentum with no classical analogue. The spin of a charged particle, the electron in this particular case, appears naturally in the relativistic wave equation, the so-called Dirac equation [9]. In condensed matter systems subject to a constant electric field appears a coupling between the spin of the particle and its momentum that lies in the perpen-

dicular plane to the electric field. The absence of inversion symmetry yields systems with Rashba spin-orbit coupling [10], while Dresselhaus spin-orbit coupling appears in systems without bulk symmetry [11]. The eigenstates of noninteracting Rashba-coupled Fermi systems can be labelled according to the projection of the spin of the particle onto its momentum — the helicity —, thus the eigenstates have positive and negative helicity. The two-branches structure of the eigenstates has been observed recently in Refs. [12, 13]. Albeit strange, ultracold neutral particles can reproduce the dynamics of charged particles by means of laser-engineered gauge fields [14–19]. Different systems have been mimicked, such as synthetic electric force [20], synthetic magnetic field [21]. Synthetic spin-orbit coupling has attracted special attention recently [22–24], reporting the first experimental realisation of synthetic spin-orbit coupling in a BEC [25].

Since an important part of this thesis is related to interactions, in Chapter 3 we shall briefly review some aspects of scattering theory, Green's functions and renormalisation. In scattering theory, the Transfer Matrix (T-matrix) allows us to calculate scattering amplitudes of interacting particles [26]. Modelling effective interactions with zero-range potentials in Rashba-coupled Fermi gases yields divergent quantities in the T-matrix that disappear when multichannel processes — processes that include changing the helicity — are considered [27]. In Chapter 4 we will propose a divergence-free single-branch theory for Rashba-coupled Fermi gases [28].

In Chapter 5 we will show how ultracold Rashba-coupled Fermi gases respond to a momentum kick [29]. Due to the absence of Galilean invariance the system will deform in a nontrivial way. We will see that when weak repulsive interactions in the negative-helicity branch are considered, the gas will evolve towards a finite momentum phase.

The last part of the thesis, Chapter 6, is dedicated to the field of open quantum systems. These are quantum systems that interact with the environment [30] and are described using master equations for the reduced-density matrix of the system. Depending on the effect of the environment onto the system, a master equations can describe Markov — memoryless — processes, where the master equation is written in Lindblad form [31, 32], or non-Markovian processes where the past history of the system determines its future evolution, where the master equation can also be written in Lindblad-like form [33]. In this chapter we will analyse the validity of the master equation approach using two different Hamiltonians that yield the same non-Markovian master equation.

Chapter 2

Spin-orbit coupling in cold Fermi gases

"Begin at the beginning," the King said, very gravely, "and go on till you come to the end: then stop."

Lewis Carroll, *Alice in Wonderland*

In this Chapter we introduce the origin of spin-orbit coupling and how to treat a spin-orbit coupled system in the non-relativistic limit. We will explain how a moving particle couples its spin and its momentum to give rise to a particular two dimensional spin-orbit coupling called Rashba spin-orbit coupling. We describe the main properties of two and three dimensional noninteracting Rashba-coupled Fermi gases in order to set the scene for the first part of the thesis.

2.1 Spin-orbit coupling

The spin of a particle is a quantum mechanical angular momentum that does not have any analog in classical physics. It appears as a consequence of treating a particle using relativistic quantum mechanics. The idea of a particle spinning in a certain manner is not correct and does not give a correct picture of its properties. The spin is related to the symmetry of the Lagrangian describing the physics of a particle under rotations, i.e. the Lagrangian for a particle with spin 1 is invariant under rotation of 2π, while a particle of spin-1/2 looks the same when it is rotated by 4π. In general, the Lagrangian of a spin-S particle is invariant under a $\theta = 2\pi/S$-rotation of its spin.

The first attempt to find a relativistic equation for a quantum particle gave the Klein-Gordon equation in 1926, a second order differential equation in position and time. In order to solve the time evolution it is necessary to know not only the initial value and its first spatial derivative of the wave function but also its time derivative. In 1928 Dirac proposed a linearised version of the Klein-Gordon equation, where position and time were treated equally, and is Lorentz invariant. We aim to work with a non-relativistic Hamiltonian that includes spin. Hence we show the derivation of the non-relativistic-Schrödinger equation for a spin-1/2 particle [34–36].

Let us begin with the relativistic expression for the energy E_R

$$E_R = \sqrt{c^2 p^2 + m^2 c^4}, \tag{2.1}$$

where c is the speed of light, $p = |\mathbf{p}|$ is the momentum of the particle and m is its mass. Identifying the relativistic energy, given by Eq. (2.1), with the Hamiltonian allows to construct a wave equation for a relativistic free particle, formally, as

$$\left(\sqrt{-c^2\hbar^2\nabla^2 + m^2c^4}\right)\psi\left(\mathbf{r},t\right) = i\hbar\frac{\partial}{\partial t}\psi\left(\mathbf{r},t\right), \tag{2.2}$$

where h and $\hbar = h/2\pi$ are Planck's constant and the reduced Planck constant, respectively. In Eq. (2.2) the momentum and the relativistic energy are written using their differential operator counterparts

$$\mathbf{p} \to -i\hbar\nabla,\ E_R \to i\hbar\frac{\partial}{\partial t}. \tag{2.3}$$

Applying twice the energy operator, Eq. (2.3), to the wave function $\psi\left(\mathbf{r},t\right)$ yields the Klein-Gordon equation

$$-\hbar^2\frac{\partial^2}{\partial t^2}\psi\left(\mathbf{r},t\right) = \left(-c^2\hbar^2\nabla^2 + m^2c^4\right)\psi\left(\mathbf{r},t\right), \tag{2.4}$$

which needs the knowledge of $\partial\psi/\partial t$ at $t = 0$ in order to determine its time evolution. Dirac realised that the relativistic energy, Eq. (2.1), can be linear in the particle's momentum $\mathbf{p}$ if it is written as

$$E_R^2 = \left(c\sum_{i=1}^{3}\alpha_i p_i + \beta mc^2\right)\left(c\sum_{j=1}^{3}\alpha_j p_j + \beta mc^2\right). \tag{2.5}$$

The above equation only holds if the coefficients α_i and β obey the following relations

$$\begin{aligned} \{\alpha_i, \alpha_j\} &= 2\delta_{i,j}, \\ \alpha_i\beta + \beta\alpha_i &= 0, \\ \beta^2 &= \mathbb{1}, \end{aligned} \tag{2.6}$$

where $i = x, y, z$ and $\delta_{i,j}$ is the Kronecker delta. Therefore α_i and β correspond to a representation of the generators of the Clifford algebra.[1] In the Dirac representation α_i and β read

$$\alpha_i = \begin{pmatrix} 0 & \sigma_i \\ \sigma_i & 0 \end{pmatrix}, \ \beta = \begin{pmatrix} \mathbb{1} & 0 \\ 0 & -\mathbb{1} \end{pmatrix}, \tag{2.7}$$

where σ_i are the spin-1/2 Pauli matrices

$$\sigma_x = \begin{pmatrix} 0 & 1 \\ 1 & 0 \end{pmatrix}, \sigma_y = \begin{pmatrix} 0 & -i \\ i & 0 \end{pmatrix}, \sigma_z = \begin{pmatrix} 1 & 0 \\ 0 & -1 \end{pmatrix}. \tag{2.8}$$

The linearised Dirac Hamiltonian reads

$$\mathcal{H}_D = c\,\boldsymbol{\alpha}\cdot\mathbf{p} + \beta mc^2, \tag{2.9}$$

where $\boldsymbol{\alpha} = (\alpha_x, \alpha_y, \alpha_z)$ is the vector of Dirac matrices. The eigenstates Ψ of the Dirac Hamiltonian (2.9) are 4-dimensional objects called spinors. Although the Hamiltonian (2.9) is a 4×4 Hamiltonian, the structure of the Dirac matrices α allows to decompose the Hamiltonian (2.9) in 2×2 blocks. In consequence it is possible to decompose the spinor Ψ into two components. In matrix form we have

$$\begin{pmatrix} mc^2 & c\,\mathbf{p}\cdot\boldsymbol{\sigma} \\ c\,\mathbf{p}\cdot\boldsymbol{\sigma} & -mc^2 \end{pmatrix} \begin{pmatrix} \Psi_+ \\ \Psi_- \end{pmatrix} = E_R \begin{pmatrix} \Psi_+ \\ \Psi_- \end{pmatrix}. \tag{2.10}$$

The objects $\Psi_\pm$ are the positive and negative mass solutions of the Dirac equation (2.10) for a spin-1/2 particle and correspond to the particle and its antiparticle, respectively. Expanding Eq. (2.10) for $v^2/c^2 \ll 1$ and clearing Ψ_- in favour of Ψ_+ yields the Schrödinger equation for a free electron. We will show next how this is done when a charged particle

[1] The elements of the Clifford algebra are matrices γ_μ where $\mu = 0, 1, 2, 3$, with the following anticommutation relations $\{\gamma_\mu, \gamma_\nu\} = 2\eta_{\mu\nu}\mathbb{1}_{4\times4}$ where $\eta_{\mu\nu} = \text{diag}\,(1, -1, -1, -1)$ is the Minkowski metric and $\mathbb{1}_{4\times4}$ is the four dimensional identity matrix.

moves in an electromagnetic field.

We introduce the effect of an electromagnetic field via the minimal coupling

$$\mathbf{p} \to \mathbf{p} - \frac{q}{c}\mathbf{A},\ E_R \to E_R - q\phi, \tag{2.11}$$

where q is the charge, $\mathbf{A}$ is the vector potential and ϕ is the electric potential, we use gaussian units since the $1/c$ dependance is explicit. Dirac's Hamiltonian (2.9) is transformed to

$$\mathcal{H}_D = c\,\boldsymbol{\alpha}\cdot\left(\mathbf{p} - \frac{q}{c}\mathbf{A}\right)^2 + q\phi + \beta mc^2, \tag{2.12}$$

which in matrix form reads

$$\begin{pmatrix} q\phi + mc^2 & c\,\boldsymbol{\sigma}\cdot\left(\mathbf{p} - \frac{q}{c}\mathbf{A}\right) \\ c\,\boldsymbol{\sigma}\cdot\left(\mathbf{p} - \frac{q}{c}\mathbf{A}\right) & q\phi - mc^2 \end{pmatrix} \begin{pmatrix} \Psi_+ \\ \Psi_- \end{pmatrix} = E_R \begin{pmatrix} \Psi_+ \\ \Psi_- \end{pmatrix}. \tag{2.13}$$

From Eq. (2.13) it is possible to write the negative-mass[2] solution Ψ_- in terms of the positive-mass solution Ψ_+ as

$$\Psi_- = \frac{1}{E_R - q\phi + mc^2} c\,\boldsymbol{\sigma}\cdot\left(\mathbf{p} - \frac{q}{c}\mathbf{A}\right)\Psi_+. \tag{2.14}$$

Equation (2.14) yields an expression for the positive mass solution as

$$-\left(E_R - q\phi - mc^2\right)\Psi_+ + c^2\,\boldsymbol{\sigma}\cdot\left(\mathbf{p} - \frac{q}{c}\mathbf{A}\right)\frac{1}{E_R - q\phi + mc^2}\boldsymbol{\sigma}\cdot\left(\mathbf{p} - \frac{q}{c}\mathbf{A}\right)\Psi_+ = 0. \tag{2.15}$$

So far no approximation has been done. Expanding the relativistic energy E_R, Eq. (2.1), for $mc^2 \gg c^2p^2$ we have $E_R \approx E + mc^2$, where $E = p^2/2m$ is the non-relativistic energy. Substituting $E_R \approx E + mc^2$ into Eq. (2.15) and using $1/(1+x) \approx 1 - x$, where $|x| = |E - q\phi|/2mc^2 \ll 1$, we obtain

$$-\left(E - q\phi\right)\Psi_+ + \frac{1}{2m}\boldsymbol{\sigma}\cdot\left(\mathbf{p} - \frac{q}{c}\mathbf{A}\right)\boldsymbol{\sigma}\cdot\left(\mathbf{p} - \frac{q}{c}\mathbf{A}\right)\Psi_+ = 0. \tag{2.16}$$

Using the following identity for the Pauli matrices

$$\left(\boldsymbol{\sigma}\cdot\mathbf{A}\right)\left(\boldsymbol{\sigma}\cdot\mathbf{B}\right) = \mathbf{A}\cdot\mathbf{B} + i\left(\mathbf{A}\times\mathbf{B}\right)\cdot\boldsymbol{\sigma}, \tag{2.17}$$

[2] Ψ_+ and Ψ_- are also called large and small component due to the difference in the sign in front of mc^2 in Eq. (2.13).

where $\mathbf{A}$ and $\mathbf{B}$ are arbitrary vectors in $\mathbb{C}^2$, the second term in Eq. (2.16) can be reduced to

$$\boldsymbol{\sigma}\cdot\left(\mathbf{p}-\frac{q}{c}\mathbf{A}\right)\boldsymbol{\sigma}\cdot\left(\mathbf{p}-\frac{q}{c}\mathbf{A}\right)=\left(\mathbf{p}-\frac{q}{c}\mathbf{A}\right)^2+i\sum_{i,j,k}\epsilon_{ijk}\left(p_j-\frac{q}{c}A_j\right)\left(p_k-\frac{q}{c}A_k\right)\sigma_i, \tag{2.18}$$

where ϵ_{ijk} is the Levi-Civita (or totally antisymmetric) tensor. The terms p_jp_k, A_jA_k and A_jp_j form a symmetric second rank tensor, so they vanish when contracted with ϵ_{ijk}.[3] The only non-vanishing term

$$\sum_{i,j,k}\epsilon_{ijk}p_jA_k\sigma_i=\boldsymbol{\sigma}\cdot(\mathbf{p}\times\mathbf{A}) \tag{2.19}$$

produces a coupling term between the magnetic field and the spin of the particle

$$-i\hbar\,\boldsymbol{\sigma}\cdot(\nabla\times\mathbf{A})=-i\hbar\,\boldsymbol{\sigma}\cdot\mathbf{B}. \tag{2.20}$$

We arrive at the non-relativistic equation for the spin-1/2 particle[4] in an electromagnetic field

$$\left[\frac{1}{2m}\left(\mathbf{p}-\frac{q}{c}\mathbf{A}\right)^2-\frac{q\hbar}{2mc}\boldsymbol{\sigma}\cdot\mathbf{B}+q\phi\right]\Psi=E\Psi. \tag{2.21}$$

An earlier version of Eq.(2.21) was derived by Pauli in 1927 as a limiting case of the Schrödinger equation for a charged spin-1/2 particle in an electromagnetic field, therefore Pauli's equation is non-relativistic and it predicted wrongly the magnetic moment of a charged spin-1/2 particle. On the other hand, Eq. (2.21) is the non-relativistic limit of a relativistic equation (2.13), hence Eq. (2.21) ensures a correct treatment of spin. In this case, the predicted magnetic moment is correct and is given by

$$\boldsymbol{\mu}=-\frac{q\hbar}{2mc}\boldsymbol{\sigma}=-g\mathbf{S}, \tag{2.22}$$

where g is the gyromagnetic moment of the charged particle. The magnetic moment of the electron is called Bohr's magneton and it is given by $\mu_B=e\hbar/2m_ec$, where e and m_e are the electron charge and mass, respectively. The gyromagnetic factor of the electron is

[3] We specify it for second rank tensors, but it applies to any rank. A second rank symmetric tensor $C_{ij}=C_{ji}$ contracted with an antisymmetric second rank tensor $D_{ij}=-D_{ij}$ gives $C_{ij}D^{ji}=\left(C_{ij}D^{ji}+C_{ij}D^{ji}\right)/2=\left(C_{ij}D^{ji}-C_{ji}D^{ij}\right)/2$, relabelling $\left(C_{ij}D^{ji}-C_{ij}D^{ji}\right)/2=0$, where Einstein's summation criteria for repeated indices was used.

[4] From now onwards all the particles we refer to correspond to the positive mass solution.

predicted[5] to be $g_e = 2$. Finally we arrive at the effective non-relativistic Hamiltonian for a charged spin-1/2 particle in an electromagnetic field

$$\mathcal{H}_{SO} = \frac{1}{2m}\left(\mathbf{p} - \frac{q}{c}\mathbf{A}\right)^2 + \boldsymbol{\mu}\cdot\mathbf{B} + q\phi. \tag{2.23}$$

See Ref. [37] for an extensive monograph on spin-orbit coupling in solid state and condensed matter systems.

2.2 Rashba spin-orbit coupling

Nowadays Rashba spin-orbit coupling cannot only be measured directly [12] but it can also be achieved by synthetic gauge fields [22, 38, 39] in neutral bosonic [25] condensates or fermionic condensates [13]. It is also important the strength of the spin-orbit coupling as it plays a major role in the formation of two-body bound states [40, 41]. Moreover, the crossover between a BEC of molecules and a BCS superfluid state can be driven by the spin-orbit coupling alone when the s-wave scattering length is fixed in two-dimensional and three-dimensional systems [42, 43].

In this section we show how to derive the effective two dimensional Rashba spin-orbit Hamiltonian for a spin-1/2 particle in an electromagnetic field. We begin by expanding Eq. (2.23) in order to simplify the general spin-orbit Hamiltonian

$$\mathcal{H}_{SO} = \frac{1}{2m}\mathbf{p}^2 - \frac{q}{2mc}\left(\mathbf{p}\cdot\mathbf{A} + \mathbf{A}\cdot\mathbf{p}\right) + \frac{q^2}{2mc^2}\mathbf{A}^2 + \boldsymbol{\mu}\cdot\mathbf{B} + q\phi. \tag{2.24}$$

The first simplification comes from using the Coulomb gauge, given by $\nabla\cdot\mathbf{A} = 0$, which allows to choose $\phi = 0$. The second assumption considers the contribution from the diamagnetic term $q^2\mathbf{A}^2/c^2$, negligible when compared to the rest of the Hamiltonian, which is of order $\mathcal{O}\left(c^{-1}\right)$. The third premise assumes a constant magnetic field, hence the vector potential can be written as

$$\mathbf{A} = \frac{1}{2}\mathbf{B}\times\mathbf{r}. \tag{2.25}$$

Substituting the vector potential, Eq. (2.25), into the paramagnetic term proportional to

[5] The actual value of the electron gyromagnetic factor is 2.002319. This correction comes from higher order diagrams in quantum electrodynamics.

$\mathbf{A} \cdot \mathbf{p}$ yields

$$\frac{q}{2mc}\mathbf{A} \cdot \mathbf{p} = \frac{q}{4mc}\left(\mathbf{B} \times \mathbf{r}\right) \cdot \mathbf{p}. \tag{2.26}$$

Writing Eq. (2.26) in components and using the differential operator form of $\mathbf{p}$ leads to

$$\begin{aligned} -\frac{iq\hbar}{4mc}\sum_{i,j,k}\epsilon_{ijk}B_j r_k \frac{\partial}{\partial r_i} &= -\frac{iq\hbar}{4mc}\sum_{i,j,k}\epsilon_{ijk}B_i r_j \frac{\partial}{\partial r_k}, \\ &= -\frac{iq\hbar}{4mc}\mathbf{B} \cdot \left(\nabla \times \mathbf{r}\right). \end{aligned} \tag{2.27}$$

Finally, identifying the orbital angular momentum as $\mathbf{L} = -i\hbar\,\mathbf{r} \times \nabla$ allows to write the paramagnetic term as

$$\frac{q}{2mc}\mathbf{A} \cdot \mathbf{p} = \frac{q}{4mc}\mathbf{B} \cdot \mathbf{L}. \tag{2.28}$$

The Hamiltonian, Eq. (2.24), for a particle in an electromagnetic field is simplified to

$$\mathcal{H}_{SO} = \frac{\mathbf{p}^2}{2m} - \frac{q}{4mc}\mathbf{B} \cdot \mathbf{L} + \boldsymbol{\mu} \cdot \mathbf{B} + \mathcal{O}\left(c^{-2}\right). \tag{2.29}$$

Rashba spin-orbit coupling appears when a constant electric field $\mathbf{E}$ in the z direction is applied. Under this circumstance, a moving charge feels a magnetic field $\mathbf{B}'$ in the reference frame where the particle is at rest. The applied electric field $\mathbf{E}$ and the induced magnetic field $\mathbf{B}'$ are related via a Lorentz transformation [44]

$$\mathbf{E}' = \gamma\left(\mathbf{E} + \frac{1}{c}\mathbf{v} \times \mathbf{B}\right) - \frac{\gamma^2}{1+\gamma}\frac{\mathbf{v}}{c}\left(\frac{\mathbf{v}}{c} \cdot \mathbf{E}\right), \tag{2.30}$$

$$\mathbf{B}' = \gamma\left(\mathbf{B} + \frac{1}{c}\mathbf{v} \times \mathbf{E}\right) - \frac{\gamma^2}{1+\gamma}\frac{\mathbf{v}}{c}\left(\frac{\mathbf{v}}{c} \cdot \mathbf{B}\right), \tag{2.31}$$

where $\mathbf{v}$ is the speed of the particle and $\gamma = 1/\sqrt{1 - v^2/c^2}$. A constant electric field in the z direction $\mathbf{E} = E_0 e_z$ induces a magnetic field

$$\begin{aligned} \mathbf{B}' &= \frac{\gamma}{c^2}E_0\left(v_y e_x - v_x e_y\right) \\ &= \frac{\gamma\hbar}{mc^2}E_0\left(k_y e_x - k_x e_y\right), \end{aligned} \tag{2.32}$$

where $\{e_x, e_y, e_z\}$ is the Cartesian orthonormal basis, while in the particle's co-moving

reference frame the interaction of the particle with the magnetic field reads

$$\begin{aligned}\boldsymbol{\mu}\cdot\mathbf{B} &= g_e\frac{\hbar}{2}\frac{\gamma\hbar}{mc^2}E_0\boldsymbol{\sigma}\cdot(-k_y,k_x,0)\\ &= \frac{\hbar^2\lambda}{m}\left(k_x\sigma_y-k_y\sigma_x\right),\end{aligned} \tag{2.33}$$

where the coupling constant is $\lambda = g_e\gamma E_0/2c^2$. The Rashba spin-orbit Hamiltonian[6] is given by

$$\mathcal{H}_{SO} = \frac{\mathbf{p}^2}{2m} + \frac{\hbar^2\lambda}{m}\left(k_x\sigma_y - k_y\sigma_x\right), \tag{2.34}$$

where the orbital angular momentum is $\mathbf{L} = 0$. In this thesis we write the Rashba Hamiltonian as

$$\mathcal{H}_{SO} = \frac{\mathbf{p}^2}{2m} + \frac{\hbar^2\lambda}{m}\mathbf{k}\cdot\boldsymbol{\sigma}. \tag{2.35}$$

In order to get from Eq. (2.34) to Eq. (2.35), the Pauli matrices, Eq. (2.8), are rotated by an unitary matrix $\mathcal{R} = \text{diag}\left(e^{-i\pi/8}, e^{i\pi/8}\right)$ [27]. This transformation yields

$$\mathcal{R}^{-1}\sigma_x\mathcal{R} = \frac{\sigma_x-\sigma_y}{\sqrt{2}}, \tag{2.36}$$

$$\mathcal{R}^{-1}\sigma_y\mathcal{R} = \frac{\sigma_x+\sigma_y}{\sqrt{2}}. \tag{2.37}$$

Renaming the wave vectors k_x and k_y in the Hamiltonian (2.34) according to the canonical transformation $k_{x,y} \to (k_x \mp k_y)/\sqrt{2}$ after transforming the Pauli matrices in Eq. (2.34) according to the rotation given by Eqs. (2.36) and (2.37) gives the Rashba spin-orbit Hamiltonian (2.35).

2.2.1 Helicity formalism

The helicity $\boldsymbol{\sigma}\cdot\mathbf{p}$, defined as the projection of the momentum onto the spin of the particle, is a convenient quantity used in relativistic quantum mechanics and quantum field theory [46, 47]. The helicity operator commutes with the Hamiltonian (2.35) and the momentum $\mathbf{p}$. This implies that the eigenstates of Eq. (2.35) can be labeled according to their helicity. The helicity operator for a spin-1/2 particle is defined as the projection of the

[6] As we already mentioned, Rashba spin-orbit Hamiltonian (2.35) is not the only two dimensional spin-orbit Hamiltonian. Dresselhaus spin-orbit coupling appears in systems where there is a lack of bulk inversion [11] and the coupling is $\mathcal{H}_D \propto k_x\sigma_y + k_y\sigma_x$. Experimental evidence of simultaneous and equal Rashba-Dresselhaus coupling measurements in Fermi gases was reported in Refs. [12, 45], respectively.

normalised momentum onto the direction of the spin

$$\mathrm{h} = \frac{\hbar \mathbf{k} \cdot \boldsymbol{\sigma}}{k}, \tag{2.38}$$

where $k = |\mathbf{k}|$. With the use of the Pauli matrices, Eq. (2.8), a matrix representation for the helicity is given by

$$\mathrm{h} = \frac{\hbar}{k} \begin{pmatrix} k_z & k_x - ik_y \\ k_x + ik_y & -k_z \end{pmatrix}. \tag{2.39}$$

The symmetry of the helicity matrix, Eq. (2.39), makes it is most convenient to work in cylindrical coordinates

$$k_x = k_\perp \cos(\gamma_k), \tag{2.40}$$

$$k_y = k_\perp \sin(\gamma_k), \tag{2.41}$$

$$k_z = k_z, \tag{2.42}$$

where $k_\perp = \sqrt{k_x^2 + k_y^2}$ and $\gamma_k = \arctan\left(k_y/k_x\right)$. The helicity, Eq. (2.39), becomes

$$\mathrm{h} = \frac{\hbar}{k} \begin{pmatrix} k_z & k_\perp e^{-i\gamma_k} \\ k_\perp e^{i\gamma_k} & -k_z \end{pmatrix}. \tag{2.43}$$

Diagonalising the helicity (2.43) shows that the helicity has two different branches of eigenvectors. They represent the parallel and antiparallel projections of the momentum onto the spin. The helicity eigenstates are

$$\left|\psi_{\mathbf{k}}^{(\alpha)}\right\rangle = \frac{1}{\sqrt{1 + \left(\frac{k_z - \alpha k_\perp}{k_\perp}\right)^2}} \begin{pmatrix} 1 \\ -\frac{k_z - \alpha k_\perp}{k_\perp} e^{i\gamma_k} \end{pmatrix}, \tag{2.44}$$

where $\alpha = \pm 1$ represent the parallel and antiparallel projection, respectively. In order to define a spin basis to work with, we introduce the eigenvectors, $|\uparrow\rangle$ and $|\downarrow\rangle$, of the z component of the spin $\mathbf{S}$ as

$$S_z |\uparrow\rangle = \frac{\hbar}{2} |\uparrow\rangle \tag{2.45}$$

$$S_z |\downarrow\rangle = -\frac{\hbar}{2} |\downarrow\rangle . \tag{2.46}$$

In spin-space, the eigenvectors of S_z define the spin-1/2 basis $\{|\uparrow\rangle, |\downarrow\rangle\}$. The identity matrix is written as

$$\mathbb{1} = |\uparrow\rangle\langle\uparrow| + |\downarrow\rangle\langle\downarrow|. \tag{2.47}$$

With the use of the spin-1/2 basis the eigenvectors of the helicity (2.44) read

$$\left|\psi_{\mathbf{k}}^{(\alpha)}\right\rangle = \frac{1}{\sqrt{1+\left(\frac{k_z-\alpha k_\perp}{k_\perp}\right)^2}}\left(|\uparrow\rangle - \frac{k_z-\alpha k_\perp}{k_\perp}e^{i\gamma_k}|\downarrow\rangle\right). \tag{2.48}$$

The corresponding eigenvalues are

$$h_\alpha = \alpha\hbar, \tag{2.49}$$

where $\alpha = \pm 1$ for the positive and negative helicity respectively.

2.2.2 Single-particle physics

In this section we describe how to diagonalise the Rashba-coupled spin-orbit Hamiltonian (2.35) using the helicity formalism. We begin by expressing the Hamiltonian in second quantisation as

$$\mathcal{H}_{SO} = \sum_{\mathbf{k}} \begin{pmatrix} c_{\mathbf{k},\uparrow}^\dagger & c_{\mathbf{k},\downarrow}^\dagger \end{pmatrix} \left(\frac{\hbar^2}{2m}\left[\mathbf{k}^2+\lambda^2\right]\mathbb{1} + \frac{\hbar^2\lambda}{m}\mathbf{k}_\perp\cdot\boldsymbol{\sigma}\right) \begin{pmatrix} c_{\mathbf{k},\uparrow} \\ c_{\mathbf{k},\downarrow} \end{pmatrix}, \tag{2.50}$$

where $c_{\mathbf{k},\sigma}$ ($c_{\mathbf{k},\sigma}^\dagger$) annihilates (creates) a fermion of momentum $\hbar\mathbf{k}$ and z-spin component σ and $\mathbf{k}_\perp = (k_x, k_y, 0)$ is the xy-plane wave vector. These operators obey canonical anti-commutation relations[7]

$$\left\{c_{\mathbf{q},\sigma'}, c_{\mathbf{k},\sigma}^\dagger\right\} = \delta_{\sigma,\sigma'}\delta_{\mathbf{k},\mathbf{q}},\ \left\{c_{\mathbf{q},\sigma'}, c_{\mathbf{k},\sigma}\right\} = \left\{c_{\mathbf{q},\sigma'}^\dagger, c_{\mathbf{k},\sigma}^\dagger\right\} = 0. \tag{2.51}$$

As mentioned before, the helicity commutes with the free particle term in the Hamiltonian (2.50). Therefore there is a common basis of vectors of the helicity and the Hamiltonian. To show this we compute the commutator between the terms corresponding to the free evolution and the helicity. We first rewrite the Hamiltonian (2.50) in a more suitable

[7] We explicitly state the commutation relations here for convenience

$$[c_{\mathbf{k},\sigma}, c_{\mathbf{q},\sigma'}] = 2c_{\mathbf{k},\sigma}c_{\mathbf{q},\sigma'},\ \left[c_{\mathbf{k},\sigma}, c_{\mathbf{q},\sigma'}^\dagger\right] = \delta_{\sigma,\sigma'}\delta_{\mathbf{k},\mathbf{q}} - 2c_{\mathbf{q},\sigma'}^\dagger c_{\mathbf{k},\sigma}.$$

way

$$\mathcal{H}_{SO} = \sum_{\mathbf{k},\sigma} \frac{\hbar^2}{2m} \left(\mathbf{k}^2 + \lambda^2\right) c^\dagger_{\mathbf{k},\sigma} c_{\mathbf{k},\sigma} + \frac{\hbar^2 \lambda}{m} \sum_{\mathbf{k}} k_\perp \left(e^{-i\gamma_k} c^\dagger_{\mathbf{k},\uparrow} c_{\mathbf{k},\downarrow} + e^{i\gamma_k} c^\dagger_{\mathbf{k},\downarrow} c_{\mathbf{k},\uparrow} \right). \tag{2.52}$$

The commutator between the free particle evolution of the Hamiltonian and the first term of the helicity is[8]

$$\begin{aligned}
&\sum_{\mathbf{k},\mathbf{q},\sigma} k_\perp e^{-i\gamma_k} \left[c^\dagger_{\mathbf{k},\sigma} c_{\mathbf{k},\sigma}, c^\dagger_{\mathbf{q},\uparrow} c_{\mathbf{q},\downarrow} \right] \\
&= \sum_{\mathbf{k},\mathbf{q},\sigma} k_\perp e^{-i\gamma_k} \Big(c^\dagger_{\mathbf{k},\sigma} c^\dagger_{\mathbf{q},\uparrow} \left[c_{\mathbf{k},\sigma}, c_{\mathbf{q},\downarrow} \right] + c^\dagger_{\mathbf{k},\sigma} \left[c_{\mathbf{k},\sigma}, c^\dagger_{\mathbf{q},\uparrow} \right] c_{\mathbf{q},\downarrow} \\
&\qquad\qquad + c^\dagger_{\mathbf{q},\uparrow} \left[c^\dagger_{\mathbf{k},\sigma}, c_{\mathbf{q},\downarrow} \right] c_{\mathbf{k},\sigma} + \left[c^\dagger_{\mathbf{k},\sigma}, c^\dagger_{\mathbf{q},\uparrow} \right] c_{\mathbf{q},\downarrow} c_{\mathbf{k},\sigma} \Big) \\
&= \sum_{\mathbf{k},\mathbf{q},\sigma} k_\perp e^{-i\gamma_k} \Big(2 c^\dagger_{\mathbf{k},\sigma} c^\dagger_{\mathbf{q},\uparrow} c_{\mathbf{k},\sigma} c_{\mathbf{q},\downarrow} - 2 c^\dagger_{\mathbf{k},\sigma} c^\dagger_{\mathbf{q},\uparrow} c_{\mathbf{k},\sigma} c_{\mathbf{q},\downarrow} + \delta_{\mathbf{k},\mathbf{q}} \delta_{\sigma,\uparrow} c^\dagger_{\mathbf{k},\sigma} c_{\mathbf{q},\downarrow} \\
&\qquad\qquad - 2 c^\dagger_{\mathbf{q},\uparrow} c^\dagger_{\mathbf{k},\sigma} c_{\mathbf{q},\downarrow} c_{\mathbf{k},\sigma} - \delta_{\mathbf{k},\mathbf{q}} \delta_{\sigma,\downarrow} c^\dagger_{\mathbf{q},\uparrow} c_{\mathbf{k},\sigma} + 2 c^\dagger_{\mathbf{q},\uparrow} c^\dagger_{\mathbf{k},\sigma} c_{\mathbf{q},\downarrow} c_{\mathbf{k},\sigma} \Big) \\
&= \sum_{\mathbf{k},\mathbf{q}} k_\perp e^{-i\gamma_k} \left(\delta_{\mathbf{k},\mathbf{q}} c^\dagger_{\mathbf{k},\uparrow} c_{\mathbf{q},\downarrow} - \delta_{\mathbf{k},\mathbf{q}} c^\dagger_{\mathbf{q},\uparrow} c_{\mathbf{k},\downarrow} \right) = 0,
\end{aligned} \tag{2.53}$$

where the anticommutation relations (2.51) have been used.

Due to the absence of spin-orbit coupling in the z direction the helicity (2.43) has a simpler expression if it is written as a matrix

$$\mathrm{h} = \hbar k_\perp \begin{pmatrix} 0 & e^{-i\gamma_k} \\ e^{i\gamma_k} & 0 \end{pmatrix}, \tag{2.54}$$

and its eigenvalues are given by $h_\alpha = \alpha \hbar k_\perp$, with $\alpha = \pm 1$. The corresponding eigenvectors are

$$\begin{aligned}
\left| \psi^{(\alpha)}_{\mathbf{k}} \right\rangle &= \frac{1}{\sqrt{2}} \begin{pmatrix} 1 \\ \alpha e^{i\gamma_k} \end{pmatrix} \\
&= \frac{1}{\sqrt{2}} \left(|\uparrow\rangle + \alpha e^{i\gamma_k} |\downarrow\rangle \right).
\end{aligned} \tag{2.55}$$

With the use of Eq. (2.54) the Hamiltonian (2.52) can be expressed as a matrix as

$$\mathcal{H}_{SO} = \frac{\hbar^2}{2m} \begin{pmatrix} k_\perp^2 + k_z^2 + \lambda^2 & 2k_\perp e^{-i\gamma} \lambda \\ 2k_\perp e^{i\gamma} \lambda & k_\perp^2 + k_z^2 + \lambda^2 \end{pmatrix}. \tag{2.56}$$

[8] The complex conjugated term is calculated in the same way, therefore it is not calculated explicitly here.

When diagonalised, the spin-orbit coupling mixes spin components giving rise to two different gapless energy bands (see Ref. [12]),

$$\epsilon_{\pm}\left(\mathbf{k}\right)=\frac{\hbar^{2}}{2m}\left[\left(k_{\perp}\pm\lambda\right)^{2}+k_{z}^{2}\right], \tag{2.57}$$

with the corresponding eigenvectors

$$\left|\Psi_{\mathbf{k}}^{(\pm)}\left(\mathbf{r}\right)\right\rangle=\frac{1}{\sqrt{2}}e^{i\mathbf{k}\cdot\mathbf{r}}\left(\left|\uparrow\right\rangle\pm e^{i\gamma_{k}}\left|\downarrow\right\rangle\right). \tag{2.58}$$

In second quantisation, diagonalising the Hamiltonian (2.52) corresponds to changing from a set of operators $c_{\mathbf{k},\sigma}^{\dagger}$ and $c_{\mathbf{k},\sigma}$ for fermions with spin σ to another set of operators $d_{\mathbf{k},h}^{\dagger}$ and $d_{\mathbf{k},h}$ that create and annihilate fermions with positive or negative helicity h[9]. The relation between the two sets of operators is given by the canonical transformation

$$\left(\begin{array}{c} d_{\mathbf{k},\uparrow}\\ d_{\mathbf{k},\downarrow}\end{array}\right)=\frac{1}{\sqrt{2}}\left(\begin{array}{cc} 1 & e^{-i\gamma_{k}}\\ 1 & -e^{-i\gamma_{k}}\end{array}\right)\left(\begin{array}{c} c_{\mathbf{k},\uparrow}\\ c_{\mathbf{k},\downarrow}\end{array}\right). \tag{2.59}$$

The new operators satisfy the canonical anticommutation relations for fermions

$$\left\{d_{\mathbf{q},\sigma'},d_{\mathbf{k},\sigma}^{\dagger}\right\}=\delta_{\sigma,\sigma'}\delta_{\mathbf{k},\mathbf{q}},\ \left\{d_{\mathbf{q},\sigma'},d_{\mathbf{k},\sigma}\right\}=\left\{d_{\mathbf{q},\sigma'}^{\dagger},d_{\mathbf{k},\sigma}^{\dagger}\right\}=0. \tag{2.60}$$

In the diagonal basis, the Rashba spin-orbit (SO) Hamiltonian is given by

$$\mathcal{H}_{SO}=\sum_{\mathbf{k}}\left(\epsilon_{+}\left(\mathbf{k}\right)d_{\mathbf{k},\uparrow}^{\dagger}d_{\mathbf{k},\uparrow}+\epsilon_{-}\left(\mathbf{k}\right)d_{\mathbf{k},\downarrow}^{\dagger}d_{\mathbf{k},\downarrow}\right). \tag{2.61}$$

The two-band structure, Fig. 2.1, and the energy gap in Rashba-coupled systems makes as ideal candidates to realise topological s-wave superconductors [48]. Topologically protected Majorana fermions [49] enhanced by spin-orbit coupling are promising candidates to develop a platform for quantum computing using Rashba spin-orbit coupling [50] or Rashba-Dresselhaus spin-orbit coupling [51].

[9]The helicity is also a representation of the spin, and we will keep the notation $\sigma=\uparrow,\downarrow$ for positive and negative helicity.

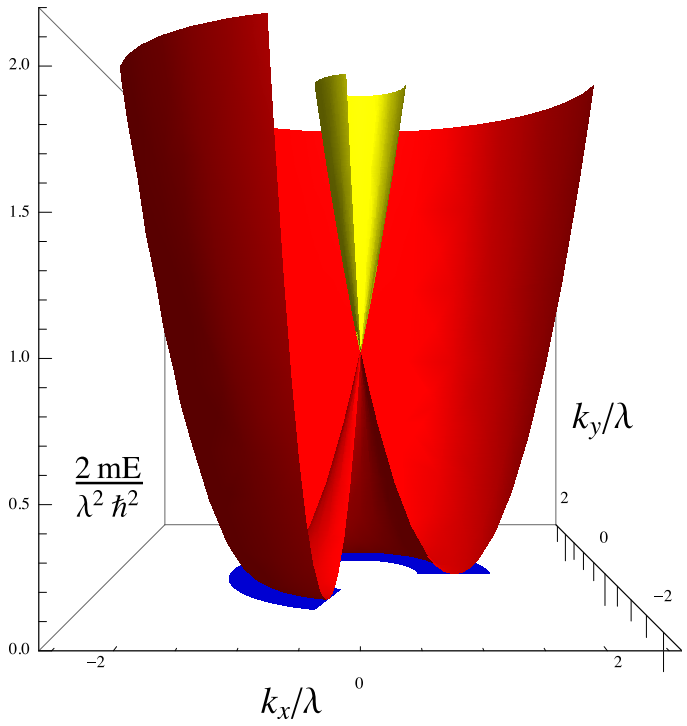

Figure 2.1: Representation of the positive (yellow) and negative (red) helicity branches for a constant $k_z/\lambda = 0$. The projection onto the plane (blue) represents the two-dimensional Fermi sea.

2.3 Noninteracting Rashba-coupled Fermi gas at low densities

Let us consider a noninteracting Rashba-coupled Fermi gas. At low density the ground state only populates the negative helicity branch and we can work with the projection

$$\mathcal{H}_{(-)} = \sum_{\mathbf{k}} \epsilon_{-}(\mathbf{k})\, d^{\dagger}_{\mathbf{k}} d_{\mathbf{k}}, \tag{2.62}$$

where for simplicity we have changed notation from $d^{\dagger}_{\mathbf{k},\downarrow}$ ($d_{\mathbf{k},\downarrow}$) to $d^{\dagger}_{\mathbf{k}}$ ($d_{\mathbf{k}}$).[10]

We define the Fermi energy E_F for the negative helicity branch as the maximum single-particle energy a fermion has inside the Fermi sea

$$\epsilon_{-}(\mathbf{k}_F) = \frac{\hbar^2 k_F^2}{2m}, \tag{2.63}$$

where $k_F = |\mathbf{k}_F|$ is the Fermi wave vector. The Fermi sea becomes saturated when the positive helicity branch is populated in the noninteracting ground state.

The number operator gives the occupation of states with well defined momentum $\hbar\mathbf{k}$

[10]The operators with explicit dependance in the spin $d_{\mathbf{k},\sigma}$ ($d^{\dagger}_{\mathbf{k},\sigma}$) are written when there is any chance of confusion, otherwise it will be implicit that we refer to the lower branch.

and negative helicity in the Fermi sea. It is defined as

$$N_{\mathbf{k}} = d_{\mathbf{k}}^{\dagger} d_{\mathbf{k}}. \tag{2.64}$$

When applied to the Fermi sea $|FS\rangle$ gives

$$N_{\mathbf{k}} \left|\mathrm{FS}\right\rangle = \Theta_I \left(\mathbf{k}\right) \left|\mathrm{FS}\right\rangle, \tag{2.65}$$

where

$$\Theta_I \left(\mathbf{k}\right) = \begin{cases} 1 & \text{if } \mathbf{k} \in \mathrm{FS} \\ 0 & \text{if } \mathbf{k} \notin \mathrm{FS}. \end{cases} \tag{2.66}$$

It is convenient to also define the function $\Theta_O \left(\mathbf{k}\right) = 1 - \Theta_I \left(\mathbf{k}\right)$. This will be useful when multiple wave vectors involving particles and holes appear in the corresponding integrals in perturbation theory.

2.4 Properties of noninteracting Rashba-coupled Fermi gases in two and three dimensions

In this section we show different properties of two and three dimensional Rashba-coupled spin-orbit Fermi gases. The properties outlined in this section will be extensively used in Chapters 4 and 5.

2.4.1 Fermi sea

Fermions loose their individuality to become part of a many-body noninteracting ground state [52] called the Fermi sea. The Fermi sea is the condensed matter physics equivalent to the vacuum in quantum optics. In this section we describe the Fermi sea for a Rashba-coupled Fermi gas in two and three dimensions. We first work through the properties of the three dimensional case. Afterwards we analyse to the two dimensional case. The Fermi energy E_F sets an upper bound for the single particle energy of the fermions in the noninteracting many-body ground state.

The single particle energy in three dimensions is given by Eq. (2.57), which allows to

define the occupation limit values of k_z as

$$|k_z| \leq \sqrt{k_F^2 - (k_\perp - \lambda)^2}. \tag{2.67}$$

The minimum and maximum values for the in-plane momentum $k_\perp = \sqrt{k_x^2 + k_y^2}$ come from

$$k_F^2 - (k_\perp - \lambda)^2 \geq 0. \tag{2.68}$$

This inequality yields

$$k_\perp \in [\lambda - k_F, \lambda + k_F]\,. \tag{2.69}$$

Therefore the Fermi sea is the volume defined by the vectors $(\gamma, k_z, k_\perp)$ whose components belong to

$$\mathrm{FS}_{3D} = [0, 2\pi) \times \left[-\sqrt{k_F^2 - (k_\perp - \lambda)^2}, \sqrt{k_F^2 - (k_\perp - \lambda)^2}\right] \times [\lambda - k_F, \lambda + k_F]\,. \tag{2.70}$$

In Ref. [53] Kohl *et al.* reported the observation of the Fermi surface in a three-dimensional lattice. The Fermi sea in two dimensions is simply defined eliminating the z-direction in three dimensions

$$\mathrm{FS}_{2D} = [0, 2\pi) \times [\lambda - k_F, \lambda + k_F]\,. \tag{2.71}$$

2.4.2 Number of states

The number of fermions in the Fermi sea comes from evaluating the expectation value of the number operator. In three dimensions is

$$\begin{aligned} N_{3D} &= \langle \mathrm{FS}| \sum_{\mathbf{k}\in \mathrm{FS}} N_{\mathbf{k}} \,|\mathrm{FS}\rangle \\ &= \sum_{\mathbf{k}\in \mathrm{FS}} \Theta_I\left(\mathbf{k}\right) \\ &= \frac{V}{(2\pi)^3} \int_{\mathrm{FS}} \mathrm{d}\mathbf{k} \\ &= \frac{V}{(2\pi)^3} \int_0^{2\pi} \mathrm{d}\gamma \int_{\lambda - k_F}^{\lambda + k_F} \mathrm{d}k_\perp k_\perp \int_{-\sqrt{k_F - (k_\perp - \lambda)^2}}^{\sqrt{k_F - (k_\perp - \lambda)^2}} \mathrm{d}k_z \\ &= V\frac{\lambda k_F^2}{4\pi}, \end{aligned} \tag{2.72}$$

where V is the volume of the system. The density of fermions is

$$\rho_{3D} = \frac{\lambda k_F^2}{4\pi}. \tag{2.73}$$

The number of states in two dimensions is easily obtained from expression (2.72) if the integral over k_z is removed and $V/(2\pi)^3$ is substituted by $S/(2\pi)^2$, where S is the surface of the system. We have then

$$\begin{aligned} N_{2D} &= \frac{S}{(2\pi)^2} \int_0^{2\pi} \mathrm{d}\gamma \int_{\lambda - k_F}^{\lambda + k_F} \mathrm{d}k_\perp k_\perp \\ &= \frac{S\lambda k_F}{\pi}. \end{aligned} \tag{2.74}$$

The two-dimensional density of fermions in the negative helicity branch is

$$\rho_{2D} = \frac{\lambda k_F}{\pi}. \tag{2.75}$$

2.4.3 Ground state energy

The filled Fermi sea is the many-body ground state of the Hamiltonian (2.52). Its total energy is the sum of all occupied single-particle energies. In three dimensions we have

$$\begin{aligned} E_0^{(3D)} &= \langle \mathrm{FS} | \, \mathcal{H}_{(-)} \, | \mathrm{FS} \rangle \\ &= \sum_{\mathbf{k} \in \mathrm{FS}} \langle \mathrm{FS} | \, \epsilon_- (\mathbf{k}) \, d_{\mathbf{k}}^\dagger d_{\mathbf{k}} \, | \mathrm{FS} \rangle \\ &= \sum_{\mathbf{k} \in \mathrm{FS}} \epsilon_- (\mathbf{k}) \, \Theta_I (\mathbf{k}) \\ &= \frac{V}{(2\pi)^3} \frac{\hbar^2}{2m} \int_{\mathrm{FS}} \mathrm{d}\mathbf{k} \left[(k_\perp - \lambda)^2 - k_z^2 \right] \\ &= \frac{V}{(2\pi)^3} \frac{\hbar^2}{2m} \int_0^{2\pi} \mathrm{d}\gamma \int_{\lambda - k_F}^{\lambda + k_F} \mathrm{d}k_\perp k_\perp \int_{-\sqrt{k_F - (k_\perp - \lambda)^2}}^{\sqrt{k_F - (k_\perp - \lambda)^2}} \mathrm{d}k_z \left[(k_\perp - \lambda)^2 - k_z^2 \right]. \end{aligned} \tag{2.76}$$

The last integral above gives the energy per unit volume as

$$\frac{E_0^{(3D)}}{V} = \frac{\hbar^2 \lambda k_F^4}{16\pi m}, \tag{2.77}$$

or in terms of the density (2.73)

$$\frac{E_0^{(3D)}}{V} = \frac{\pi \hbar^2}{m\lambda} \rho_{3D}^2. \tag{2.78}$$

For the two-dimensional case we remove the k_z integral in Eq. (2.76) and we again replace $V/(2\pi)^3 \to S/(2\pi)^2$. We obtain the energy density

$$\begin{aligned}\frac{E_0^{(2D)}}{S} &= \frac{1}{(2\pi)^2}\frac{\hbar^2}{2m}\int_0^{2\pi} \mathrm{d}\gamma \int_{\lambda-k_F}^{\lambda+k_F} \mathrm{d}k_\perp k_\perp \left(k_\perp - \lambda\right)^2 \\ &= \frac{\hbar^2\lambda}{6\pi m}k_F^3. \end{aligned} \tag{2.79}$$

In terms of the two-dimensional density, defined in Eq. (2.75), the ground state energy reads

$$\frac{E_0^{(2D)}}{S} = \frac{\hbar^2\pi^2}{6m\lambda^2}\rho_{2D}^3. \tag{2.80}$$

2.5 Conclusions

In this Chapter we have introduced the spin of a charged quantum particle as a consequence of describing its dynamics by special relativity and quantum mechanics. In this framework, the helicity allows to distinguish between the two different projections of the spin onto the momentum of the particle, which labels the eigenvalues as positive-helicity eigenvalues for the parallel projection and negative-helicity eigenvalues for the antiparallel projection. The coupling between the spin of a particle and its momentum yields an in-plane spin-orbit coupling called Rashba spin-orbit coupling. Rashba spin-orbit coupling has become an active field in condensed matter physics, since it is a good candidate to enhance superconductivity [54], quantum computation [50] or as a potential platform to observe Majorana fermions [55, 56]. Along this Chapter we briefly reviewed the main concepts related to spin-orbit Rashba-coupled Fermi gases that will be used during the rest of the thesis.

Chapter 3

Scattering theory and renormalisation

Scattering theory provides the tools to calculate effective particle-particle interactions using the T-matrix [26, 34, 57], that can be calculated as a perturbative expansion in the potential using Green's functions. This expansion is the Born series. The techniques used in scattering theory have been adapted to condensed matter physics in order to compute interactions in fermionic and bosonic systems [58, 59], where Rashba spin-orbit coupling is present [60]. When the interactions considered are modelled by zero-range s-wave contact interactions, ultraviolet (UV) divergences appear. In order to have a meaningful theory that includes interactions, divergences need to be renormalised. Hence, in this Chapter we begin by introducing scattering theory and Green's functions. We conclude the Chapter by explaining the basics of renormalisation and applying them to a typical case similar to what we will encounter in the following Chapters.

3.1 Scattering states and Green's functions

In this section we introduce the basics of stationary scattering theory and how it is related to time-independent Green's functions for interacting and noninteracting systems. We also explain some concepts such as the T-matrix and the Born series which we will use in Chapter 4.

3.1.1 Stationary scattering states

First, let us tackle the problem of a particle interacting with a finite-range potential $\mathcal{V}$, where $\mathcal{H}_I = \lambda\mathcal{V}$ is the interacting Hamiltonian and λ the coupling constant. We define the

incident wave $|\psi_0\rangle$ as an eigenstate of the noninteracting Hamiltonian $\mathcal{H}_0$ with energy E, and the stationary wave as $|\psi\rangle$, eigenfunction of the Schrödinger equation. The stationary scattering wave function can be written as

$$|\psi\rangle = |\psi_0\rangle + |\psi_S\rangle\,, \tag{3.1}$$

where $|\psi_S\rangle$ is the scattered part. The stationary Schrödinger equation is given by

$$(\mathcal{H}_0 + \lambda\mathcal{V})\,|\psi\rangle = E\,|\psi\rangle\,, \tag{3.2}$$

where E is the energy associated with $|\psi\rangle$, since we look for a stationary scattering wave solution such that $\mathcal{H}_0\,|\psi\rangle = E\,|\psi\rangle$ and $|\psi\rangle \to |\psi_0\rangle$ when $\mathcal{V} \to 0$. Substituting Eq. (3.1) into the Schrödinger equation (3.2) gives

$$\lambda\mathcal{V}\,|\psi\rangle = (E - \mathcal{H}_0)\,(|\psi_0\rangle + |\psi_S\rangle)\,. \tag{3.3}$$

As $\mathcal{H}_0\,|\psi_0\rangle = E\,|\psi_0\rangle$, we can relate $|\psi\rangle$ with the scattered term $|\psi_S\rangle$ as

$$\lambda\mathcal{V}\,|\psi\rangle = (E - \mathcal{H}_0)\,|\psi_S\rangle\,. \tag{3.4}$$

Therefore the scattered wave reads, formally

$$|\psi_S\rangle = \lambda\,(E - \mathcal{H}_0)^{-1}\,\mathcal{V}\,|\psi\rangle\,. \tag{3.5}$$

In order to avoid double counting of $|\psi_0\rangle$ and to ensure causality the energy is replaced by $E + i\eta$, where $\eta \to 0^+$. Substituting the scattered part $|\psi_S\rangle$ given by Eq. (3.5), into the stationary scattering wave, Eq. (3.1), gives the Lippmann-Schwinger equation [61]

$$|\psi\rangle = |\psi_0\rangle + \lambda\,(E + i\eta - \mathcal{H}_0)^{-1}\,\mathcal{V}\,|\psi\rangle\,, \tag{3.6}$$

which allows us to write the state $|\psi\rangle$ in terms of the incident state $|\psi_0\rangle$

$$|\psi\rangle = \frac{1}{1 - \lambda\,(E + i\eta - \mathcal{H}_0)^{-1}\,\mathcal{V}}\,|\psi_0\rangle\,. \tag{3.7}$$

It is also possible to solve Eq. (3.6) by iteration. The first-order solution comes when the interacting term is not considered, thence $|\psi\rangle = |\psi_0\rangle$. The second-order solution

corresponds to substituting $|\psi\rangle = |\psi_0\rangle$ in the right hand side (RHS) of Eq.(3.6), this yields

$$|\psi\rangle \approx \left(1 + \lambda \left(E + i\eta - \mathcal{H}_0\right)^{-1} \mathcal{V}\right) |\psi_0\rangle \,. \tag{3.8}$$

Subsequently the third iteration gives

$$|\psi\rangle \approx \left(1 + \lambda \left(E + i\eta - \mathcal{H}_0\right)^{-1} \mathcal{V} + \lambda^2 \left(E + i\eta - \mathcal{H}_0\right)^{-1} \mathcal{V} \left(E + i\eta - \mathcal{H}_0\right)^{-1} \mathcal{V}\right) |\psi_0\rangle \tag{3.9}$$

This iteration procedure yields the Born series, which we explain and expand later in Sec. 3.1.3. Equation (3.9) can be rewritten as

$$|\psi\rangle \approx \left(E + i\eta - \mathcal{H}_0\right)^{-1} \left[\left(E + i\eta - \mathcal{H}_0\right) + \lambda\mathcal{V} + \lambda^2 \mathcal{V} \left(E + i\eta - \mathcal{H}_0\right)^{-1} \mathcal{V}\right] |\psi_0\rangle \,. \tag{3.10}$$

Finally, we get to

$$|\psi\rangle \approx |\psi_0\rangle + \left(E + i\eta - \mathcal{H}_0\right)^{-1} \left(\lambda\mathcal{V} + \lambda^2 \mathcal{V} \left(E + i\eta - \mathcal{H}_0\right)^{-1} \mathcal{V}\right) |\psi_0\rangle \,. \tag{3.11}$$

Obviously it is possible to keep iterating the series to express the stationary scattering wave $|\psi\rangle$ as the sum of all the possible scattering events.

3.1.2 Green's function

The scattered wave function in Eq. (3.5) is written in terms of the operator $\left(E + i\eta - \mathcal{H}_0\right)^{-1}$, which is also the central part of the iterative expansion in Eq. (3.9). The operator $\left(E + i\eta - \mathcal{H}_0\right)^{-1}$ is called the noninteracting Green's function. Let us define Green's functions for a general time-independent Hamiltonian. Given the Hamiltonian $\mathcal{H}$ of a system, the Green's function is defined as

$$\mathcal{G}\left(z\right) = \left(z - \mathcal{H}\right)^{-1} , \tag{3.12}$$

where z is a complex variable with dimensions of energy. Although it was mentioned earlier, we introduce now the noninteracting Green's function $\mathcal{G}_0\left(z\right)$ as

$$\mathcal{G}_0\left(z\right) = \left(z - \mathcal{H}_0\right)^{-1} . \tag{3.13}$$

From the general definition in Eq. (3.12) it is clear that Green's functions are not Hermitian and $\mathcal{G}\left(z^*\right) = \left[\mathcal{G}\left(z\right)\right]^\dagger$.

We now introduce an equivalent definition of the Green's function. From the nonin-

teracting Green's function defined in Eq. (3.13) we have the following identity

$$(z - \mathcal{H}_0)\,\mathcal{G}_0\,(z) = 1. \tag{3.14}$$

Multiplying Eq. (3.14) on the left by $\langle \mathbf{r}' |$ and on the right by $|\mathbf{r}\rangle$ and using the differential operator representation for the momentum, Eq. (2.3), we obtain

$$\left(\frac{\hbar^2\nabla^2}{2m} + z\right) \left\langle \mathbf{r}' \right| \mathcal{G}_0\,(z)\,|\mathbf{r}\rangle = \delta\left(\mathbf{r} - \mathbf{r}'\right), \tag{3.15}$$

where we have used $\langle \mathbf{r}'|\mathbf{r}\rangle = \delta\,(\mathbf{r} - \mathbf{r}')$. We extend the definition to the interacting Green's function $\mathcal{G}\,(z)$ as the function that solves Eq. (3.15), where $\mathcal{H}_0 \to \mathcal{H}_0 + \mathcal{H}_I$.

In order to show some properties of the Green's function let us now calculate the eigenvalues and eigenstates of the interacting Green's function, defined by Eq. (3.12). Let us assume the spectrum $\sigma\,(\mathcal{H})$ of $\mathcal{H}$ is known and its basis of eigenstates is $\{|\psi_k\rangle\,, k = 1, \ldots, N_{\mathbb{H}}\}$ being $N_{\mathbb{H}}$ the dimension of the Hilbert space $\mathbb{H}$. We apply the Green's function to the eigenstates of $\mathcal{H}$ to get

$$\mathcal{G}\,(z)\,|\psi_k\rangle = \frac{1}{z - E_k}\,|\psi_k\rangle\,, \tag{3.16}$$

which implies that $(z - \mathcal{H})^{-1}$ is meromorphic[1]. According to Eqs. (3.12) and (3.16), Green's functions are not defined when z is an eigenvalue of the Hamiltonian. Hence the knowledge of the singularities of the Green's function is equivalent to the knowledge of the spectrum of the Hamiltonian. In the particular case of considering scattering states, where there is a continuous and positive spectrum, $\mathcal{G}$ is not defined in $\mathbb{R}^+$ and is singular at the bound state energies.

The interacting and noninteracting Green's functions are related with the interacting Hamiltonian via the identity[2]

$$\mathcal{G}\,(z) = \mathcal{G}_0\,(z) + \mathcal{G}_0\,(z)\,\mathcal{H}_I\mathcal{G}\,(z)\,, \tag{3.17}$$

or alternatively

$$\mathcal{G}\,(z) = \mathcal{G}_0\,(z) + \mathcal{G}\,(z)\,\mathcal{H}_I\mathcal{G}_0\,(z)\,. \tag{3.18}$$

[1] A complex function is said to be meromorphic in an open subset $\mathcal{U}$ of $\mathbb{C}$ if it is complex differentiable at every point of $\mathcal{U}$ except the poles (see Ref. [62]).

[2] For any operators A and B, it holds $A^{-1} = B^{-1} + B^{-1}\,(B - A)\,A^{-1}$. Write $A = z - \mathcal{H}$ and $B = z - \mathcal{H}_0$ to obtain (3.17) or $A \leftrightarrow B$ to get (3.18) (see Ref. [26])

From Eqs. (3.17) and (3.18) it is obvious that

$$\mathcal{G}_0(z)\,\mathcal{H}_I\mathcal{G}(z) = \mathcal{G}(z)\,\mathcal{H}_I\mathcal{G}_0(z) \tag{3.19}$$

if $\mathcal{G}_0(z)$ and $\mathcal{G}(z)$ exist.

3.1.3 *T*-matrix

The *T*-matrix is defined in terms of the interacting Hamiltonian ($\mathcal{H}_I = \lambda\mathcal{V}$) and the interacting Green's function as

$$T(z) = \mathcal{H}_I + \mathcal{H}_I\mathcal{G}(z)\,\mathcal{H}_I. \tag{3.20}$$

We can write now the stationary scattering wave $|\psi\rangle$, given by Eq. (3.11), as

$$|\psi\rangle = [1 + \mathcal{G}_0(z)\,T(z)]\,|\psi_0\rangle\,. \tag{3.21}$$

Therefore the scattered wave in Eq. (3.5) is

$$|\psi_S\rangle = \mathcal{G}_0(z)\,T(z)\,|\psi_0\rangle\,. \tag{3.22}$$

Multiplying the *T*-matrix in Eq. (3.20) on the left by $\mathcal{G}_0(z)$ and using Eq. (3.17) we obtain

$$\mathcal{G}_0(z)\,T(z) = \mathcal{G}(z)\,\mathcal{H}_I. \tag{3.23}$$

Or alternatively multiplying on the right and using Eq. (3.18) gives

$$T(z)\,\mathcal{G}_0(z) = \mathcal{H}_I\mathcal{G}(z)\,. \tag{3.24}$$

Therefore it is possible to write a relation between the noninteracting Green's function, the interacting Green's function and the *T*-matrix as

$$\mathcal{G}(z) = \mathcal{G}_0(z) + \mathcal{G}_0(z)\,T(z)\,\mathcal{G}_0(z)\,. \tag{3.25}$$

Substituting Eq. (3.23) into the equation for the *T*-matrix (3.20) yields an integral equation for the *T*-matrix similar to that for $\mathcal{G}(z)$ in Eq. (3.17)

$$T(z) = \mathcal{H}_I + \mathcal{H}_I\mathcal{G}_0(z)\,T(z)\,. \tag{3.26}$$

This is called the Lippmann-Schwinger equation for the T-matrix. Equation (3.26) is the starting point to construct the Born series. We solve Eq. (3.26) iteratively as we did to obtain $|\psi\rangle$, Eq. (3.8), with the difference that we use now operators instead of wave functions. Thus the first term corresponds to

$$T(z) \approx \mathcal{H}_I. \tag{3.27}$$

Substituting Eq. (3.27) into the RHS of Eq. (3.26) yields a second order term in the interacting Hamiltonian $\mathcal{H}_I$

$$T(z) \approx \mathcal{H}_I + \mathcal{H}_I \mathcal{G}_0(z) \mathcal{H}_I. \tag{3.28}$$

Iterating this process yields the Born series for the T-matrix

$$T(z) = \sum_{n=0}^{\infty} \lambda^n T^{(n)}(z). \tag{3.29}$$

Above we have written the dependence of the interacting Hamiltonian in the coupling constant λ explicitly. The Born series is not necessarily convergent. For weak potentials or high energy collisions the series in Eq. (3.29) may converge. If the coupling parameter λ is small enough that the series in Eq. (3.29) converges for all momenta $\mathbf{p}$, then it can be proved that there are no bound states [26]. Conversely, if it is known that the Hamiltonian has some bound state, then the Born series does not converge for all momenta $\mathbf{p}$. Proving the convergence of the Born series can give extra information of the structure of the spectrum of the Hamiltonian, though the calculations can be rather hard [26].

3.2 Renormalisation

> *It doesn't matter how beautiful your theory is, it doesn't matter how smart you are. If it doesn't agree with the experiments, it's wrong.*
>
> Richard P. Feynman

Sometimes, certain calculations yield results that are not compatible with the experiments, including finite experimental results when theoretical calculations predict divergent quantities. As there is no experimental evidence of infinities, and so far Nature is

finite, these infinities have to disappear from the theory or else the theory has little-to-no predictive power. The process of annihilating the infinities is called renormalisation. Since H. Bethe applied perturbative renormalisation for the first time in 1947 to compute Lamb's shift in the Hydrogen atom, it has become an extremely active field in Physics [63–66], giving rise to several Nobel prizes[3].

The first step to renormalise a theory that shows divergent quantities is to regularise the theory. Here we will consider cut-off regularisation, although there are different regularisation schemes.[4] Although different regularisation schemes give different intermediate results, the final result must be independent of the regularisation scheme. Regularising a divergent theory consists of parametrising the divergences into the sensitivity to a parameter Ξ called regulator.

In Sec. 4.3 we will encounter linear and logarithmic ultraviolet (UV) divergences in the calculation of the *T*-matrix for a Rashba-coupled Fermi gas. They appear because of integrating over all the possible momenta in the interaction and the use of approximate low-energy interactions. The linear divergence is renormalised using minimal subtraction or the Tan-Valiente distribution [67, 68] (see Sec. 3.2.2), while the logarithmic divergence is removed by renormalisation of the coupling constant.

3.2.1 Renormalisation process

We now explain how to renormalise a single-parameter divergent theory [69]. We do not specify how the divergence appears or which regulator is used as the purpose of this section is to show how to eliminate the divergent terms in favour of physical quantities.

Let us start by introducing a single-parameter theory with a bare coupling constant g_0 that can be for instance the strength of the interaction in the Hamiltonian. A function $\mathcal{F}(\mathbf{r})$ is a measurable or calculable quantity that depends on the only scale $\mathbf{r}$ of the theory. From the experiment or Gedanken experiment we know that

$$\mathcal{F}(\mathbf{r}_0) = g_R, \tag{3.30}$$

where g_R is called the renormalised coupling constant at $\mathbf{r}_0$. Equation (3.30) is the only "experimental" information we have on the system and it shows a disagreement between the "theoretical" g_0 and the "experimental" g_R values of the coupling constant.

[3] K. Wilson for his application to Statistical Mechanics (1982) and to M. Veltman and G. t' Hooft for their work in Particle Physics.

[4] Different regularisation schemes include lattice regularisation, minimal subtraction or coupling constant renormalisation.

The coupling constants g_0 and g_R disagree because a function in the theory is expanded in a mathematically inconsistent way. Equation (3.30) is used as the starting point in the renormalisation process and it is called renormalisation condition. On the other hand, the quantity $\mathcal{F}(\mathbf{r})$ admits a formal perturbative expansion in powers of the bare coupling g_0

$$\mathcal{F}(\mathbf{r}) = g_0 + g_0^2 \mathcal{F}_1(\mathbf{r}) + g_0^3 \mathcal{F}_2(\mathbf{r}) + \cdots \tag{3.31}$$

The functions $\mathcal{F}_i(\mathbf{r})$ are ill-defined (divergent) for all $\mathbf{r}$. The first step in the renormalisation protocol consists in choosing an appropriate regularisation scheme. Substituting the ill-defined functions $\mathcal{F}_i$ by other functions $\mathcal{F}_{i,\Xi}$ where the divergence is parametrised into the sensitivity to an external parameter Ξ as it goes to infinity. The functions $\mathcal{F}_{i,\Xi}$ are finite if Ξ is finite, but they still diverge if the regulator Ξ goes to infinity. We write the expansion in Eq. (3.31) using the regularised functions $\mathcal{F}_{i,\Xi}$

$$\mathcal{F}_\Xi(\mathbf{r}) = g_0 + g_0^2 \mathcal{F}_{1,\Xi}(\mathbf{r}) + g_0^3 \mathcal{F}_{2,\Xi}(\mathbf{r}) + \cdots \tag{3.32}$$

Now the expansion in Eq. (3.32) is well defined for $\mathbf{r}_0$ as long as Ξ is finite. When the limit $\Xi \to \infty$ is taken, the expansion (3.32) is still divergent at all orders. The main idea consists now of adjusting the terms in Eq. (3.32) so the renormalisation condition, given by Eq. (3.30), is fulfilled and once the theory is renormalised then

$$\lim_{\Xi \to \infty} \mathcal{F}_\Xi(\mathbf{r}) = \mathcal{F}(\mathbf{r}). \tag{3.33}$$

Now Eq. (3.33) is free of divergences under quite general conditions (in particular, if the divergence is $\mathbf{r}$-independent). The general renormalisation process can be summarised as follows:

- Regularise the theory: Find a suitable way of defining the regulator Ξ and the functions $\mathcal{F}_{i,\Xi}(\mathbf{r})$.
- The regularised functions $\mathcal{F}_{i,\Xi}(\mathbf{r})$ must obey the renormalisation condition, Eq. (3.30), at any order, therefore we set $\mathcal{F}_\Xi(\mathbf{r}_0) = g_R$. The regularised functions $\mathcal{F}_{i,\Xi}(\mathbf{r})$ must have the same functional form as the ill-defined functions $\mathcal{F}_i(\mathbf{r})$.
- The renormalisation condition, Eq. (3.30), imposes $\mathcal{F}(\mathbf{r}_0) = \mathcal{F}_\Xi(\mathbf{r}_0)$ when $\Xi \to \infty$. As we will show, the divergent term of order n in (3.31) cancels with the $n-1$ term that comes from the renormalisation process. In order to cancel a divergent term we must add another divergent term that needs to cancel out a higher order correction.

This process is repeated *ad infinitum*.

Renormalisation to second order

We now show the general and formal procedure of renormalisation to second order. In Sec. 4.3 we follow this approach to renormalise into the coupling constant the logarithmic UV divergence that appears in the T-matrix of a Rashba-coupled Fermi gas. The renormalisation condition, Eq. (3.30), imposes $\mathcal{F}(\mathbf{r}_0) = \mathcal{F}_\Xi(\mathbf{r}_0)$ to any order of the expansion of $\mathcal{F}_\Xi(\mathbf{r})$, given by Eq. (3.32). Thence, to first order we expand the bare coupling g_0 in terms of the renormalised coupling g_R as

$$g_0 = g_R + \mathcal{O}\left(g_R^2\right). \tag{3.34}$$

Introducing Eq. (3.34) into the regularised expansion of $\mathcal{F}_\Xi(\mathbf{r})$, given by Eq. (3.32), and retaining only the second order terms gives

$$\mathcal{F}_\Xi(\mathbf{r}) = g_R + g_R^2 \mathcal{F}_{1,\Xi}(\mathbf{r}) + \mathcal{O}\left(g_R^3\right). \tag{3.35}$$

Still the function defined by Eq. (3.35) is divergent when $\Xi \to \infty$. To eliminate this term, we substitute the expansion of g_0 in terms of g_R, Eq. (3.34), into the expansion of $\mathcal{F}_\Xi(\mathbf{r})$, Eq. (3.32), to obtain

$$\mathcal{F}_\Xi(\mathbf{r}) = g_R + \mathcal{O}\left(g_R^2\right) + \left[g_R + \mathcal{O}\left(g_R^2\right)\right]^2 \mathcal{F}_{1,\Xi}(\mathbf{r}) + \cdots \tag{3.36}$$

The idea consists now of finding $\mathcal{O}\left(g_R^2\right)$ such that it cancels the divergent term $\mathcal{F}_{1,\Xi}$ in Eq. (3.36). The renormalisation condition $\mathcal{F}_\Xi(\mathbf{r}_0) = g_R$ gives

$$\mathcal{O}\left(g_R^2\right) = -g_R^2 \mathcal{F}_{1,\Xi}(\mathbf{r}_0) \tag{3.37}$$

as the correction to second order in the renormalised coupling g_R. Substituting the correction, Eq. (3.37), into Eq. (3.36) and retaining only the terms to second order yields

$$\mathcal{F}_\Xi(\mathbf{r}) = g_R + g_R^2 \left[\mathcal{F}_{1,\Xi}(\mathbf{r}) - \mathcal{F}_{1,\Xi}(\mathbf{r}_0)\right] + \mathcal{O}\left(g_R^3\right). \tag{3.38}$$

Equation (3.38) gives the correct result if $[\mathcal{F}_{1,\Xi}(\mathbf{r}) - \mathcal{F}_{1,\Xi}(\mathbf{r}_0)]$ is finite for all $\mathbf{r}$ when $\Xi \to \infty$. We introduced a divergent term $\mathcal{O}\left(g_R^2\right)$ in the expansion of the bare coupling constant g_0, Eq. (3.34), in order to cancel the divergence $\mathcal{F}_{1,\Xi}$ that comes from the expansion of

$\mathcal{F}_{\Xi}(\mathbf{r})$ in Eq. (3.32).

3.2.2 *s*-wave contact interaction

Contact s-wave interactions described by $\delta(\mathbf{r})$ functions can be good approximations to scattering off short-range potentials. However, they give rise to UV divergences when short distances (large momenta) are considered. Hence the δ-interaction has to be renormalised. This can be done using the Tan-Valiente Λ distribution. The Λ distribution was introduced by S. Tan [67] to renormalise the Fermi-Huang-Lee pseudopotential [70]. Later M. Valiente found the momentum representation of Λ [68]. In this section we begin by showing the origin and main properties of Λ and we finish with a calculation as an example of the type of renormalisation procedure we encounter in Sec. 4.1.

Let us follow the same approach as S. Tan in [67]. We assume the interaction between two particles with different spin states is mediated by the zero-range Fermi-Huang-Lee pseudopotential [70]

$$V(\mathbf{r})\,\psi(\mathbf{r}) = \frac{4\pi a}{\mu}\delta(\mathbf{r})\,\frac{\partial}{\partial r}\left[r\psi(\mathbf{r})\right], \tag{3.39}$$

where a is the s-wave scattering length, μ is the reduced mass and r is the interparticle distance. The pseudo-potential (3.39) is valid when the effective range r_0 is much smaller than $|a|$. The Schrödinger equation reads

$$-\frac{\hbar^2\nabla^2}{\mu}\psi(\mathbf{r}) + \frac{4\pi a}{\mu}\delta(\mathbf{r})\,\frac{\partial}{\partial r}\left[r\,\psi(\mathbf{r})\right] = E\psi(\mathbf{r}). \tag{3.40}$$

Since we want to relate the properties of Λ in momentum space to the Fermi-Huang-Lee pseudopotential, we Fourier transform the Schrödinger equation (3.40)

$$\int\frac{\mathrm{d}\mathbf{k}}{(2\pi)^3}\left(E-\frac{\hbar^2k^2}{\mu}\right)e^{i\mathbf{k}\cdot\mathbf{r}}\psi(\mathbf{k}) = \frac{4\pi a}{\mu}\int\frac{\mathrm{d}\mathbf{k}}{(2\pi)^3}\psi(\mathbf{k})\,\delta(\mathbf{r})\,\frac{\partial}{\partial r}\left(re^{i\mathbf{k}\cdot\mathbf{r}}\right). \tag{3.41}$$

The Λ distribution is defined as

$$\delta(\mathbf{r})\,\Lambda(\mathbf{k}) = \delta(\mathbf{r})\,\frac{\partial}{\partial r}\left(re^{i\mathbf{k}\cdot\mathbf{r}}\right), \tag{3.42}$$

where $\Lambda(\mathbf{k})$ is an unknown distribution of $\mathbf{k}$. The equality in Eq. (3.42) cannot be taken term by term. By taking the limit $\mathbf{r}\to 0$ while keeping $\mathbf{k}$ finite in both sides of Eq. (3.42)

we get to

$$\Lambda\left(\mathbf{k}\right)=1 \text{ if } k<\infty. \tag{3.43}$$

One of the great advantages of using the Λ distribution relies on the absence of UV linear divergences. To show this, let us perform the typical integral that leads to UV linear divergences. In order to do so, we multiply both sides of Eq. (3.42) by k^{-2} and integrate over $\mathbf{k}$

$$\delta\left(\mathbf{r}\right)\int\frac{\mathbf{dk}}{\left(2\pi\right)^{3}}\frac{\Lambda\left(\mathbf{k}\right)}{k^{2}}=\delta\left(\mathbf{r}\right)\frac{\partial}{\partial r}\left[\int\frac{\mathbf{dk}}{\left(2\pi\right)^{3}}\frac{re^{i\mathbf{k}\cdot\mathbf{r}}}{k^{2}}\right] \tag{3.44}$$

Integrating the RHS of Eq. (3.44) yields a constant value, hence the derivative with respect to r is zero. Therefore

$$\int\frac{\mathbf{dk}}{\left(2\pi\right)^{3}}\frac{\Lambda\left(\mathbf{k}\right)}{k^{2}}=0 \tag{3.45}$$

annihilates the UV linear divergences in the theory. We can enumerate the most important mathematical properties of Λ [67]

$$\begin{aligned}\Lambda\left(-\mathbf{k}\right)&=\Lambda\left(\mathbf{k}\right)\\ \Lambda\left(c\mathbf{k}\right)&=\Lambda\left(\mathbf{k}\right)\\ \Lambda^{*}\left(\mathbf{k}\right)&=\Lambda\left(\mathbf{k}\right),\end{aligned} \tag{3.46}$$

where $c\neq0$ is a real constant.

So far the properties of $\Lambda\left(\mathbf{k}\right)$ are well established but its form is unknown. The explicit momentum representation for the Λ distribution was given by M. Valiente in [68] and formally, it has the form

$$\Lambda\left(\mathbf{k}\right)=1-\frac{\delta\left(1/k\right)}{k}. \tag{3.47}$$

Equation (3.47) can be modified to include the effects of a cutoff for numerical calculations, therefore

$$\Lambda_{c}\left(\mathbf{k}\right)=\theta\left(k_{c}-k\right)-\frac{\delta\left(1/k-1/k_{c}\right)}{k}, \tag{3.48}$$

where k_c is the high-momentum cutoff. We use now Eq. (3.48) to explicitly integrate an

expression similar to Eq. (3.45), hence

$$\begin{aligned}\int_0^\infty \mathrm{d}k \frac{k^2}{1+k^2}\Lambda_c\left(\mathbf{k}\right) &= \int_0^\infty \mathrm{d}k \frac{k^2}{1+k^2}\left[\theta\left(k_c-k\right)-\frac{\delta\left(1/k-1/k_c\right)}{k}\right] \\ &= \lim_{k_c\to\infty}\left[\int_0^{k_c}\mathrm{d}k\frac{k^2}{1+k^2}-\int_{1/k_c}^\infty \mathrm{d}k\frac{k\,\delta\left(1/k-1/k_c\right)}{1+k^2}\right] \\ &= \lim_{k_c\to\infty}\left[k_c-\arctan k_c^2+\int_{1/k_c}^\infty \mathrm{d}u\frac{\delta\left(u-1/k_c\right)}{u^2\left(u+1\right)}\right] \\ &= \lim_{k_c\to\infty}\left[k_c-\arctan k_c+\frac{k_c}{1+1/k_c^2}\right] \\ &= -\frac{\pi}{2}, \end{aligned} \tag{3.49}$$

where the substitution $k = 1/u$ is used. The result of the integral (3.49) shows how the Tan-Valiente distribution renormalises the bare contact *s*-wave interaction so no UV divergences appear.

3.3 Conclusions

In this Chapter we reviewed the most important concepts in scattering theory and renormalisation, which will be addressed in Chapter 4 and Chapter 5. We showed the importance of Green's functions in the framework of computing effective interactions using the *T*-matrix. We approached renormalisation with the humble purpose of clarifying the origin of different UV divergences. We showed how linear divergences can be nicely renormalised using the Tan-Valiente distribution [67, 68], while logarithmic UV divergences can be renormalised into the coupling constant.

Chapter 4

Single-branch theory of ultracold Fermi gases with artificial Rashba spin-orbit coupling

In previous Chapters we introduced and described the properties of noninteracting Rashba-coupled Fermi gases. We outlined the helicity formalism to distinguish two different set of eigenstates. In this Chapter we will describe contact s-wave interactions between negative-helicity fermions. As proved by Ozawa and Baym [27], the multichannel theory shows no logarithmic UV divergences in the T-matrix. Here we show how the single-channel T-matrix is renormalised using the correct multi-channel T-matrix by Ozawa, yielding a divergent-free theory for the negative-helicity branch with a finite correction to the energy in second order perturbation theory [28].

The outline of this Chapter is as follows: we start introducing the negative-helicity contact s-wave interaction. We then describe the first and second approximation in the Born series, Eq. (3.29), and show the linear and logarithmic divergences. The linear divergence is renormalised using the Tan-Valiente distribution [67, 68], while we renormalise the logarithmic divergence into the coupling constant. We conclude by showing that the energy of the interacting ground state is renormalisable, therefore finite, to second order in perturbation theory.

4.1 Contact interactions in Rashba-coupled Fermi gases

In Chapter 2 we described the main properties of noninteracting Rashba-coupled Fermi gases in two and three dimensions. For single-branch theories, introducing a contact

s-wave interaction leads to a non-renormalisable logarithmic divergence [71, 72] in the T-matrix that is renormalised when the multichannel T-matrix is considered [27]. Our starting point to develop a divergent-free single-branch theory for a Rashba-coupled many-body problem at low densities is the interaction term[1] in the spin-1/2 basis [27]

$$\mathcal{H}_I = \frac{g_*}{V} \sum_{\mathbf{k}_1+\mathbf{k}_2=\mathbf{k}_3+\mathbf{k}_4} c^\dagger_{\mathbf{k}_4,\uparrow} c^\dagger_{\mathbf{k}_3,\downarrow} c_{\mathbf{k}_2,\downarrow} c_{\mathbf{k}_1,\uparrow}, \tag{4.1}$$

where V is the volume and g_* is the bare coupling constant. With the use of the noninteracting spin-orbit Hamiltonian (2.52), the interacting Hamiltonian reads

$$\mathcal{H} = \sum_{\mathbf{k},\sigma} \frac{\hbar^2}{2m} \left(\mathbf{k}^2 + \lambda^2\right) c^\dagger_{\mathbf{k},\sigma} c_{\mathbf{k},\sigma} + \frac{\hbar^2 \lambda}{m} \sum_{\mathbf{k}} k_\perp \left(e^{-i\gamma_k} c^\dagger_{\mathbf{k},\uparrow} c_{\mathbf{k},\downarrow} + e^{i\gamma_k} c^\dagger_{\mathbf{k},\downarrow} c_{\mathbf{k},\uparrow} \right) + \frac{g_*}{V} \sum_{\mathbf{k}_1+\mathbf{k}_2=\mathbf{k}_3+\mathbf{k}_4} c^\dagger_{\mathbf{k}_4,\uparrow} c^\dagger_{\mathbf{k}_3,\downarrow} c_{\mathbf{k}_2,\downarrow} c_{\mathbf{k}_1,\uparrow}. \tag{4.2}$$

We express the interacting Hamiltonian (4.2) in the helicity basis, where the noninteracting Hamiltonian (2.52) is diagonal. The inverse transformation of Eq. (2.59) is

$$\begin{pmatrix} c_{\mathbf{k},\uparrow} \\ c_{\mathbf{k},\downarrow} \end{pmatrix} = \frac{1}{\sqrt{2}} \begin{pmatrix} 1 & 1 \\ e^{i\gamma_k} & -e^{i\gamma_k} \end{pmatrix} \begin{pmatrix} d_{\mathbf{k},\uparrow} \\ d_{\mathbf{k},\downarrow} \end{pmatrix}. \tag{4.3}$$

Writing the interaction Hamiltonian (4.1) in the helicity basis yields

$$\mathcal{H}_I = \frac{g_*}{4V} \sum_{\mathbf{k}_1+\mathbf{k}_2=\mathbf{k}_3+\mathbf{k}_4} e^{-i\gamma_3} e^{i\gamma_2} \left(d^\dagger_{\mathbf{k}_4,\uparrow} + d^\dagger_{\mathbf{k}_4,\downarrow} \right) \left(d^\dagger_{\mathbf{k}_3,\uparrow} - d^\dagger_{\mathbf{k}_3,\downarrow} \right) \left(d_{\mathbf{k}_2,\uparrow} - d_{\mathbf{k}_2,\downarrow} \right) \left(d_{\mathbf{k}_1,\uparrow} + d_{\mathbf{k}_1,\downarrow} \right). \tag{4.4}$$

Expanding Eq. (4.4) gives all the possible interactions in the system. Since at low density only the lowest branch is energetically relevant, we only retain that term in Eq. (4.4). Therefore the effective Hamiltonian is reduced to

$$\mathcal{V} = \frac{g_*}{4V} \sum_{\mathbf{k}_1+\mathbf{k}_2=\mathbf{k}_3+\mathbf{k}_4} e^{-i\gamma_3} e^{i\gamma_2} d^\dagger_{\mathbf{k}_4,\downarrow} d^\dagger_{\mathbf{k}_3,\downarrow} d_{\mathbf{k}_2,\downarrow} d_{\mathbf{k}_1,\downarrow}, \tag{4.5}$$

where $\mathcal{V}$ represents the interaction Hamiltonian in the negative-helicity branch. The interaction only depends in the incident angle γ_2 and the outgoing angle γ_3. In order to have an interaction that depends on the parameters of all the particles involved, we pro-

[1] Any wave vector labeled using numbers $\mathbf{k}_i$ where $i = 1, 2, ...$ corresponds to a creation or annihilation operator that appears in the effective interaction no matter the basis chosen.

ceed to symmetrise Eq. (4.5). Permuting the indices (from here onwards we omit again the spin indices as we always refer to the negative helicity branch) yields

$$\begin{aligned}\mathcal{V} =& \frac{g_*}{8V} \sum_{\mathbf{k}_1+\mathbf{k}_2=\mathbf{k}_3+\mathbf{k}_4} \left(e^{-i\gamma_3} e^{i\gamma_2} d^\dagger_{\mathbf{k}_4} d^\dagger_{\mathbf{k}_3} d_{\mathbf{k}_2} d_{\mathbf{k}_1} + e^{-i\gamma_4} e^{i\gamma_2} d^\dagger_{\mathbf{k}_3} d^\dagger_{\mathbf{k}_4} d_{\mathbf{k}_2} d_{\mathbf{k}_1} \right) \\ =& \frac{g_*}{16V} \sum_{\mathbf{k}_1+\mathbf{k}_2=\mathbf{k}_3+\mathbf{k}_4} \Big(e^{-i\gamma_3} e^{i\gamma_2} d^\dagger_{\mathbf{k}_4} d^\dagger_{\mathbf{k}_3} d_{\mathbf{k}_2} d_{\mathbf{k}_1} + e^{-i\gamma_3} e^{i\gamma_1} d^\dagger_{\mathbf{k}_4} d^\dagger_{\mathbf{k}_3} d_{\mathbf{k}_1} d_{\mathbf{k}_2} \\ &+ e^{-i\gamma_4} e^{i\gamma_2} d^\dagger_{\mathbf{k}_3} d^\dagger_{\mathbf{k}_4} d_{\mathbf{k}_2} d_{\mathbf{k}_1} + e^{-i\gamma_4} e^{i\gamma_1} d^\dagger_{\mathbf{k}_3} d^\dagger_{\mathbf{k}_4} d_{\mathbf{k}_1} d_{\mathbf{k}_2} \Big). \end{aligned} \tag{4.6}$$

The anticommutation relations, Eq. (2.60), allow to write Eq. (4.6) as

$$\mathcal{V} = \frac{g_*}{16V} \sum_{\mathbf{k}_1+\mathbf{k}_2=\mathbf{k}_3+\mathbf{k}_4} d^\dagger_{\mathbf{k}_4} d^\dagger_{\mathbf{k}_3} d_{\mathbf{k}_2} d_{\mathbf{k}_1} \left(e^{-i\gamma_3} e^{i\gamma_2} - e^{-i\gamma_3} e^{i\gamma_1} - e^{-i\gamma_4} e^{i\gamma_2} + e^{-i\gamma_4} e^{i\gamma_1} \right), \tag{4.7}$$

which is rearranged as

$$\mathcal{V} = -\frac{g_*}{16V} \sum_{\mathbf{k}_1+\mathbf{k}_2=\mathbf{k}_3+\mathbf{k}_4} d^\dagger_{\mathbf{k}_4} d^\dagger_{\mathbf{k}_3} d_{\mathbf{k}_2} d_{\mathbf{k}_1} \left(e^{i\gamma_1} - e^{i\gamma_2} \right) \left(e^{-i\gamma_3} - e^{-i\gamma_4} \right). \tag{4.8}$$

We finally write the negative-helicity bare interaction Hamiltonian as

$$\mathcal{V} = \frac{g_*}{2V} \sum_{\mathbf{k}_1+\mathbf{k}_2=\mathbf{k}_3+\mathbf{k}_4} \Delta\left(\gamma_1, \gamma_2, \gamma_3, \gamma_4\right) d^\dagger_{\mathbf{k}_4} d^\dagger_{\mathbf{k}_3} d_{\mathbf{k}_2} d_{\mathbf{k}_1}, \tag{4.9}$$

where the angular details of the interaction are given by

$$\Delta\left(\gamma_1, \gamma_2, \gamma_3, \gamma_4\right) = -\frac{1}{8} \left(e^{i\gamma_1} - e^{i\gamma_2} \right) \left(e^{-i\gamma_3} - e^{-i\gamma_4} \right). \tag{4.10}$$

In App. A.4 we summarise the main properties of the Δ function, Eq. (4.10).

Since the total momentum is conserved, we separate the centre of mass (CM) and relative coordinates. From Fig. 4.1 we define the incident wave vectors as $\mathbf{k}_1$ and $\mathbf{k}_2$ and the outgoing wave vectors as $\mathbf{k}_3$ and $\mathbf{k}_4$. The relative incident momentum $\hbar\mathbf{p}$ and the CM momentum $\hbar\mathbf{Q}$ are defined in terms of the incident wave vectors as

$$\mathbf{p} = \frac{\mathbf{k}_2 - \mathbf{k}_1}{2}, \tag{4.11}$$

$$\mathbf{Q} = \mathbf{k}_1 + \mathbf{k}_2. \tag{4.12}$$

Conservation of momentum leads to the same relations for the outgoing momenta $\mathbf{k}_3$ and

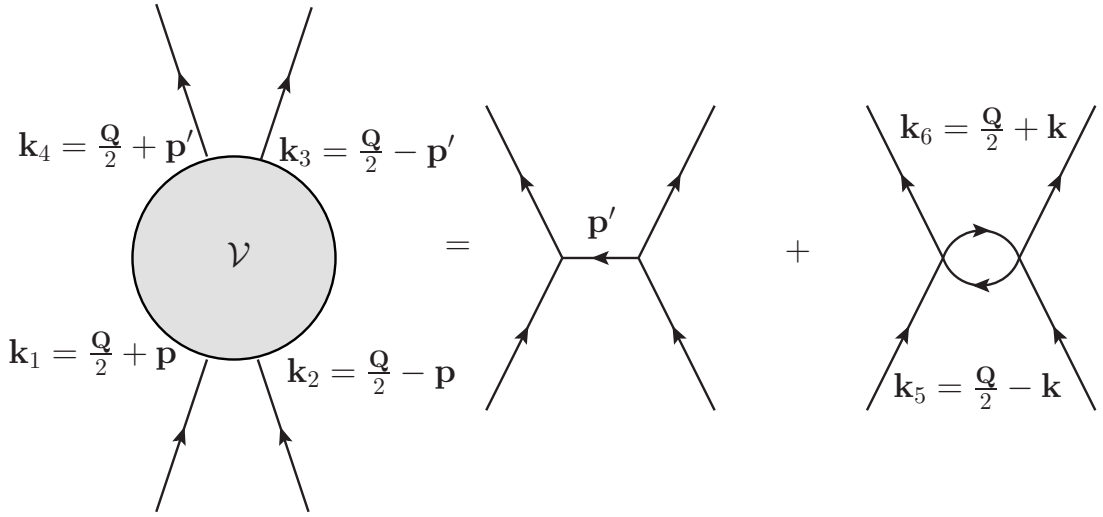

Figure 4.1: Pictorial representation of the negative helicity interaction $\mathcal{V}$ to first and second order.

$\mathbf{k}_4$ and the relative outgoing momentum $\hbar\mathbf{p}'$

$$\mathbf{k}_3 = \frac{\mathbf{Q}}{2} - \mathbf{p}', \tag{4.13}$$

$$\mathbf{k}_4 = \frac{\mathbf{Q}}{2} + \mathbf{p}'. \tag{4.14}$$

4.2 Single channel *T*-matrix

In this section we compute the single-channel T-matrix for an interacting Rashba-coupled Fermi gas. We begin by computing the first and second term in the Born series, Eq. (3.29), to show how the second term in the Born series yields a logarithmic UV divergence. The linear UV divergence is removed by re-parametrising the zero-range s-wave interaction (4.10) using the Tan-Valiente distribution, see Sec. 3.2.2.

4.2.1 First Born approximation

The first term in the Born series, Eq. (3.29), comes from evaluating the matrix elements of the interaction $\mathcal{V}$. We define $|\mathbf{k},\mathbf{q}\rangle = d^\dagger_{\mathbf{k}} d^\dagger_{\mathbf{q}} |0\rangle$ and $|\mathbf{k}',\mathbf{q}'\rangle = d^\dagger_{\mathbf{k}'} d^\dagger_{\mathbf{q}'} |0\rangle$ as incident and outgoing states respectively. Hence, the matrix elements read

$$\begin{aligned}\left\langle \mathbf{q}',\mathbf{k}' \right| \mathcal{V} \left| \mathbf{k},\mathbf{q} \right\rangle &= \frac{g_*}{2V} \sum_{\mathbf{k}_1+\mathbf{k}_2=\mathbf{k}_3+\mathbf{k}_4} \Delta\left(\gamma_1,\gamma_2,\gamma_3,\gamma_4\right) \Lambda\left(\mathbf{p}\right) \left\langle \mathbf{q}',\mathbf{k}' \right| d^\dagger_{\mathbf{k}_4} d^\dagger_{\mathbf{k}_3} d_{\mathbf{k}_2} d_{\mathbf{k}_1} \left| \mathbf{k},\mathbf{q} \right\rangle \\ &= \frac{g_*}{2V} \sum_{\mathbf{k}_1+\mathbf{k}_2=\mathbf{k}_3+\mathbf{k}_4} \Delta\left(\gamma_1,\gamma_2,\gamma_3,\gamma_4\right) \Lambda\left(\mathbf{p}\right) \left\langle 0 \right| d_{\mathbf{q}} d_{\mathbf{k}} d^\dagger_{\mathbf{k}_4} d^\dagger_{\mathbf{k}_3} d_{\mathbf{k}_2} d_{\mathbf{k}_1} d^\dagger_{\mathbf{k}} d^\dagger_{\mathbf{q}} \left| 0 \right\rangle ,\end{aligned} \tag{4.15}$$

where $\Lambda(\mathbf{p})$ is the Tan-Valiente distribution and $\mathbf{p} = (\mathbf{k}_2 - \mathbf{k}_1)/2$ the relative momentum. The expectation value in Eq. (4.15) is easily obtained using Wick's theorem (see Appendix A.5). From the eight contractions that do not leave any operator unpaired, let us show first the four contractions that give a non-vanishing contribution to the T-matrix. Afterwards, we will show how the remaining four terms vanish. The first term in the Born series reads

$$T^{(1)} = \frac{g_*}{2V} \sum_{\mathbf{k}_1+\mathbf{k}_2=\mathbf{k}_3+\mathbf{k}_4} \Delta(\gamma_1,\gamma_2,\gamma_3,\gamma_4)\,\Lambda(\mathbf{p}) \times \langle 0| \left(\overbrace{d_{\mathbf{q}'} d_{\mathbf{k}'} d^\dagger_{\mathbf{k}_4}} d^\dagger_{\mathbf{k}_3} + \overbrace{d_{\mathbf{q}'} d_{\mathbf{k}'} d^\dagger_{\mathbf{k}_4}} d^\dagger_{\mathbf{k}_3} \right) \left(\overbrace{d_{\mathbf{k}_2} d_{\mathbf{k}_1} d^\dagger_{\mathbf{k}}} d^\dagger_{\mathbf{q}} + \overbrace{d_{\mathbf{k}_2} d_{\mathbf{k}_1} d^\dagger_{\mathbf{k}}} d^\dagger_{\mathbf{q}} \right) |0\rangle . \tag{4.16}$$

Substituting the contractions by their values we get

$$T^{(1)} = \frac{g_*}{2V} \sum_{\mathbf{k}_1+\mathbf{k}_2=\mathbf{k}_3+\mathbf{k}_4} \Delta(\gamma_1,\gamma_2,\gamma_3,\gamma_4)\,\Lambda(\mathbf{p}) \times \Big[\delta_{\mathbf{q}',\mathbf{k}_3}\delta_{\mathbf{k}',\mathbf{k}_4} - \delta_{\mathbf{q}',\mathbf{k}_4}\delta_{\mathbf{k}',\mathbf{k}_3}\Big]\Big[-\delta_{\mathbf{q},\mathbf{k}_1}\delta_{\mathbf{k},\mathbf{k}_2} + \delta_{\mathbf{q},\mathbf{k}_2}\delta_{\mathbf{k},\mathbf{k}_1}\Big]. \tag{4.17}$$

In order to simplify this expression we interchange the dummy indices to obtain

$$T^{(1)} = \frac{g_*}{2V} \sum_{\mathbf{k}_1+\mathbf{k}_2=\mathbf{k}_3+\mathbf{k}_4} \delta_{\mathbf{q},\mathbf{k}_1}\delta_{\mathbf{k},\mathbf{k}_2}\delta_{\mathbf{k}',\mathbf{k}_3}\delta_{\mathbf{q}',\mathbf{k}_4}\Lambda(\mathbf{p}) \Big[-\Delta(\gamma_1,\gamma_2,\gamma_4,\gamma_3) + \Delta(\gamma_2,\gamma_1,\gamma_4,\gamma_3) + \Delta(\gamma_1,\gamma_2,\gamma_3,\gamma_4) - \Delta(\gamma_2,\gamma_1,\gamma_3,\gamma_4)\Big]. \tag{4.18}$$

The antisymmetry of Δ, Eq. (A.18), allows us to write Eq. (4.18) as

$$T^{(1)} = \frac{2g_*}{V} \sum_{\mathbf{k}_1+\mathbf{k}_2=\mathbf{k}_3+\mathbf{k}_4} \delta_{\mathbf{q},\mathbf{k}_1}\delta_{\mathbf{k},\mathbf{k}_2}\delta_{\mathbf{k}',\mathbf{k}_3}\delta_{\mathbf{q}',\mathbf{k}_4}\Delta(\gamma_1,\gamma_2,\gamma_3,\gamma_4)\,\Lambda(\mathbf{p}). \tag{4.19}$$

Finally summing over all momenta gives the first term in the Born series

$$T^{(1)} = \frac{2g_*}{V}\Delta\left(\gamma_q,\gamma_k,\gamma_{k'},\gamma_{q'}\right). \tag{4.20}$$

The four contractions that give a vanishing contribution to the T-matrix are given by

$$t^{(1)} = \frac{g_*}{2V} \sum_{\mathbf{k}_1+\mathbf{k}_2=\mathbf{k}_3+\mathbf{k}_4} \Delta(\gamma_1,\gamma_2,\gamma_3,\gamma_4)\,\Lambda(\mathbf{p}) \times \langle 0| \left(\overbrace{d_{\mathbf{q}'} d_{\mathbf{k}'} d^\dagger_{\mathbf{k}}} d^\dagger_{\mathbf{q}} + \overbrace{d_{\mathbf{q}'} d_{\mathbf{k}'} d^\dagger_{\mathbf{k}}} d^\dagger_{\mathbf{q}} \right) \left(\overbrace{d_{\mathbf{k}_2} d_{\mathbf{k}_1} d^\dagger_{\mathbf{k}_4}} d^\dagger_{\mathbf{k}_3} + \overbrace{d_{\mathbf{k}_2} d_{\mathbf{k}_1} d^\dagger_{\mathbf{k}_4}} d^\dagger_{\mathbf{k}_3} \right) |0\rangle . \tag{4.21}$$

Equation (4.21) yields

$$t^{(1)} = \frac{g_*}{2V} \sum_{\mathbf{k}_1+\mathbf{k}_2=\mathbf{k}_3+\mathbf{k}_4} \Delta\left(\gamma_1,\gamma_2,\gamma_3,\gamma_4\right)\Lambda\left(\mathbf{p}\right)\times \\ \left[\delta_{\mathbf{q},\mathbf{q}'}\delta_{\mathbf{k},\mathbf{k}'} - \delta_{\mathbf{q},\mathbf{k}'}\delta_{\mathbf{k},\mathbf{q}'}\right]\left[\delta_{\mathbf{k}_1,\mathbf{k}_4}\delta_{\mathbf{k}_2,\mathbf{k}_3} - \delta_{\mathbf{k}_1,\mathbf{k}_3}\delta_{\mathbf{k}_2,\mathbf{k}_4}\right]. \tag{4.22}$$

A first inspection of Eq. (4.22) suggests that this set of contractions corresponds to a non-interacting process. All the indices that correspond to incident ($\mathbf{q}$ and $\mathbf{k}$) or outgoing ($\mathbf{q}'$ and $\mathbf{k}'$) operators are not *mixed* with numeric indices that describe operators that come from the interaction, Eq. (4.9). Let us operate on the Kronecker deltas that are not affected by the sum. Due to conservation of momentum we write the Kronecker delta $\delta_{\mathbf{q}+\mathbf{k},\mathbf{q}'+\mathbf{k}'}$ explicitly to obtain

$$\Big[-\delta_{\mathbf{q},\mathbf{q}'}\delta_{\mathbf{k},\mathbf{k}'} + \delta_{\mathbf{q},\mathbf{k}'}\delta_{\mathbf{k},\mathbf{q}'}\Big]\delta_{\mathbf{q}+\mathbf{k},\mathbf{q}'+\mathbf{k}'} = -\delta_{\mathbf{q},\mathbf{q}'}\delta_{\mathbf{k},\mathbf{q}+\mathbf{k}-\mathbf{q}'} + \delta_{\mathbf{q},\mathbf{k}'}\delta_{\mathbf{k},\mathbf{k}+\mathbf{q}-\mathbf{k}'}, \tag{4.23}$$

which simplifies to $(-\delta_{\mathbf{k},\mathbf{k}} + \delta_{\mathbf{k},\mathbf{k}}) = 0$. Contractions that involve incident operators with outgoing operators, and subsequently contraction of operators that come from the interaction in Eq. (4.9) correspond to noninteracting processes, therefore they do not contribute to the T-matrix, see Fig. 4.2.

4.2.2 Second Born approximation

The second term in the Born series comes from evaluating the matrix elements of $\mathcal{V}\mathcal{G}_0\left(z\right)\mathcal{V}$, Eq. (3.28). The resolution of the identity for a two-particle system in the relative momentum $\mathbf{p}$ basis, Eq. (4.11), for a fixed CM momentum, Eq. (4.12), reads

$$\mathbb{1} = \sum_{\mathbf{p}} \left|\frac{\mathbf{Q}}{2}+\mathbf{p}, \frac{\mathbf{Q}}{2}-\mathbf{p}\right\rangle\left\langle\frac{\mathbf{Q}}{2}-\mathbf{p}, \frac{\mathbf{Q}}{2}+\mathbf{p}\right|, \tag{4.24}$$

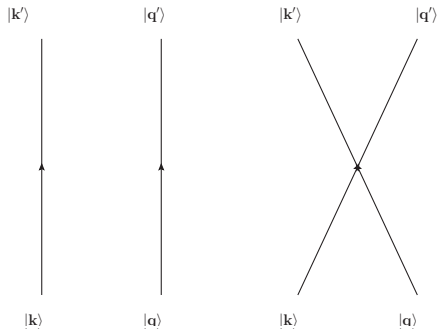

Figure 4.2: Vanishing contractions in the first term of the Born series.

hence the noninteracting Green's function is

$$\mathcal{G}_0(z) = \sum_{\mathbf{p}} \frac{1}{z - \mathcal{H}_{(-)}} \left| \frac{\mathbf{Q}}{2} + \mathbf{p}, \frac{\mathbf{Q}}{2} - \mathbf{p} \right\rangle \left\langle \frac{\mathbf{Q}}{2} - \mathbf{p}, \frac{\mathbf{Q}}{2} + \mathbf{p} \right|. \tag{4.25}$$

The two-particle state $|\mathbf{Q}/2 + \mathbf{p}, \mathbf{Q}/2 - \mathbf{p}\rangle$ is an eigenstate of the noninteracting single-branch Hamiltonian (2.61), therefore

$$\mathcal{H}_{(-)} \left| \frac{\mathbf{Q}}{2} + \mathbf{p}, \frac{\mathbf{Q}}{2} - \mathbf{p} \right\rangle = \left[\epsilon_- \left(\frac{\mathbf{Q}}{2} + \mathbf{p} \right) + \epsilon_- \left(\frac{\mathbf{Q}}{2} - \mathbf{p} \right) \right] \left| \frac{\mathbf{Q}}{2} + \mathbf{p}, \frac{\mathbf{Q}}{2} - \mathbf{p} \right\rangle \tag{4.26}$$

allows us to write the noninteracting Green's function, Eq. (4.25), as

$$\mathcal{G}_0(z) = \sum_{\mathbf{p}} \frac{1}{z - \epsilon_-(\mathbf{Q}/2 + \mathbf{p}) - \epsilon_-(\mathbf{Q}/2 - \mathbf{p})} \left| \frac{\mathbf{Q}}{2} + \mathbf{p}, \frac{\mathbf{Q}}{2} - \mathbf{p} \right\rangle \left\langle \frac{\mathbf{Q}}{2} - \mathbf{p}, \frac{\mathbf{Q}}{2} + \mathbf{p} \right|. \tag{4.27}$$

Making use of Eq. (4.27), the second term in the Born series reads

$$\begin{aligned} \left\langle \mathbf{q}', \mathbf{k}' \right| \mathcal{V} \mathcal{G}_0(z) \mathcal{V} \left| \mathbf{k}, \mathbf{q} \right\rangle = \left(\frac{g_*}{2V} \right)^2 \sum_{\mathbf{p}} \frac{\delta_{\mathbf{k}+\mathbf{q}, \mathbf{k}'+\mathbf{q}'}}{z - \epsilon_-(\mathbf{Q}/2 + \mathbf{p}) - \epsilon_-(\mathbf{Q}/2 - \mathbf{p})} \times \\ \sum_{\mathbf{k}_5 + \mathbf{k}_6 = \mathbf{k}_7 + \mathbf{k}_8} \Delta(\gamma_5, \gamma_6, \gamma_7, \gamma_8) \Lambda(\mathbf{p}'') \left\langle 0 \right| d_{\mathbf{q}'} d_{\mathbf{k}'} d^\dagger_{\mathbf{k}_8} d^\dagger_{\mathbf{k}_7} d_{\mathbf{k}_6} d_{\mathbf{k}_5} d^\dagger_{\mathbf{Q}/2+\mathbf{p}} d^\dagger_{\mathbf{Q}/2-\mathbf{p}} \left| 0 \right\rangle \\ \sum_{\mathbf{k}_1 + \mathbf{k}_2 = \mathbf{k}_3 + \mathbf{k}_4} \Delta(\gamma_1, \gamma_2, \gamma_3, \gamma_4) \Lambda(\mathbf{p}') \left\langle 0 \right| d_{\mathbf{Q}/2-\mathbf{p}} d_{\mathbf{Q}/2+\mathbf{p}} d^\dagger_{\mathbf{k}_4} d^\dagger_{\mathbf{k}_3} d_{\mathbf{k}_2} d_{\mathbf{k}_1} d^\dagger_{\mathbf{k}} d^\dagger_{\mathbf{q}} \left| 0 \right\rangle, \end{aligned} \tag{4.28}$$

where the relative momentum are given by $\mathbf{p}' = (\mathbf{k}_2 - \mathbf{k}_1)/2$, and $\mathbf{p}'' = (\mathbf{k}_6 - \mathbf{k}_5)/2$. As explained at the end of Sec. 4.2.1 there are certain contractions that do not contribute to the T-matrix, therefore we will not compute them. We name the two vacuum expectation values in Eq. (4.28) as $\langle T_1^{(2)} \rangle$ and $\langle T_2^{(2)} \rangle$, respectively. From the first vacuum expectation value we have

$$\begin{aligned} \langle T_1^{(2)} \rangle = \sum_{\mathbf{k}_5 + \mathbf{k}_6 = \mathbf{k}_7 + \mathbf{k}_8} \Delta(\gamma_5, \gamma_6, \gamma_7, \gamma_8) \Lambda(\mathbf{p}'') \left(\delta_{\mathbf{k}_8, \mathbf{k}'} \delta_{\mathbf{k}_7, \mathbf{q}'} - \delta_{\mathbf{k}_8, \mathbf{q}'} \delta_{\mathbf{k}_7, \mathbf{k}'} \right) \times \\ \left(\delta_{\mathbf{k}_6, \mathbf{Q}/2-\mathbf{p}} \delta_{\mathbf{k}_5, \mathbf{Q}/2+\mathbf{p}} - \delta_{\mathbf{k}_6, \mathbf{Q}/2+\mathbf{p}} \delta_{\mathbf{k}_5, \mathbf{Q}/2-\mathbf{p}} \right), \end{aligned} \tag{4.29}$$

which yields

$$\begin{aligned}\langle T_1^{(2)}\rangle =&4 \sum_{\mathbf{k}_5+\mathbf{k}_6=\mathbf{k}_7+\mathbf{k}_8} \Delta\left(\gamma_5,\gamma_6,\gamma_7,\gamma_8\right)\Lambda\left(\mathbf{p}''\right)\delta_{\mathbf{k}_5,\mathbf{Q}/2+\mathbf{p}}\delta_{\mathbf{k}_6,\mathbf{Q}/2-\mathbf{p}}\delta_{\mathbf{k}_7,\mathbf{q}'}\delta_{\mathbf{k}_8,\mathbf{k}'}\\ =&4\,\Delta\left(\gamma_{\mathbf{Q}/2+\mathbf{p}},\gamma_{\mathbf{Q}/2-\mathbf{p}},\gamma_{q'},\gamma_{k'}\right)\Lambda\left(\mathbf{p}\right). \end{aligned} \tag{4.30}$$

For the second vacuum expectation value in the second Born term, Eq. (4.28), we simply interchange indices as

$$\begin{aligned}\mathbf{q}'&\to\frac{\mathbf{Q}}{2}-\mathbf{p},\\ \mathbf{k}'&\to\frac{\mathbf{Q}}{2}+\mathbf{p},\\ \frac{\mathbf{Q}}{2}+\mathbf{p}&\to\mathbf{k},\\ \frac{\mathbf{Q}}{2}-\mathbf{p}&\to\mathbf{q},\\ \mathbf{p}''&\to\mathbf{p}',\end{aligned} \tag{4.31}$$

and the numerical indices as $\mathbf{k}_4\to\mathbf{k}_8$, $\mathbf{k}_3\to\mathbf{k}_7$, $\mathbf{k}_2\to\mathbf{k}_6$ and $\mathbf{k}_1\to\mathbf{k}_5$ to get to

$$\langle T_2^{(2)}\rangle = 4\,\Delta\left(\gamma_k,\gamma_q,\gamma_{\mathbf{Q}/2-\mathbf{p}},\gamma_{\mathbf{Q}/2+\mathbf{p}}\right)\Lambda\left(\mathbf{p}\right). \tag{4.32}$$

Substituting $\langle T_1^{(2)}\rangle$ and $\langle T_2^{(2)}\rangle$, Eqs. (4.30) and (4.32) respectively, into Eq. (4.28), we obtain the second term in the Born series

$$\begin{aligned}T^{(2)} =&16\,\delta_{\mathbf{k}+\mathbf{q},\mathbf{k}'+\mathbf{q}'}\left(\frac{g_*}{2V}\right)^2\times\\ &\sum_{\mathbf{p}}\Lambda\left(\mathbf{p}\right)\frac{\Delta\left(\gamma_k,\gamma_q,\gamma_{\mathbf{Q}/2-\mathbf{p}},\gamma_{\mathbf{Q}/2+\mathbf{p}}\right)\Delta\left(\gamma_{\mathbf{Q}/2+\mathbf{p}},\gamma_{\mathbf{Q}/2-\mathbf{p}},\gamma_{q'},\gamma_{k'}\right)}{z-\epsilon_-\left(\mathbf{Q}/2+\mathbf{p}\right)-\epsilon_-\left(\mathbf{Q}/2-\mathbf{p}\right)}.\end{aligned} \tag{4.33}$$

The composition property (A.21) of Δ yields

$$\begin{aligned}T^{(2)} =&\delta_{\mathbf{k}+\mathbf{q},\mathbf{k}'+\mathbf{q}'}\left(\frac{2g_*}{V}\right)^2\Delta\left(\gamma_k,\gamma_q,\gamma_{q'},\gamma_{k'}\right)\times\\ &\sum_{\mathbf{p}}\Lambda\left(\mathbf{p}\right)\frac{\Delta\left(\gamma_{\mathbf{Q}/2+\mathbf{p}},\gamma_{\mathbf{Q}/2-\mathbf{p}},\gamma_{\mathbf{Q}/2+\mathbf{p}},\gamma_{\mathbf{Q}/2-\mathbf{p}}\right)}{z-\epsilon_-\left(\mathbf{Q}/2+\mathbf{p}\right)-\epsilon_-\left(\mathbf{Q}/2-\mathbf{p}\right)}.\end{aligned} \tag{4.34}$$

We express $\Delta\left(\gamma_{\mathbf{Q}/2+\mathbf{p}}, \gamma_{\mathbf{Q}/2-\mathbf{p}}, \gamma_{\mathbf{Q}/2+\mathbf{p}}, \gamma_{\mathbf{Q}/2-\mathbf{p}}\right)$ using Eq. (A.20) and we write the sum in Eq. (4.34) as an integral to finally obtain the second term in the Born series

$$T^{(2)} = \delta_{\mathbf{k}+\mathbf{q},\mathbf{k}'+\mathbf{q}'}\left(\frac{g_*}{V}\right)^2 \Delta\left(\gamma_k, \gamma_q, \gamma_{k'}, \gamma_{q'}\right) \times \\ \frac{V}{(2\pi)^3}\int \mathrm{d}\mathbf{p}\, \Lambda\left(\mathbf{p}\right) \frac{1-\cos\left(\gamma_{\mathbf{Q}/2-\mathbf{p}} - \gamma_{\mathbf{Q}/2+\mathbf{p}}\right)}{z - \epsilon_-\left(\mathbf{Q}/2+\mathbf{p}\right) - \epsilon_-\left(\mathbf{Q}/2-\mathbf{p}\right)}. \tag{4.35}$$

Finally, the first and second term in the Born series, Eqs. (4.20) and (4.35) respectively, give the T-matrix to second order in the Born series

$$\left\langle \mathbf{q}', \mathbf{k}' \right| T \left| \mathbf{k}, \mathbf{q} \right\rangle = \delta_{\mathbf{k}+\mathbf{q},\mathbf{k}'+\mathbf{q}'} \frac{2g_*}{V} \Delta\left(\gamma_q, \gamma_k, \gamma_{k'}, \gamma_{q'}\right) \\ \times \left[1 - \frac{g_*}{2}\int \frac{\mathrm{d}\mathbf{p}}{(2\pi)^3} \Lambda\left(\mathbf{p}\right) \frac{1-\cos\left(\gamma_{\mathbf{Q}/2-\mathbf{p}} - \gamma_{\mathbf{Q}/2+\mathbf{p}}\right)}{z - \epsilon_-\left(\mathbf{Q}/2+\mathbf{p}\right) - \epsilon_-\left(\mathbf{Q}/2-\mathbf{p}\right)}\right]. \tag{4.36}$$

4.2.3 Logarithmic divergence

The single-channel T-matrix (4.36) contains a genuine linear UV divergence coming from the zero-range s-wave interaction and a logarithmic UV divergence caused by considering only the negative helicity branch [27]. In this section we will explicitly compute the linear and logarithmic UV divergences in Eq. (4.36). To show the linear UV divergence we remove the Tan-Valiente distribution from Eq. (4.36). The integral reads

$$\int \frac{\mathrm{d}\mathbf{p}}{(2\pi)^3} \frac{1-\cos\left(\gamma_{\mathbf{Q}/2-\mathbf{p}} - \gamma_{\mathbf{Q}/2+\mathbf{p}}\right)}{z - \epsilon_-\left(\mathbf{Q}/2+\mathbf{p}\right) - \epsilon_-\left(\mathbf{Q}/2-\mathbf{p}\right)}. \tag{4.37}$$

Let us first rewrite the denominator in Eq. (4.37) using Eq. (2.57). For $|\mathbf{p}| \gg |\mathbf{Q}_\perp|/2$ we have

$$\epsilon_-\left(\frac{\mathbf{Q}}{2} \pm \mathbf{p}\right) = \frac{\hbar^2}{2m}\left[\left(\left|\frac{\mathbf{Q}_\perp}{2} \pm \mathbf{p}_\perp\right| - \lambda\right)^2 + \left(\frac{q_z}{2} \pm p_z\right)^2\right] \\ \approx \frac{\hbar^2}{2m}\left[\left(p_\perp - \lambda\right)^2 + p_z^2\right]. \tag{4.38}$$

In cylindrical coordinates the identity $k_x + ik_y = k_\perp e^{i\gamma_k}$ allows us to write

$$\frac{Q_\perp}{2} e^{i\gamma_Q} \pm p_\perp e^{i\gamma_p} = e^{i\gamma_{\mathbf{Q}/2\pm\mathbf{p}}}\left|\frac{\mathbf{Q}_\perp}{2} \pm \mathbf{p}_\perp\right|, \tag{4.39}$$

hence the product $e^{i\gamma_{\mathbf{Q}/2+\mathbf{p}}}e^{-i\gamma_{\mathbf{Q}/2-\mathbf{p}}}$ reads

$$\begin{aligned} e^{i\gamma_{\mathbf{Q}/2+\mathbf{p}}}e^{-i\gamma_{\mathbf{Q}/2-\mathbf{p}}} &= \frac{\left(\frac{Q_\perp}{2}e^{i\gamma_Q}-p_\perp e^{i\gamma_p}\right)}{\left|\frac{\mathbf{Q}_\perp}{2}-\mathbf{k}_\perp\right|}\frac{\left(\frac{Q_\perp}{2}e^{-i\gamma_Q}+p_\perp e^{-i\gamma_p}\right)}{\left|\frac{\mathbf{Q}_\perp}{2}+\mathbf{p}_\perp\right|} \\ &= \frac{\frac{Q_\perp^2}{4}-p_\perp^2+iQ_\perp p_\perp\sin\left(\gamma_Q-\gamma_p\right)}{\left|\frac{\mathbf{Q}_\perp}{2}-\mathbf{p}_\perp\right|\left|\frac{\mathbf{Q}_\perp}{2}+\mathbf{p}_\perp\right|}. \end{aligned} \tag{4.40}$$

The cosine in Eq. (4.37) is written as

$$\cos\left(\gamma_{\mathbf{Q}/2-\mathbf{p}}-\gamma_{\mathbf{Q}/2+\mathbf{p}}\right)=\frac{\frac{Q_\perp^2}{4}-p_\perp^2}{\left|\frac{\mathbf{Q}_\perp}{2}-\mathbf{p}_\perp\right|\left|\frac{\mathbf{Q}_\perp}{2}+\mathbf{p}_\perp\right|}, \tag{4.41}$$

or alternatively as a function of the angles γ_Q and γ_p

$$\cos\left(\gamma_{\mathbf{Q}/2-\mathbf{p}}-\gamma_{\mathbf{Q}/2+\mathbf{p}}\right)=\frac{\frac{Q_\perp^2}{4}-p_\perp^2}{\sqrt{\left(\frac{Q_\perp^2}{4}+p_\perp^2\right)^2-p_\perp^2Q_\perp^2\cos^2\left(\gamma_p-\gamma_Q\right)}}. \tag{4.42}$$

For large values of the in-plane wave vector $p_\perp$ the cosine in Eq. (4.42) tends to -1 and the single-particle energy can be written as Eq. (4.38), substituting these two results into Eq. (4.37) gives

$$\begin{aligned} \frac{2m}{\hbar^2}\int^\Lambda\frac{\mathrm{d}\mathbf{p}}{(2\pi)^3}\frac{1}{\left(p_\perp-\lambda\right)^2+p_z^2} &= \frac{m}{\hbar^2}\int^\Lambda\frac{\mathrm{d}p_\perp p_\perp}{2\pi}\int\frac{\mathrm{d}p_z}{2\pi}\frac{1}{\left(p_\perp-\lambda\right)^2+p_z^2} \\ &= \frac{m}{2\hbar^2}\int^\Lambda\frac{\mathrm{d}p_\perp}{2\pi}\frac{p_\perp}{p_\perp-\lambda} \\ &= \frac{m}{4\pi\hbar^2}\left(\Lambda+\lambda\ln\frac{\Lambda}{\Lambda_0}\right), \end{aligned} \tag{4.43}$$

where Λ is the high momentum cutoff and Λ_0 is a finite, arbitrary momentum scale with the only purpose of rendering the argument of the logarithm dimensionless. Therefore the *T*-matrix for large cutoff Λ behaves as

$$\frac{T^*}{g_*\Delta}\sim 1-\frac{g_*m}{16\pi\hbar^2}\left(\Lambda+\lambda\ln\frac{\Lambda}{\Lambda_0}\right). \tag{4.44}$$

The linear divergence in Eq. (4.44) can be removed using the Tan-Valiente distribution, Eq. (3.47), while the logarithmic divergence will be absorbed by the coupling constant.

4.3 Renormalization of the coupling constant

In this section we renormalise the coupling constant to cure the logarithmic divergence in the single-channel T-matrix, Eq. (4.36). We use the divergence-free multichannel T-matrix computed in [27] as the renormalisation condition, Eq. (3.30), while the linear divergence is renormalised by means of the Tan-Valiente distribution, Sec. 3.2.2.

Ozawa and Baym proved that the T-matrix for a Rashba-coupled Fermi gas does not have logarithmic UV-divergences when both branches are considered [27]. The exact divergence-free T-matrix is

$$\left\langle \mathbf{q}', \mathbf{k}' \right| T \left| \mathbf{k}, \mathbf{q} \right\rangle = \frac{g\Delta\left(\gamma_q, \gamma_k, \gamma_{k'}, \gamma_{q'}\right)}{1 + \frac{mg\lambda\hbar}{4\pi}\mathcal{F}\left(\frac{\mathbf{Q}}{2}\right)}, \tag{4.45}$$

where $g = 4\pi a/m$ is the renormalised coupling constant, with a the s-wave scattering length. The function $\mathcal{F}$ is given by

$$\mathcal{F}\left(\frac{\mathbf{Q}}{2}\right) = \frac{\pi}{m\lambda\hbar}\int \frac{\mathrm{d}\mathbf{p}}{(2\pi)^3}\Lambda\left(\mathbf{p}\right)\left[\frac{1-\cos\left(\gamma_{\mathbf{Q}/2-\mathbf{p}} - \gamma_{\mathbf{Q}/2+\mathbf{p}}\right)}{\epsilon_-\left(\frac{\mathbf{Q}}{2}-\mathbf{p}\right) + \epsilon_-\left(\frac{\mathbf{Q}}{2}+\mathbf{p}\right)}\right.$$
$$\left. + \frac{1-\cos\left(\gamma_{\mathbf{Q}/2-\mathbf{p}} - \gamma_{\mathbf{Q}/2+\mathbf{p}}\right)}{\epsilon_+\left(\frac{\mathbf{Q}}{2}-\mathbf{p}\right) + \epsilon_+\left(\frac{\mathbf{Q}}{2}+\mathbf{p}\right)} + 2\frac{1+\cos\left(\gamma_{\mathbf{Q}/2-\mathbf{p}} - \gamma_{\mathbf{Q}/2+\mathbf{p}}\right)}{\epsilon_-\left(\frac{\mathbf{Q}}{2}+\mathbf{p}\right) + \epsilon_+\left(\frac{\mathbf{Q}}{2}-\mathbf{p}\right)}\right]. \tag{4.46}$$

As explained in Sec. 3.2.1, the renormalisation condition, Eq. (3.30), is given by the exact divergence-free T-matrix, Eq. (4.45), at zero-energy, which means setting $z = 0$ in the denominator of the Green's function. We begin the renormalisation process by expanding the bare coupling constant g_* in powers of its renormalised counterpart g

$$g_*(\lambda, Q) = g + \alpha_{\lambda,Q}g^2 + \mathcal{O}(g^3), \tag{4.47}$$

where $\alpha_{\lambda,Q}$ is an unknown function of the CM momentum $\hbar\mathbf{Q}$ and spin-orbit coupling constant λ. The divergence-free T-matrix, Eq. (4.45), to first order in g reads

$$\left\langle \mathbf{q}', \mathbf{k}' \right| T \left| \mathbf{k}, \mathbf{q} \right\rangle \approx g\Delta\left(\gamma_q, \gamma_k, \gamma_{k'}, \gamma_{q'}\right)\left[1 - \frac{mg\lambda\hbar}{4\pi}\mathcal{F}\left(\frac{\mathbf{Q}}{2}\right) + \mathcal{O}\left(g^2\right)\right]. \tag{4.48}$$

We substitute now the expansion of the bare coupling g_* in terms of the renormalised

coupling g, Eq. (4.47), into the single-channel UV-divergent T-matrix given by Eq. (4.36)

$$\left\langle \mathbf{q}', \mathbf{k}' \right| T^* \left| \mathbf{k}, \mathbf{q} \right\rangle = \left(g + \alpha_{\lambda,Q} g^2\right) \Delta\left(\gamma_q, \gamma_k, \gamma_{k'}, \gamma_{q'}\right) \times \left(1 - \frac{g + \alpha_{\lambda,Q} g^2}{4} \int \frac{\mathrm{d}\mathbf{p}}{(2\pi)^3} \Lambda\left(\mathbf{p}\right) \frac{1 - \cos\left(\gamma_{\mathbf{Q}/2-\mathbf{p}} - \gamma_{\mathbf{Q}/2+\mathbf{p}}\right)}{\epsilon_-\left(\frac{\mathbf{Q}}{2} - \mathbf{p}\right) + \epsilon_-\left(\frac{\mathbf{Q}}{2} + \mathbf{p}\right)}\right) + \mathcal{O}\left(g_*^3\right). \tag{4.49}$$

Comparing terms to second order in the renormalised coupling constant g between the divergence-free T-matrix, Eq. (4.48), and the single-channel T-matrix in Eq. (4.49) yields

$$-\frac{m\lambda\hbar}{4\pi} \mathcal{F}\left(\frac{\mathbf{Q}}{2}\right) = \alpha_{\lambda,Q} - \frac{1}{4} \int \frac{\mathrm{d}\mathbf{p}}{(2\pi)^3} \Lambda\left(\mathbf{p}\right) \frac{1 - \cos\left(\gamma_{\mathbf{Q}/2-\mathbf{p}} - \gamma_{\mathbf{Q}/2+\mathbf{p}}\right)}{\epsilon_-\left(\frac{\mathbf{Q}}{2} - \mathbf{p}\right) + \epsilon_-\left(\frac{\mathbf{Q}}{2} + \mathbf{p}\right)}. \tag{4.50}$$

Hence, solving Eq. (4.50) for $\alpha_{\lambda,Q}$ gives

$$\alpha_{\lambda,Q} = -\frac{m\lambda\hbar}{4\pi} \mathcal{F}\left(\frac{\mathbf{Q}}{2}\right) + \frac{1}{4} \int \frac{\mathrm{d}\mathbf{p}}{(2\pi)^3} \Lambda\left(\mathbf{p}\right) \frac{1 - \cos\left(\gamma_{\mathbf{Q}/2-\mathbf{p}} - \gamma_{\mathbf{Q}/2+\mathbf{p}}\right)}{\epsilon_-\left(\frac{\mathbf{Q}}{2} - \mathbf{p}\right) + \epsilon_-\left(\frac{\mathbf{Q}}{2} + \mathbf{p}\right)}. \tag{4.51}$$

Substituting the definition of $\mathcal{F}$, Eq. (4.46), into the above equation gives a more compact expression for $\alpha_{\lambda,Q}$

$$\alpha_{\lambda,Q} = -\frac{1}{4} \int \frac{\mathrm{d}\mathbf{p}}{(2\pi)^3} \Lambda\left(\mathbf{p}\right) \left[\frac{1 - \cos\left(\gamma_{\mathbf{Q}/2-\mathbf{p}} - \gamma_{\mathbf{Q}/2+\mathbf{p}}\right)}{\epsilon_+\left(\frac{\mathbf{Q}}{2} - \mathbf{k}\right) + \epsilon_+\left(\frac{\mathbf{Q}}{2} + \mathbf{k}\right)} + 2\frac{1 + \cos\left(\gamma_{\mathbf{Q}/2-\mathbf{p}} - \gamma_{\mathbf{Q}/2+\mathbf{p}}\right)}{\epsilon_-\left(\frac{\mathbf{Q}}{2} + \mathbf{k}\right) + \epsilon_+\left(\frac{\mathbf{Q}}{2} - \mathbf{k}\right)}\right]. \tag{4.52}$$

The integrals in Eq. (4.52) are of the same kind as that in Eq. (4.37), which we proved to be divergent. Hence $\alpha_{\lambda,Q}$ is a logarithmically divergent function that will cancel the logarithmic divergence in the renormalised single-channel T-matrix (4.49). We now rearrange the renormalised single-channel T-matrix to second order in g, Eq. (4.49), as

$$\left\langle \mathbf{q}', \mathbf{k}' \right| T^* \left| \mathbf{k}, \mathbf{q} \right\rangle = g\Delta\left(\gamma_q, \gamma_k, \gamma_{k'}, \gamma_{q'}\right) \times \left[1 + \alpha_{\lambda,Q} g - \frac{g}{4} \int \frac{\mathrm{d}\mathbf{p}}{(2\pi)^3} \Lambda\left(\mathbf{p}\right) \frac{1 - \cos\left(\gamma_{\mathbf{Q}/2-\mathbf{p}} - \gamma_{\mathbf{Q}/2+\mathbf{p}}\right)}{\epsilon_-\left(\frac{\mathbf{Q}}{2} - \mathbf{p}\right) + \epsilon_-\left(\frac{\mathbf{Q}}{2} + \mathbf{p}\right)}\right]. \tag{4.53}$$

Substituting the expression for $\alpha_{\lambda,Q}$, Eq. (4.51), into Eq. (4.53) yields

$$\left\langle \mathbf{q}', \mathbf{k}' \right| T^* \left| \mathbf{k}, \mathbf{q} \right\rangle = g\Delta\left(\gamma_q, \gamma_k, \gamma_{k'}, \gamma_{q'}\right) \left[1 - \frac{mg\lambda\hbar}{4\pi} \mathcal{F}\left(\frac{\mathbf{Q}}{2}\right)\right]. \tag{4.54}$$

The renormalised single-channel T-matrix corresponds to the weak coupling expansion of the multichannel T-matrix (4.48).

4.4 Energy of the interacting Rashba-coupled Fermi gas

The energy of a Rashba-coupled Fermi gas changes when contact s-wave interactions are included. We now compute the contribution to the energy using perturbation theory to first and second order in the renormalised coupling constant and show that the many-body problem is renormalisable. We also show that the second order term proves to be finite when the renormalised coupling constant g is used.

4.4.1 First order correction

The first order correction to the energy (Hartree-shift) comes from evaluating $\langle \mathrm{FS}| \mathcal{V} |\mathrm{FS}\rangle$. Hence, substituting $\mathcal{V}$, Eq. (4.9), yields

$$\langle \mathrm{FS}| \mathcal{V} |\mathrm{FS}\rangle = \frac{g_*}{2V} \sum_{\mathbf{k}_1+\mathbf{k}_2=\mathbf{k}_3+\mathbf{k}_4} \Delta(\gamma_1,\gamma_2,\gamma_3,\gamma_4)\, \Lambda(\mathbf{p})\, \langle \mathrm{FS}| d^\dagger_{\mathbf{k}_4} d^\dagger_{\mathbf{k}_3} d_{\mathbf{k}_2} d_{\mathbf{k}_1} |\mathrm{FS}\rangle\,, \tag{4.55}$$

where the relative momentum is $\mathbf{p} = (\mathbf{k}_2 - \mathbf{k}_1)/2$. In principle, the four momenta involved in the expectation value in the equation above do not have any restriction besides total momentum conservation. But in order to have a non-vanishing contribution it is necessary that holes are created inside the Fermi sea, hence $\mathbf{k}_1$ and $\mathbf{k}_2$ belong to the Fermi sea. On the other hand, $\mathbf{k}_3$ and $\mathbf{k}_4$ also need to belong to the Fermi sea so the initial state is recovered. Therefore applying Wick's theorem to Eq. (4.55) gives

$$\begin{aligned}
\langle \mathrm{FS}| \mathcal{V} |\mathrm{FS}\rangle =& \frac{g_*}{2V} \sum_{\mathbf{k}_1+\mathbf{k}_2=\mathbf{k}_3+\mathbf{k}_4} \Delta(\gamma_1,\gamma_2,\gamma_3,\gamma_4)\, \Lambda(\mathbf{p}) \\
&\times \langle 0| \left(\overbrace{d^\dagger_{\mathbf{k}_4} d^\dagger_{\mathbf{k}_3} d_{\mathbf{k}_2} d_{\mathbf{k}_1}} - \overbrace{d^\dagger_{\mathbf{k}_4} d^\dagger_{\mathbf{k}_3} d_{\mathbf{k}_2} d_{\mathbf{k}_1}} \right) |0\rangle\, \Theta_I(\mathbf{k}_4)\, \Theta_I(\mathbf{k}_3)\, \Theta_I(\mathbf{k}_2)\, \Theta_I(\mathbf{k}_1) \\
=& \frac{g_*}{2V} \sum_{\mathbf{k}_1+\mathbf{k}_2=\mathbf{k}_3+\mathbf{k}_4} \Delta(\gamma_1,\gamma_2,\gamma_3,\gamma_4)\, \Lambda(\mathbf{p})\, (\delta_{\mathbf{k}_1,\mathbf{k}_4}\delta_{\mathbf{k}_2,\mathbf{k}_3} - \delta_{\mathbf{k}_1,\mathbf{k}_3}\delta_{\mathbf{k}_2,\mathbf{k}_4}) \\
&\times \Theta_I(\mathbf{k}_4)\, \Theta_I(\mathbf{k}_3)\, \Theta_I(\mathbf{k}_2)\, \Theta_I(\mathbf{k}_1)\,,
\end{aligned} \tag{4.56}$$

relabelling the dummy indices in Eq. (4.56) yields

$$E^{(1)} = \frac{g_*}{2V} \sum_{\mathbf{k}_1+\mathbf{k}_2=\mathbf{k}_3+\mathbf{k}_4} \delta_{\mathbf{k}_1,\mathbf{k}_4}\delta_{\mathbf{k}_2,\mathbf{k}_3}\Lambda\left(\mathbf{p}\right)\left[\Delta\left(\gamma_1,\gamma_2,\gamma_3,\gamma_4\right) - \Delta\left(\gamma_1,\gamma_2,\gamma_4,\gamma_3\right)\right] \times \Theta_I\left(\mathbf{k}_4\right)\Theta_I\left(\mathbf{k}_3\right)\Theta_I\left(\mathbf{k}_2\right)\Theta_I\left(\mathbf{k}_1\right). \tag{4.57}$$

The antisymmetry property of Δ, Eq. (A.18), simplifies Eq. (4.57) to

$$E^{(1)} = \frac{g_*}{V} \sum_{\mathbf{k}_1+\mathbf{k}_2=\mathbf{k}_3+\mathbf{k}_4} \delta_{\mathbf{k}_1,\mathbf{k}_4}\delta_{\mathbf{k}_2,\mathbf{k}_3}\Delta\left(\gamma_1,\gamma_2,\gamma_3,\gamma_4\right)\Lambda\left(\mathbf{p}\right)\Theta_I\left(\mathbf{k}_4\right)\Theta_I\left(\mathbf{k}_3\right)\Theta_I\left(\mathbf{k}_2\right)\Theta_I\left(\mathbf{k}_1\right). \tag{4.58}$$

Summing over $\mathbf{k}_2$ and $\mathbf{k}_4$ in Eq. (4.58) gives

$$E^{(1)} = \frac{g_*}{V} \sum_{\mathbf{k}_1,\mathbf{k}_3} \Delta\left(\gamma_1,\gamma_3,\gamma_3,\gamma_1\right)\Lambda\left(\mathbf{p}\right)\Theta_I\left(\mathbf{k}_3\right)\Theta_I\left(\mathbf{k}_1\right). \tag{4.59}$$

Writing the sums in Eq. (4.59) as integrals and using Eq. (A.20) to express Δ as a cosine function gives the energy density

$$\begin{aligned}\frac{E^{(1)}}{V} &= -g_* \int_{\mathrm{FS}} \frac{\mathrm{d}\mathbf{k}_1}{(2\pi)^3} \int_{\mathrm{FS}} \frac{\mathrm{d}\mathbf{k}_3}{(2\pi)^3} \Delta\left(\gamma_1,\gamma_3,\gamma_1,\gamma_3\right) \\ &= \frac{g_*}{4} \int_{\mathrm{FS}} \frac{\mathrm{d}\mathbf{k}_1}{(2\pi)^3} \int_{\mathrm{FS}} \frac{\mathrm{d}\mathbf{k}_3}{(2\pi)^3} \left[1 - \cos\left(\gamma_3 - \gamma_1\right)\right],\end{aligned} \tag{4.60}$$

where the Tan-Valiente distribution is removed as the integrals in the Fermi sea do not yield any UV divergence. The integral involving the cosine function in Eq. (4.60) vanishes when the angular integral is performed. Therefore, the energy reads

$$\begin{aligned}\frac{E^{(1)}}{V} &= \frac{g_*}{4}\left[\int_{\mathrm{FS}} \frac{\mathrm{d}\mathbf{k}}{(2\pi)^3}\right]^2 \\ &= \frac{g_*}{4}\rho^2.\end{aligned} \tag{4.61}$$

The first order correction in perturbation theory to the energy gives a constant term which is proportional to the bare coupling g_* and the density of the Rashba-coupled Fermi gas, Eq. (2.73). The renormalisation condition, Eq. (4.47), to first order imposes $g_* = g$, hence the energy density reads

$$\frac{E^{(1)}}{V} = \frac{g}{4}\rho^2. \tag{4.62}$$

The noninteracting ground state energy (2.78) and the first correction (4.62) give a total energy for the system

$$\frac{E}{V} = \left(\frac{\pi\hbar^2}{m\lambda} + \frac{g}{4}\right)\rho^2. \tag{4.63}$$

4.4.2 Second order correction

The energy to second order in the renormalised coupling constant g comes from two different contributions. The renormalisation process to second order, Eq. (3.35), yields a divergent term of order g^2 in the renormalised coupling constant. On the other hand, second order perturbation theory in g_*^2 gives another logarithmically-divergent term of order g^2 when the bare coupling constant is substituted by its renormalised counterpart. As we will show, the energy to second order in the renormalised coupling is finite.

We start by computing the contribution to the energy from the renormalisation process. Substituting Eq. (4.47), into the interacting Hamiltonian (4.9) yields

$$\mathcal{V} = \sum_{\mathbf{k}_1+\mathbf{k}_2=\mathbf{k}_3+\mathbf{k}_4} \frac{g+\alpha_{\lambda,Q}g^2}{2V}\Delta\left(\gamma_1,\gamma_2,\gamma_3,\gamma_4\right)\Lambda\left(\mathbf{p}\right) d^\dagger_{\mathbf{k}_4} d^\dagger_{\mathbf{k}_3} d_{\mathbf{k}_2} d_{\mathbf{k}_1}, \tag{4.64}$$

where $\mathbf{p} = \left(\mathbf{k}_2 - \mathbf{k}_1\right)/2$ is the relative momentum. Equation (4.64) yields two terms, one proportional to g, Eq. (4.62), the other proportional to g^2

$$E_1^{(2)} = \frac{g^2}{2V}\sum_{\mathbf{k}_1+\mathbf{k}_2=\mathbf{k}_3+\mathbf{k}_4} \alpha_{\lambda,Q}\Delta\left(\gamma_1,\gamma_2,\gamma_3,\gamma_4\right)\Lambda\left(\mathbf{p}\right) \langle \mathrm{FS}| d^\dagger_{\mathbf{k}_4} d^\dagger_{\mathbf{k}_3} d_{\mathbf{k}_2} d_{\mathbf{k}_1} |\mathrm{FS}\rangle \\ \times \Theta_I\left(\mathbf{k}_4\right)\Theta_I\left(\mathbf{k}_3\right)\Theta_I\left(\mathbf{k}_2\right)\Theta_I\left(\mathbf{k}_1\right). \tag{4.65}$$

Performing the same steps and calculations as in Sec. 4.4.1 we obtain

$$\frac{E_1^{(2)}}{V} = \frac{g^2}{4}\int_{\mathrm{FS}}\frac{\mathrm{d}\mathbf{k}_1}{(2\pi)^3}\int_{\mathrm{FS}}\frac{\mathrm{d}\mathbf{k}_3}{(2\pi)^3}\alpha_{\lambda,Q}\Lambda\left(\mathbf{p}\right)\left[1-\cos\left(\gamma_3-\gamma_1\right)\right]. \tag{4.66}$$

The above equation is logarithmically divergent due to the presence of $\alpha_{\lambda,Q}$. Performing the integration in Eq. (4.66) yields

$$\frac{E_1^{(2)}}{V} = \frac{g^2}{4}\rho^2\alpha_{\lambda,Q}. \tag{4.67}$$

Substituting $\alpha_{\lambda,Q}$, Eq. (4.52), into Eq. (4.67) gives

$$\frac{E_1^{(2)}}{V} = -\frac{g^2\rho^2}{16}\int \frac{\mathrm{d}\mathbf{p}}{(2\pi)^3}\Lambda\left(\mathbf{p}\right) \times \left[\frac{1-\cos\left(\gamma_{\mathbf{Q}/2-\mathbf{p}}-\gamma_{\mathbf{Q}/2+\mathbf{p}}\right)}{\epsilon_+\left(\frac{\mathbf{Q}}{2}-\mathbf{p}\right)+\epsilon_+\left(\frac{\mathbf{Q}}{2}+\mathbf{p}\right)} + 2\frac{1+\cos\left(\gamma_{\mathbf{Q}/2-\mathbf{p}}-\gamma_{\mathbf{Q}/2+\mathbf{p}}\right)}{\epsilon_-\left(\frac{\mathbf{Q}}{2}+\mathbf{p}\right)+\epsilon_+\left(\frac{\mathbf{Q}}{2}-\mathbf{p}\right)}\right]. \quad (4.68)$$

Since it will show useful, we perform the integral in Eq. (4.68) for large in-plane momentum $|\mathbf{p}_\perp| \gg |\mathbf{Q}_\perp|/2$. Therefore, Eq. (4.68) gives

$$\frac{E_1^{(2)}}{V} \approx -\frac{1}{2}\left(\frac{g\rho}{2}\right)^2 \int^{\Lambda} \frac{\mathrm{d}\mathbf{p}}{(2\pi)^3}\Lambda\left(\mathbf{p}\right)\frac{1}{\left(p_\perp-\lambda\right)^2+p_z^2}, \quad (4.69)$$

which, obviously, is the same integral as in Eq. (4.43).

The remaining contribution to the energy in order g^2 comes from calculating the second order correction to the energy in perturbation theory. In this case, we obtain a correction to the energy proportional to g_*^2. Imposing the renormalisation condition to first order in the coupling ($g_* \approx g$) yields a second order correction in g^2. Let us begin by writing the second order correction to the energy

$$E_2^{(2)} = \sum_{|n\rangle\notin \mathrm{FS}} \frac{\left|\langle \mathrm{FS}|\,\mathcal{V}\,|n\rangle\right|^2}{E_0-\epsilon_n}, \quad (4.70)$$

where E_0 is the energy of the ground state (2.78), and ϵ_n is the energy associated to the intermediate state $|n\rangle$, which is different from the Fermi sea. The intermediate state consists of two particles ejected from the Fermi sea, hence their momenta are not inside the Fermi sea, plus two holes created in the Fermi sea, with their corresponding momenta inside the Fermi sea. The two particle-two hole state is represented as

$$|n\rangle = \Theta_O\left(\mathbf{k}\right)\Theta_O\left(\mathbf{q}\right)\Theta_I\left(\mathbf{k}'\right)\Theta_I\left(\mathbf{q}'\right) d_{\mathbf{k}}^\dagger d_{\mathbf{q}}^\dagger d_{\mathbf{k}'} d_{\mathbf{q}'}\,|\mathrm{FS}\rangle\,. \quad (4.71)$$

The energy of the excited state corresponds to the energy of the ground state E_0, Eq. (2.78), plus the energy of the two particles minus the energy of the two holes

$$\epsilon_n = E_0 + \epsilon_-\left(\mathbf{k}\right) + \epsilon_-\left(\mathbf{q}\right) - \epsilon_-\left(\mathbf{k}'\right) - \epsilon_-\left(\mathbf{q}'\right). \quad (4.72)$$

The matrix element in Eq. (4.70) reads

$$\begin{aligned}\langle \mathrm{FS}|\,\mathcal{V}\,|n\rangle = \frac{g_*}{2V}\sum_{\mathbf{k}_1+\mathbf{k}_2=\mathbf{k}_3+\mathbf{k}_4}&\Delta\left(\gamma_1,\gamma_2,\gamma_3,\gamma_4\right)\Lambda\left(\mathbf{p}\right)\\ &\times\langle \mathrm{FS}|\,d^\dagger_{\mathbf{k}_4}d^\dagger_{\mathbf{k}_3}d_{\mathbf{k}_2}d_{\mathbf{k}_1}d^\dagger_{\mathbf{k}}d^\dagger_{\mathbf{q}}d_{\mathbf{k}'}d_{\mathbf{q}'}\,|\mathrm{FS}\rangle\,\Theta_O\left(\mathbf{k}\right)\Theta_O\left(\mathbf{q}\right)\Theta_I\left(\mathbf{k}'\right)\Theta_I\left(\mathbf{q}'\right),\end{aligned}\tag{4.73}$$

where $\mathbf{p}=\left(\mathbf{k}_2-\mathbf{k}_1\right)/2$ is the relative momenta. The non-vanishing contractions that come from applying Wick's theorem to the matrix element in Eq. (4.73) are

$$\langle \mathrm{FS}|\,d^\dagger_{\mathbf{k}_4}d^\dagger_{\mathbf{k}_3}d_{\mathbf{k}_2}d_{\mathbf{k}_1}d^\dagger_{\mathbf{k}}d^\dagger_{\mathbf{q}}d_{\mathbf{k}'}d_{\mathbf{q}'}\,|\mathrm{FS}\rangle = \left(\delta_{\mathbf{k},\mathbf{k}_1}\delta_{\mathbf{q},\mathbf{k}_2}-\delta_{\mathbf{k},\mathbf{k}_2}\delta_{\mathbf{q},\mathbf{k}_1}\right)\left(\delta_{\mathbf{k}',\mathbf{k}_3}\delta_{\mathbf{q}',\mathbf{k}_4}-\delta_{\mathbf{k}',\mathbf{k}_4}\delta_{\mathbf{q}',\mathbf{k}_3}\right).\tag{4.74}$$

Inserting Eq. (4.74) into Eq. (4.73) gives

$$\begin{aligned}\langle \mathrm{FS}|\,\mathcal{V}\,|n\rangle =&\frac{g_*}{2V}\sum_{\mathbf{k}_1+\mathbf{k}_2=\mathbf{k}_3+\mathbf{k}_4}\Delta\left(\gamma_1,\gamma_2,\gamma_3,\gamma_4\right)\Lambda\left(\mathbf{p}\right)\left[\delta_{\mathbf{k},\mathbf{k}_1}\delta_{\mathbf{q},\mathbf{k}_2}-\delta_{\mathbf{k},\mathbf{k}_2}\delta_{\mathbf{q},\mathbf{k}_1}\right]\\ &\times\left[\delta_{\mathbf{k}',\mathbf{k}_3}\delta_{\mathbf{q}',\mathbf{k}_4}-\delta_{\mathbf{k}',\mathbf{k}_4}\delta_{\mathbf{q}',\mathbf{k}_3}\right]\Theta_O\left(\mathbf{k}\right)\Theta_O\left(\mathbf{q}\right)\Theta_I\left(\mathbf{k}'\right)\Theta_I\left(\mathbf{q}'\right)\\ =&\frac{g_*}{2V}\sum_{\mathbf{k}_1+\mathbf{k}_2=\mathbf{k}_3+\mathbf{k}_4}\delta_{\mathbf{k},\mathbf{k}_1}\delta_{\mathbf{q},\mathbf{k}_2}\delta_{\mathbf{k}',\mathbf{k}_3}\delta_{\mathbf{q}',\mathbf{k}_4}\Lambda\left(\mathbf{p}\right)\Big[\Delta\left(\gamma_1,\gamma_2,\gamma_3,\gamma_4\right)-\Delta\left(\gamma_1,\gamma_2,\gamma_4,\gamma_3\right)\\ &-\Delta\left(\gamma_2,\gamma_1,\gamma_3,\gamma_4\right)+\Delta\left(\gamma_2,\gamma_1,\gamma_4,\gamma_3\right)\Big]\Theta_O\left(\mathbf{k}\right)\Theta_O\left(\mathbf{q}\right)\Theta_I\left(\mathbf{k}'\right)\Theta_I\left(\mathbf{q}'\right)\\ =&\frac{2g_*}{V}\Delta\left(\gamma_k,\gamma_q,\gamma_{q'},\gamma_{k'}\right)\Lambda\left(\mathbf{p}\right)\Theta_O\left(\mathbf{k}\right)\Theta_O\left(\mathbf{q}\right)\Theta_I\left(\mathbf{k}'\right)\Theta_I\left(\mathbf{q}'\right),\end{aligned}\tag{4.75}$$

where Eq. (A.18) has been used. Substituting the matrix element (4.75) into the expression for the energy at second order, Eq. (4.70), yields

$$\begin{aligned}E_2^{(2)}=&\sum_{|n\rangle\notin\mathrm{FS}}\frac{\langle \mathrm{FS}|\,\mathcal{V}\,|n\rangle\,\langle n|\,\mathcal{V}\,|\mathrm{FS}\rangle}{E_0-\epsilon_n}\\ =&\left(\frac{2g_*}{V}\right)^2\sum_{|n\rangle\notin\mathrm{FS}}\Lambda\left(\mathbf{p}\right)\frac{\Delta\left(\gamma_k,\gamma_q,\gamma_{q'},\gamma_{k'}\right)\Delta\left(\gamma_{k'},\gamma_{q'},\gamma_q,\gamma_k\right)}{\epsilon_-\left(\mathbf{k}\right)+\epsilon_-\left(\mathbf{q}\right)-\epsilon_-\left(\mathbf{k}'\right)-\epsilon_-\left(\mathbf{q}'\right)}\\ &\times\Theta_O\left(\mathbf{k}\right)\Theta_O\left(\mathbf{q}\right)\Theta_I\left(\mathbf{k}'\right)\Theta_I\left(\mathbf{q}'\right)\\ =&-\left(\frac{2g_*}{V}\right)^2\frac{1}{16}\sum_{|n\rangle\notin\mathrm{FS}}\Lambda\left(\mathbf{p}\right)\frac{\left[1-\cos\left(\gamma_k-\gamma_q\right)\right]\left[1-\cos\left(\gamma_{k'}-\gamma_{q'}\right)\right]}{\epsilon_-\left(\mathbf{k}\right)+\epsilon_-\left(\mathbf{q}\right)-\epsilon_-\left(\mathbf{k}'\right)-\epsilon_-\left(\mathbf{q}'\right)}\\ &\times\Theta_O\left(\mathbf{k}\right)\Theta_O\left(\mathbf{q}\right)\Theta_I\left(\mathbf{k}'\right)\Theta_I\left(\mathbf{q}'\right).\end{aligned}\tag{4.76}$$

To make Eq. (4.76) more compact we introduce the following notation

$$\mathcal{C}_{\mathbf{k},\mathbf{q}} = 1 - \cos\left(\gamma_k - \gamma_q\right), \tag{4.77}$$

$$\epsilon_-\left(\mathbf{k},\mathbf{q},\mathbf{k}',\mathbf{q}'\right) = \epsilon_-\left(\mathbf{k}\right) + \epsilon_-\left(\mathbf{q}\right) - \epsilon_-\left(\mathbf{k}'\right) - \epsilon_-\left(\mathbf{q}'\right). \tag{4.78}$$

We also make explicit the conservation of momentum by including $\delta_{\mathbf{k}+\mathbf{q},\mathbf{k}'+\mathbf{q}'}$ in Eq. (4.76). Hence we get to

$$E_2^{(2)} = -\left(\frac{g_*}{2V}\right)^2 \sum_{|n\rangle\notin \mathrm{FS}} \delta_{\mathbf{k}+\mathbf{q},\mathbf{k}'+\mathbf{q}'} \Lambda\left(\mathbf{p}\right) \frac{\mathcal{C}_{\mathbf{k},\mathbf{q}}\mathcal{C}_{\mathbf{k}',\mathbf{q}'}}{\epsilon_-\left(\mathbf{k},\mathbf{q},\mathbf{k}',\mathbf{q}'\right)} \times \Theta_O\left(\mathbf{k}\right)\Theta_O\left(\mathbf{q}\right)\Theta_I\left(\mathbf{k}'\right)\Theta_I\left(\mathbf{q}'\right). \tag{4.79}$$

Performing the sum in $\mathbf{k}$ in Eq. (4.79) yields

$$E_2^{(2)} = -\left(\frac{g_*}{2V}\right)^2 \sum_{\mathbf{q},\mathbf{k}',\mathbf{q}'} \Lambda\left(\mathbf{p}\right) \frac{\mathcal{C}_{\mathbf{q}-\mathbf{k}'-\mathbf{q}',\mathbf{q}}\mathcal{C}_{\mathbf{k}',\mathbf{q}'}}{\epsilon_-\left(\mathbf{q}-\mathbf{k}'-\mathbf{q}',\mathbf{q},\mathbf{k}',\mathbf{q}'\right)} \Theta_O\left(\mathbf{q}\right)\Theta_I\left(\mathbf{k}'\right)\Theta_I\left(\mathbf{q}'\right). \tag{4.80}$$

Writing Eq. (4.80) as an integral and substituting the bare coupling constant g_* for the renormalised coupling constant g (first order renormalisation process, see Eq. (3.34)) gives the energy density to second order in perturbation theory in the thermodynamic limit

$$\frac{E_2^{(2)}}{V} = -\frac{g^2}{4}\int \frac{\mathrm{d}\mathbf{q}}{(2\pi)^3}\int_{\mathrm{FS}} \frac{\mathrm{d}\mathbf{k}'}{(2\pi)^3}\int_{\mathrm{FS}} \frac{\mathrm{d}\mathbf{q}'}{(2\pi)^3} \Lambda\left(\mathbf{p}\right) \frac{\mathcal{C}_{\mathbf{q}-\mathbf{k}'-\mathbf{q}',\mathbf{q}}\mathcal{C}_{\mathbf{k}',\mathbf{q}'}}{\epsilon_-\left(\mathbf{q}-\mathbf{k}'-\mathbf{q}',\mathbf{q},\mathbf{k}',\mathbf{q}'\right)} \Theta_O\left(\mathbf{q}\right). \tag{4.81}$$

For large momentum $|\mathbf{q}| \gg |\mathbf{Q}|/2$, we can write $1/\epsilon_-\left(\mathbf{q}-\mathbf{k}'-\mathbf{q}',\mathbf{q},\mathbf{k}',\mathbf{q}'\right) \approx 1/2\epsilon_-\left(\mathbf{q}\right) + \mathcal{O}\left(\epsilon_-^{-2}\left(\mathbf{q}\right)\right)$ since the remaining momenta $\mathbf{k}'$ and $\mathbf{q}'$ belong to the Fermi sea. Therefore, Eq. (4.81) reads

$$\frac{E_2^{(2)}}{V} \approx -\left(\frac{g\rho}{2}\right)^2 \int^{\Lambda} \frac{\mathrm{d}\mathbf{q}}{(2\pi)^3} \frac{1}{2\epsilon_-\left(\mathbf{q}\right)}, \tag{4.82}$$

which is logarithmic divergent for large values of the momenta. Finally, Eqs. (4.66) and (4.81) give the total energy to order g^2

$$\frac{E_2}{V} = \frac{g^2}{4}\int_{\mathrm{FS}} \frac{\mathrm{d}\mathbf{k}'}{(2\pi)^3}\int_{\mathrm{FS}} \frac{\mathrm{d}\mathbf{q}'}{(2\pi)^3} \mathcal{C}_{\mathbf{k}',\mathbf{q}'} \Lambda\left(\mathbf{p}'\right) \left[\alpha_{\lambda,Q} - \int \frac{\mathrm{d}\mathbf{q}}{(2\pi)^3} \Lambda\left(\mathbf{p}\right) \frac{\mathcal{C}_{\mathbf{q}-\mathbf{k}'-\mathbf{q}',\mathbf{q}'}}{\epsilon_-\left(\mathbf{k},\mathbf{q},\mathbf{k}',\mathbf{q}'\right)} \Theta_O\left(\mathbf{q}\right)\right]. \tag{4.83}$$

Equation (4.83) is finite for large relative momentum since the combination of Eq. (4.69)

and Eq. (4.82) yield a finite correction to the energy

$$\frac{E_1^{(2)}+E_2^{(2)}}{V} \approx -\frac{1}{2}\left(\frac{g\rho}{2}\right)^2 \int^{\Lambda} \frac{\mathbf{dp}}{(2\pi)^3}\Lambda\left(\mathbf{p}\right) \frac{1}{\left(p_\perp-\lambda\right)^2+p_z^2} + \frac{1}{2}\left(\frac{g\rho}{2}\right)^2 \int^{\Lambda} \frac{\mathbf{dq}}{(2\pi)^3}\frac{\Lambda\left(\mathbf{p}\right)}{\epsilon_-\left(\mathbf{q}\right)}. \tag{4.84}$$

4.5 Conclusions

In this Chapter we have introduced a renormalisable theory for interacting fermions subject to a Rashba spin-orbit coupling. The theory is valid in the dilute regime where the fermions in the noninteracting ground state occupy only the lower helicity branch. The effective single-branch model corresponds to interacting fermions in the negative-helicity branch, and thus opens the path to a simpler treatment of the many-body problem, circumventing the intricacies of the full multi-channel system. We showed that the second-order correction to the ground-state energy of the repulsive Rashba-coupled Fermi gas is finite.

As a natural extension of the single-channel theory, it would be interesting to calculate the non-Hermitian optical potential. Solving the single-channel problem with the use of the optical potential yields complex energies that are the same of the multichannel problem when outgoing boundary conditions are imposed in the time-independent Schrödinger equation [73]. The single-channel model may be also of interest for a more sophisticated treatment of the BEC-BCS crossover. In the next Chapter we will apply the single-branch model to compute the effect of applying a Fermi kick onto the system.

Chapter 5

Non-Galilean features of ultracold Rashba-Fermi gases in two dimensions

Landau's Fermi-liquid theory successfully describes Fermi systems when interactions are present. Interactions change the effective mass and the effective coupling of the particle, thus Landau's Fermi-liquid description is based on quasiparticles with different dynamical properties than those in noninteracting systems [74]. Despite Landau's Fermi-liquid theory has been widely applied, it breaks down in the vicinity of quantum critical points [75, 76], to describe copper-based high-temperature superconductors [77, 78], or to predict a phase transition to an insulating spin liquid [79]. Additionally, symmetry-breaking deformations of the Fermi surface are difficult to explain using Landau's Fermi-liquid theory, including Pomeranchuk instabilities [80], where fermion-fermion forward scattering leads to shape deformations of the Fermi surface [81]. It is also possible to induce finite momentum Fermi surface deformations in Rashba-coupled Fermi gases by exploiting the absence of Galilean invariance [29].

In this Chapter we will show how the Fermi surface is deformed when a Galilean boost is applied to a Rashba-coupled Fermi gas. We begin by revising how Galilean invariance breaks down in spin-orbit Rashba-coupled Fermi systems. Then, we show the response of the noninteracting system to an overall momentum kick. We will classify the transformations of the Fermi sea accordingly to the most favourable energy configuration. When interactions are considered, the system will exhibit a phase transition to a finite-momentum ground state. We will conclude with some experimental considerations.

5.1 Galilean invariance

A non-relativistic system is said to have Galilean symmetry if its equations of motion are invariant under a Galilean transformation [82]. The Galileo group is composed by space-time translations, rotations and boosts, hence it is a 10-generator continuous group. If rotations are not considered, a Galilean boost of speed $\mathbf{v}_0$ between two frames of reference moving with respect to each other at constant speed $\mathbf{v}_0$ corresponds to

$$\mathbf{v} \to \mathbf{v} + \mathbf{v}_0. \tag{5.1}$$

Due to the fact that the acceleration does not change, Newtonian laws of motion exhibit Galilean invariance when the velocity is not involved.[1] However, certain quantities depend on the frame of reference. If we apply a Galilean boost to a moving particle, the kinetic energy K changes as

$$K = \frac{1}{2}m\mathbf{v}^2 \to \frac{1}{2}m\left(\mathbf{v}^2 + \mathbf{v}_0^2 + 2\,\mathbf{v}\cdot\mathbf{v}_0\right) = K + K_0 + m\mathbf{v}\cdot\mathbf{v}_0, \tag{5.2}$$

making explicitly the dependance on the frame of reference, where $K_0 = m\mathbf{v}^2/2$.

Quantum mechanically, the effect of a Galilean boost (5.1) into the free particle Hamiltonian can be removed by a gauge transformation, therefore the Heisenberg equation of motion for the creation and annihilation operators are invariant under a Galilean boost. On the other hand, the spin-orbit coupling adds an extra term to the free particle Hamiltonian, Eq. (2.52).

Let us show how to remove the effect of the Galilean boost by a gauge transformation. The free Fermi gas Hamiltonian is

$$\mathcal{H}_0 = \sum_{\mathbf{k},\sigma} \frac{\hbar^2 k^2}{2m} c^\dagger_{\mathbf{k},\sigma} c_{\mathbf{k},\sigma}. \tag{5.3}$$

The equation of motion for the creation operator $c^\dagger_{\mathbf{q},\sigma'}$ in the Heisenberg picture[2] (we

[1] Lorentz's force is a clear example of a force which is not Galilean invariant $\mathbf{F} = q\left(\mathbf{E} + \mathbf{v}\times\mathbf{B}/c\right)$.

[2] A operator $\mathcal{A}$ in the Schrödinger picture is expressed in the Heisenberg picture $\mathcal{A}(t)$ via the transformation $\mathcal{A}(t) = U^\dagger(t)\,\mathcal{A}\,U(t)$, where $U(t) = \exp\left(-i\mathcal{H}t/\hbar\right)$ is the unitary time-evolution operator and $\mathcal{H}$ the Hamiltonian of the system.

make explicit now the time dependance in the operators) is

$$\begin{aligned}\frac{\mathrm{d}}{\mathrm{d}t}c^{\dagger}_{\mathbf{q},\sigma'}(t) &= \frac{i}{\hbar}\left[\mathcal{H}_0, c^{\dagger}_{\mathbf{q},\sigma'}(t)\right] \\ &= \frac{i\hbar}{2m}\sum_{\mathbf{k},\sigma} k^2\left[c^{\dagger}_{\mathbf{k},\sigma}(t)\, c_{\mathbf{k},\sigma}(t), c^{\dagger}_{\mathbf{q},\sigma'}(t)\right] \\ &= \frac{i\hbar}{2m}\sum_{\mathbf{k},\sigma} k^2\delta_{\mathbf{k},\mathbf{q}}\delta_{\sigma,\sigma'}c^{\dagger}_{\mathbf{k},\sigma}(t) \\ &= \frac{i\hbar q^2}{2m}c^{\dagger}_{\mathbf{q},\sigma'}(t)\,. \end{aligned} \tag{5.4}$$

Solving the differential equation yields

$$c^{\dagger}_{\mathbf{q},\sigma'}(t) = e^{i\hbar q^2 t/2m}c^{\dagger}_{\mathbf{q},\sigma'}(0)\,. \tag{5.5}$$

Equation (5.5) gives the usual free particle evolution. Let us assume now that a Galilean boost in the wave vector $\mathbf{k} \to \mathbf{k} + \mathbf{k}_0$ is applied to the system. The Hamiltonian changes to

$$\begin{aligned}\mathcal{H} &= \mathcal{H}_0 + \mathcal{H}_G \\ &= \frac{\hbar^2}{2m}\sum_{\mathbf{k},\sigma}\left(k^2 + k_0^2 + 2\mathbf{k}\cdot\mathbf{k}_0\right)c^{\dagger}_{\mathbf{k},\sigma}c_{\mathbf{k},\sigma}, \end{aligned} \tag{5.6}$$

where the Galilean-boosted Hamiltonian reads

$$\mathcal{H}_G = \frac{\hbar^2}{2m}\sum_{\mathbf{k},\sigma}\left(k_0^2 + 2\mathbf{k}\cdot\mathbf{k}_0\right)c^{\dagger}_{\mathbf{k},\sigma}c_{\mathbf{k},\sigma}. \tag{5.7}$$

The equation of motion for the creation operator changes to

$$\frac{\mathrm{d}}{\mathrm{d}t}c^{\dagger}_{\mathbf{q},\sigma'}(t) = \frac{i}{\hbar}\left[\mathcal{H}_0 + \mathcal{H}_G, c^{\dagger}_{\mathbf{q},\sigma'}(t)\right]. \tag{5.8}$$

Let us analyse the term $\left[\mathcal{H}_G, c^{\dagger}_{\mathbf{q},\sigma'}\right]$ independently. The commutator is given by

$$\begin{aligned}\frac{i}{\hbar}\left[\mathcal{H}_G, c^{\dagger}_{\mathbf{q},\sigma'}(t)\right] &= \frac{i\hbar}{2m}\sum_{\mathbf{k},\sigma}\left(k_0^2 + 2\mathbf{k}\cdot\mathbf{k}_0\right)\left[c^{\dagger}_{\mathbf{k},\sigma}(t)\, c_{\mathbf{k},\sigma}(t), c^{\dagger}_{\mathbf{q},\sigma'}(t)\right] \\ &= \frac{i\hbar}{2m}\left(k_0^2 + 2\mathbf{q}\cdot\mathbf{k}_0\right)c^{\dagger}_{\mathbf{q},\sigma'}(t)\,. \end{aligned} \tag{5.9}$$

Therefore, the Heisenberg equation, Eq. (5.8), for the creation operator reads

$$\frac{\mathrm{d}}{\mathrm{d}t}c^{\dagger}_{\mathbf{q},\sigma'}(t) = \frac{i\hbar}{2m}\left[q^2 + k_0^2 + 2\mathbf{q}\cdot\mathbf{k}_0\right]c^{\dagger}_{\mathbf{q},\sigma'}(t)\,. \tag{5.10}$$

The term $k_0^2 + 2\mathbf{q}\cdot\mathbf{k}_0$ in Eq. (5.10) appears from the effect of the Galilean boost in the free Fermi gas Hamiltonian. It is possible to remove this term from Eq. (5.10) by a gauge transformation

$$c^{\dagger}_{\mathbf{q},\sigma}(t) \to e^{i\mathcal{H}_G t/\hbar}c^{\dagger}_{\mathbf{q},\sigma}(t)\,e^{-i\mathcal{H}_G t/\hbar}. \tag{5.11}$$

In the case of a Rashba-coupled Fermi gas described by the Hamiltonian (2.52), the Heisenberg equation for $c^{\dagger}_{\mathbf{q},\sigma'}$ is

$$\frac{\mathrm{d}}{\mathrm{d}t}c^{\dagger}_{\mathbf{q},\sigma'}(t) = \frac{i}{\hbar}\left[\mathcal{H}_0 + \mathcal{H}_{SO}, c^{\dagger}_{\mathbf{q},\sigma'}(t)\right], \tag{5.12}$$

where the spin-orbit part of the Rashba-coupled Fermi gas Hamiltonian (2.52) is

$$\mathcal{H}_{SO} = \frac{\hbar^2\lambda}{m}\sum_{\mathbf{k}} k_{\perp}\left(e^{-i\gamma_k}c^{\dagger}_{\mathbf{k},\uparrow}c_{\mathbf{k},\downarrow} + e^{i\gamma_k}c^{\dagger}_{\mathbf{k},\downarrow}c_{\mathbf{k},\uparrow}\right). \tag{5.13}$$

Let us expand the commutator in Eq. (5.12) between the creation operator and the spin-orbit Hamiltonian, Eq. (5.13),

$$\begin{aligned}
\left[\mathcal{H}_{SO}, c^{\dagger}_{\mathbf{q},\sigma'}(t)\right] &= \frac{\lambda\hbar^2}{m}\sum_{\mathbf{k}} k_{\perp}\Bigg(e^{-i\gamma_k}\left[c^{\dagger}_{\mathbf{k},\uparrow}(t)\,c_{\mathbf{k},\downarrow}(t), c^{\dagger}_{\mathbf{q},\sigma'}(t)\right] \\
&\qquad + e^{i\gamma_k}\left[c^{\dagger}_{\mathbf{k},\downarrow}(t)\,c_{\mathbf{k},\uparrow}(t), c^{\dagger}_{\mathbf{q},\sigma'}(t)\right]\Bigg) \\
&= \frac{\lambda\hbar^2}{m}\sum_{\mathbf{k}} k_{\perp}\delta_{\mathbf{k},\mathbf{q}}\left[e^{-i\gamma_k}\delta_{\downarrow,\sigma'}c^{\dagger}_{\mathbf{k},\uparrow}(t) + e^{i\gamma_k}\delta_{\uparrow,\sigma'}c^{\dagger}_{\mathbf{k},\downarrow}(t)\right] \\
&= \frac{\lambda\hbar^2}{m}q_{\perp}\left[e^{-i\gamma_q}\delta_{\downarrow,\sigma'}c^{\dagger}_{\mathbf{q},\uparrow}(t) + e^{i\gamma_q}\delta_{\uparrow,\sigma'}c^{\dagger}_{\mathbf{q},\downarrow}(t)\right].
\end{aligned} \tag{5.14}$$

Hence substituting Eq. (5.14) into Eq. (5.12) yields

$$\frac{\mathrm{d}}{\mathrm{d}t}c^{\dagger}_{\mathbf{q},\sigma'}(t) = \frac{i\hbar}{m}\left[\left(q^2+\lambda^2\right)c^{\dagger}_{\mathbf{q},\sigma'}(t) + \lambda q_{\perp}\left(e^{-i\gamma_q}\delta_{\downarrow,\sigma'}c^{\dagger}_{\mathbf{q},\uparrow}(t) + e^{i\gamma_q}\delta_{\uparrow,\sigma'}c^{\dagger}_{\mathbf{q},\downarrow}(t)\right)\right]. \tag{5.15}$$

The information enclosed in Eq. (5.15) is easier to visualise if it is written as a system

$$\frac{\mathrm{d}}{\mathrm{d}t}c^{\dagger}_{\mathbf{q},\uparrow}(t) = \frac{i\hbar}{m}\left[\left(q^2+\lambda^2\right)c^{\dagger}_{\mathbf{q},\uparrow}(t) + \lambda q_{\perp}e^{i\gamma_q}c^{\dagger}_{\mathbf{q},\downarrow}(t)\right], \tag{5.16}$$

$$\frac{\mathrm{d}}{\mathrm{d}t}c^{\dagger}_{\mathbf{q},\downarrow}(t) = \frac{i\hbar}{m}\left[\left(q^2+\lambda^2\right)c^{\dagger}_{\mathbf{q},\downarrow}(t) + \lambda q_{\perp}e^{-i\gamma_q}c^{\dagger}_{\mathbf{q},\uparrow}(t)\right]. \tag{5.17}$$

The spin-orbit couples the dynamics of the different spin-particles. On the other hand, performing a Galilean boost to the spin-orbit Hamiltonian (2.52) gives

$$\mathcal{H}_{SOG} = \mathcal{H}_0 + \mathcal{H}_G + \frac{\hbar^2\lambda}{m}\sum_{\mathbf{k}}\left(k_{\perp}+k_{0,\perp}\right)\left(e^{-i\gamma_{k+k_0}}c^{\dagger}_{\mathbf{k},\uparrow}c_{\mathbf{k},\downarrow} + e^{i\gamma_{k+k_0}}c^{\dagger}_{\mathbf{k},\downarrow}c_{\mathbf{k},\uparrow}\right), \tag{5.18}$$

where the term in third term in the RHS of Eq. (5.18) comes from the Galilean boost applied to Eq. (5.13). There is no gauge transformation like Eq. (5.11) that simultaneously removes the effect of the Galilean boost in the free particle Hamiltonian and in the spin-orbit Hamiltonian. Although for for large spin-orbit coupling, Galilean invariance can be restored at the BEC-BCS crossover [83, 84].

5.2 Conditions and description of the system

Let us apply a momentum kick $\hbar\mathbf{k}_0$ per particle to the Rashba-coupled Fermi gas, so that the total momentum of the system is

$$\hbar\mathbf{Q} = \hbar\sum_{i}^{N}\mathbf{k}_i = N\hbar\mathbf{k}_0, \tag{5.19}$$

where N is the total number of particles in the system and $\hbar\mathbf{k}_i$ is the individual momentum of each particle of the system. For finite momentum kick $\hbar\mathbf{k}_0$, the gas will adiabatically evolve according to the minimum energy configuration it can achieve. If the momentum kick per particle $\hbar\mathbf{k}_0$ is small compared to the typical single-particle momentum $\hbar\lambda$, the finite momentum ground state in the thermodynamic limit can be modelled by infinitesimal transformations, which describe the response of the system to small momentum kicks. These infinitesimal transformations must fulfil two conditions: (i) the density ρ is preserved and (ii) the momentum per particle of the resulting Fermi sea equals $\hbar\mathbf{k}_0$. These conditions do not prevent fermions to have individual momentum different than $\hbar\mathbf{k}_0$ as long as the momentum density remains constant. If we consider infinitesimally small momenta, we can safely rule out breaking the Fermi sea into two disjoint pieces, that is, we do not allow a change in topology, which is predicted to happen in strong

Rashba spin-orbit coupling [54]. We are then left with two possibilities, namely displacements of the inner and outer circumferences and multipolar deformations of these.

The Fermi sea of a two-dimensional Rashba-coupled Fermi gas, Eq. (2.75), is an annulus with inner and outer radii $R_I = \lambda - k_F$ and $R_O = \lambda + k_F$, respectively. Due to the shape of the Fermi sea we consider the region $k < R_I$ as a virtual Fermi sea of holes with density ρ_I. On the other hand, we treat the region $k < R_O$ as a virtual Fermi sea of particles with density ρ_O, Fig. 2.1. The virtual individual densities are defined as

$$\rho_i = \int_0^{2\pi} \frac{\mathrm{d}\gamma}{2\pi} \int_0^{R_i} \frac{\mathrm{d}kk}{2\pi} = \frac{R_i^2}{4\pi}, \tag{5.20}$$

where $i = I, O$ for the inner (outer) radius. The total density of the system needs to remain constant and it is defined as the virtual density of particles minus the virtual density of holes as

$$\rho = \rho_O - \rho_I = \frac{\lambda k_F}{\pi}, \tag{5.21}$$

which is the density for the noninteracting Rashba-coupled Fermi gas in two dimensions, Eq. (2.75). An analogous relation to Eq. (5.21) can be obtained for the momentum density. Let us write the total momentum per particle $\hbar\mathbf{k}_0$ of the resulting Fermi sea as the total momentum per particle of the virtual Fermi sea of particles $\hbar\mathbf{q}_O$ minus the total momentum per particle of the virtual Fermi sea of holes $\hbar\mathbf{q}_I$. This means

$$\mathbf{k}_0\rho = \mathbf{q_O}\rho_O - \mathbf{q_I}\rho_I. \tag{5.22}$$

In order to have infinitesimal transformations of the Fermi sea, Eq. (5.21) and Eq. (5.22) need to remain fixed.

We introduce now the only dimensionless parameter that defines the strength of the density[3]-coupling ratio in a two-dimensional Rashba-coupled Fermi gas as [29]

$$z = \frac{\pi\rho}{\lambda^2}. \tag{5.23}$$

Alternatively, using Eq. (2.75) we can write $z = k_F/\lambda$. The inner and outer radius of the

[3]In this Chapter we use the two-dimensional density (2.75) $\rho_{2D} = \lambda k_F/\pi$. Since there is no chance of confusion and not to overload notation, we write from now on ρ instead of ρ_{2D}.

Fermi sea, Eq. (2.71), in terms of z read

$$R_I = \lambda - k_F = \lambda\,(1-z)\,, \tag{5.24}$$

$$R_O = \lambda + k_F = \lambda\,(1+z)\,. \tag{5.25}$$

5.2.1 Mathematical description of the displacements and deformations

Mathematically, we model displacements and deformations of the Rashba-coupled Fermi gas differently. Applying a momentum kick $\hbar\mathbf{k}_0$ to the Rashba-coupled Fermi gas can yield a displacement of the Fermi sea. The displacement is parametrised by replacing $\mathbf{k} \to \mathbf{k}+\mathbf{k}_0$ into the single-particle energy, Eq. (2.57). Therefore, the single-particle energy changes as

$$\epsilon_-\left(\mathbf{k}\right) \to \epsilon_-\left(\mathbf{k}+\mathbf{k}_0\right). \tag{5.26}$$

Since we consider small displacements $k_0 \ll k$, the single-particle energy for the negative-helicity branch, given by Eq. (2.57), is expanded as

$$\epsilon_-\left(\mathbf{k}+\mathbf{k}_0\right) \approx \frac{\hbar^2}{2m}\left(\left|\mathbf{k}+\mathbf{k}_0\right|^2 + \lambda^2 - 2\lambda k\left[1 + \frac{k_0}{k}\cos\gamma + \frac{k_0^2}{2k^2}\sin^2\gamma\right]\right), \tag{5.27}$$

where we have written the square root in Eq. (2.57) as

$$\begin{aligned}\left|\mathbf{k}+\mathbf{k}_0\right| &= \sqrt{k^2 + k_0^2 + 2kk_0\cos\gamma} \\ &\approx k\left(1 + \frac{k_0}{k}\cos\gamma + \frac{k_0^2}{2k^2}\sin^2\gamma\right) + \mathcal{O}\left(k_0^3\right).\end{aligned} \tag{5.28}$$

Let us consider now that the momentum kick $\hbar\mathbf{k}_0$ induces multipolar deformations [85] of the Fermi sea. Deformations of the Fermi sea appears in square lattices [86, 87], or as a consequence of interactions [88] that yield Pomeranchuk instabilities [81, 89]. We parametrise deformations using polar coordinates, therefore the inner and outer radii are written as

$$R_i\left(\gamma\right) = R_i + f_i\left(\gamma\right), \tag{5.29}$$

where $i = I, O$ for the inner and outer radii respectively and $f_i\left(\gamma\right)$ are real-valued functions. Since deformations do not preserve density in general, we need to impose additional conditions on the angular functions $f_{I(O)}\left(\gamma\right)$. To this end, let us calculate the

density of the deformed system using the parametrisation in Eq.(5.29). We have then

$$\begin{aligned}\rho &= \int_0^{2\pi} \frac{\mathrm{d}\gamma}{2\pi} \int_{R_I+f_I(\gamma)}^{R_O+f_O(\gamma)} \frac{\mathrm{d}kk}{2\pi} \\ &= \rho_O - \rho_I + \frac{1}{8\pi^2} \int_0^{2\pi} \mathrm{d}\gamma \left(\left[f_O\left(\gamma\right) \right]^2 - \left[f_I\left(\gamma\right) \right]^2 \right), \end{aligned} \tag{5.30}$$

where we have used the fact that $f_{I(O)}\left(\gamma\right)$ are periodic functions of the angle. In order to keep the density constant we impose

$$\int_0^{2\pi} \mathrm{d}\gamma \left[f_O\left(\gamma\right) \right]^2 = \int_0^{2\pi} \mathrm{d}\gamma \left[f_I\left(\gamma\right) \right]^2 . \tag{5.31}$$

We express now the angular functions $f_{I(O)}\left(\gamma\right)$ as a multipole expansion[4] as

$$f_i\left(\gamma\right) = \sum_{m\geq 1} c_m^{(i)} \frac{\cos\left(m\gamma\right)}{\sqrt{\pi}}, \tag{5.32}$$

where $i = I, O$ and every coefficient $c_m^{(i)}$ is real. Since we consider small deformations, we retain only the dipolar term of the expansion, hence

$$f_i\left(\gamma\right) \approx c_1^{(i)} \frac{\cos\gamma}{\sqrt{\pi}}. \tag{5.33}$$

We substitute Eq. (5.33) into Eq. (5.31) to obtain the condition for the dipolar coefficients $c_1^{(i)}$, which reads

$$\left(c_1^{(O)}\right)^2 = \left(c_1^{(I)}\right)^2. \tag{5.34}$$

Equation (5.34) yields to two types of deformations depending on whether the dipolar coefficients are equal or opposite

$$c_1^{(I)} = \pm c_1^{(O)}. \tag{5.35}$$

[4]Since $f_{I(O)}\left(\gamma\right)$ are periodic functions it is possible to write the reparametrisation in (5.29) as a cosine Fourier series as

$$f_i\left(\gamma\right) = R_i + \sum_{m=1} c_m^{(i)} \frac{\cos\left(m\gamma\right)}{\sqrt{\pi}},$$

where $i = I, O$.

For simplicity we introduce the notation

$$q_1 = \frac{c_1^{(O)}}{\sqrt{\pi}}, \tag{5.36}$$

therefore all the dipolar coefficients will be referred to q_1. We introduce now the angle-parametrisation of the inner and outer radii as

$$R_I(\gamma) = R_I + p\cos\gamma, \tag{5.37}$$

$$R_O(\gamma) = R_O + q\cos\gamma, \tag{5.38}$$

where $q = q_1$ and $p = \pm q_1$, and with the positive (negative) sign corresponding to equal (opposite) dipolar coefficients. In Sec. 5.3.2 we study the excess of energy density corresponding to equal and opposite deformations of the Fermi surface.

5.3 Energetic effects of non-Galilean transformations on the Fermi sea

In this section we analyse which of the density-preserving transformations gives the most favourable excess of energy to the noninteracting Rashba-coupled Fermi gas when a momentum kick is performed. Therefore we define the *excess of energy* due to the momentum kick as

$$\Delta\mathcal{E}_i = \mathcal{E}_i - \mathcal{E}_0. \tag{5.39}$$

Above, $\mathcal{E} = E/S$ is the energy density, $i = \mathrm{GB}, D$ denotes the energy density corresponding to a Galilean boost (GB) or D to a deformation and $\mathcal{E}_0$ is the ground state energy density of the two-dimensional noninteracting Rashba-coupled Fermi gas introduced in Eq. (2.80). Using the dimensionless variable z, Eq. (5.23), we have

$$\begin{aligned}\mathcal{E}_0 &= \frac{\hbar^2}{2m}\int_0^{2\pi}\frac{\mathrm{d}\gamma}{2\pi}\int_{\lambda(1-z)}^{\lambda(1+z)}\frac{\mathrm{d}k\,k}{2\pi}\,(k-\lambda)^2 \\ &= \frac{\hbar^2\pi}{6m}z\rho^2.\end{aligned} \tag{5.40}$$

We shall compute now the excess of energy density for a finite momentum kick $\hbar\mathbf{k}_0$ per particle to a Rashba-coupled Fermi gas. We split the analysis in the three different cases: Galilean boost, deformations and displacement along with deformations.

5.3.1 Galilean boost

The first configuration we consider corresponds to a Galilean boost to the whole Fermi sea. Due to the circular symmetry of the system we perform a momentum kick to the system in the x direction, therefore the momentum kick is $\hbar\mathbf{k}_0 = \hbar k_0 \hat{e}_x$, where $\hat{e}_x$ is the unit vector in the x-dimension. We consider both circumferences to be displaced equally. Hence the energy of the moving many-body ground state reads

$$\begin{aligned}\mathcal{E}_{\text{GB}} &= \int_{\text{FS}} \frac{\mathrm{d}\mathbf{k}}{(2\pi)^2} \epsilon_- \left(\mathbf{k} + \mathbf{k}_0\right) \\ &= \frac{\hbar^2}{2m} \int_0^{2\pi} \frac{\mathrm{d}\gamma}{2\pi} \int_{R_I}^{R_O} \frac{\mathrm{d}k\, k}{2\pi} \Big(\left|\mathbf{k} + \mathbf{k}_0\right| - \lambda \Big)^2 . \end{aligned} \tag{5.41}$$

Introducing the second order expansion in k_0 for the single-particle energy, Eq. (5.27), we get to

$$\mathcal{E}_{\text{GB}} = \frac{\hbar^2}{2m} \int_0^{2\pi} \frac{\mathrm{d}\gamma}{2\pi} \int_{R_I}^{R_O} \frac{\mathrm{d}k}{2\pi} k \left[\left(k - \lambda\right)^2 + 2k_0 \left(k - \lambda\right) \cos\gamma + k_0^2 \left(1 - \frac{\lambda}{k} \sin^2\gamma \right) \right] . \tag{5.42}$$

Performing the integral in Eq. (5.42) yields an excess of energy

$$\Delta\mathcal{E}_{\text{GB}} = \mathcal{E}_G - \mathcal{E}_0 = \frac{\hbar^2 k_0^2}{4m} \rho . \tag{5.43}$$

At the end of this section we will show that Eq. (5.43) gives an upper bound for the ground-state energy at finite momentum and it is only attained for a saturated ($z = 1$) lower branch.

5.3.2 Dipolar deformations of the Fermi surface

Let us assume now that the Fermi circumferences deform when the finite momentum kick is applied to the system. We study both cases where the dipolar coefficients of the inner and outer Fermi circumferences are equal ($q = q_1 = p$) or opposite ($q = q_1 = -p$), according to the notation introduced in Eqs. (5.37) and (5.38), see Fig. 5.1.

The energy density for a Rashba-coupled Fermi gas subject to a momentum kick $\hbar\mathbf{k}_0$ that induces dipolar deformations of the Fermi sea with dipolar coefficients q and p for the outer and inner radii, respectively, is

$$\mathcal{E}_D = \frac{\hbar^2}{2m} \int_0^{2\pi} \frac{\mathrm{d}\gamma}{2\pi} \int_{R_I + p\cos\gamma}^{R_O + q\cos\gamma} \frac{\mathrm{d}k}{2\pi} k \left(k - \lambda\right)^2 . \tag{5.44}$$

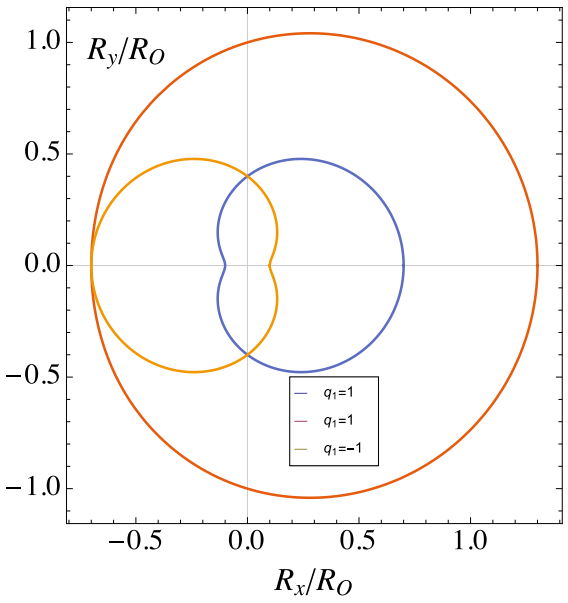

Figure 5.1: Pictorial representation of the displacement and deformation of the Fermi circumferences for equal and opposite dipolar coefficients $c_1^{(I)} = \pm c_1^{(O)}$. In order to enhance the deformation we have set $q_1/R_O = 0.3$ and $R_I/R_O = 0.4$, hence the appearance resembles a displaced curve. The red curve represents the deformation of the outer Fermi circumference $R_O(\gamma) = R_O + q_1 \cos\gamma$, while the blue (yellow) curve represent the deformation of the inner circumference $R_I(\gamma) = R_I \pm q_1 \cos\gamma$, where the positive (negative) sign corresponds to equal (opposite) dipolar coefficient q_1.

Doing the integral in Eq. (5.44) yields

$$\mathcal{E}_D = \frac{\hbar^2}{8\pi m}\frac{1}{48}\Big(9\left[q^4 - p^4\right] + 24z\lambda^2\left[2\left(q^2+p^2\right) + 3z\left(q^2-p^2\right)\right] + 64z^3\lambda^4\Big). \tag{5.45}$$

As the energy density in Eq. (5.45) is an even polynomial of q and p we can substitute $q = q_1$ and $p = \pm q_1$, where $p = q_1$ and $p = -q_1$ represent equal and opposite dipolar coefficients respectively. Both deformations yield the same expression, which is

$$\mathcal{E}_D = \frac{\hbar^2}{4m}\rho\left[q_1^2 + \frac{2\pi^2\rho^2}{3\lambda^2}\right], \tag{5.46}$$

where the second term in the RHS represents the ground state energy $\mathcal{E}_0$ computed in Eq. (5.40). Equation (5.46) shows that without any additional restriction, deformations with equal or opposite dipolar coefficients yield the same energy density. Since the momentum density $\rho\mathbf{k}_0$ needs to remain constant, Eq. (5.22) gives the additional relation between the different momenta

$$k_0\rho = \frac{1}{(2\pi)^2}\int_0^{2\pi} \mathrm{d}\gamma\cos\gamma\int_{R_I+p\cos\gamma}^{R_O+q\cos\gamma}\mathrm{d}k\,k^2. \tag{5.47}$$

Performing the integral gives

$$k_0\rho = \frac{1}{16\pi}\left[q^3 - p^3 + 4\lambda^2\Big(q\,[1+z]^2 - p\,[1-z]^2\Big)\right]. \tag{5.48}$$

Since Eq. (5.48) is an odd polynomial in q and p, substituting $q = q_1$ and $p = \pm q_1$ does not simplify it any further.

Equal dipolar coefficients

For equal dipolar coefficients ($q = q_1 = p$), the constant momentum density condition, Eq. (5.48) is

$$k_0\rho = \frac{q_1\lambda^2}{4\pi}\Big([1+z]^2 - [1-z]^2\Big). \tag{5.49}$$

Since $\rho_i = R_i^2/4\pi$ where $i = I, O$ and $R_{I(O)} = \lambda\,(1 \mp z)$, Eq. (5.49) simplifies to

$$k_0 = q_1. \tag{5.50}$$

Substituting Eq. (5.50) into Eq. (5.46) gives an excess of energy density for a deformation with equal dipolar coefficients

$$\Delta\mathcal{E}_D^{(+)} = \frac{\hbar^2 k_0^2}{4m}\rho. \tag{5.51}$$

A finite momentum kick that induces a deformation of the Fermi sea with equal dipolar coefficients yields an excess of energy, Eq. (5.51), which is equal to the excess of energy produced by a momentum kick that yields a displacement of the Fermi sea, Eq. (5.43).

Opposite dipolar coefficients

For opposite dipolar coefficients ($q = q_1 = -p$) the constant momentum density, Eq. (5.48), gives

$$k_0\rho = \frac{q_1}{8\pi}\Big[q_1^2 + 4\lambda^2\left(1+z^2\right)\Big]. \tag{5.52}$$

Intuitively, dipolar coefficients with opposite sign yield a lower energy, since from Eq. (5.52) we see that a weaker deformation is needed in order to have the required momentum k_0.

Considering only the leading order in q_1 we have

$$q_1 = \frac{2z}{1+z^2} k_0, \tag{5.53}$$

where $\rho = \lambda k_F/\pi$ has been used. Substituting Eq. (5.53) into the energy density for dipolar deformations (5.46) gives

$$\Delta\mathcal{E}_D^{(-)} = \frac{\hbar^2 k_0^2}{m}\left[\frac{z}{1+z^2}\right]^2 \rho. \tag{5.54}$$

This expression is bounded from above by the energy of a Galilean boost, Eq. (5.51), and it only reaches its maximum value in the case of a saturated gas $z = 1$.

5.3.3 General Galilean displacements and dipolar deformations of the Fermi surface

We now study the most general case. Once the momentum kick is applied, it induces a displacement and a deformation of the Fermi sea. We consider different displacements $\mathbf{q}_I$ and $\mathbf{q}_O$ for the inner and outer circumferences. As we saw in the previous section, the most favourable energetic situation corresponds to a deformation with opposite dipolar coefficients, hence the dipolar coefficients are $q = q_1 = -p$. We compute the excess of energy density as the difference between the energy $\mathcal{E}_O$ of a virtual Fermi sea of particles and that of a virtual Fermi sea of holes $\mathcal{E}_I$. Each energy density for the virtual Fermi seas is calculated as

$$\mathcal{E}_i = \frac{1}{(2\pi)^2}\int_0^{2\pi} \mathrm{d}\gamma \int_0^{R_i + f_i(\gamma)} \mathrm{d}k k \epsilon_-\left(\mathbf{k} + \mathbf{q}_i\right), \tag{5.55}$$

where $i = I, O$. Introducing the limits of integration and the single-particle energy, Eq. (5.27), for $k \gg k_0$ yields

$$\begin{aligned}\mathcal{E}_i &= \frac{\hbar^2}{2m}\frac{1}{(2\pi)^2}\int_0^{2\pi}\mathrm{d}\gamma\int_0^{R_i \pm q_1\cos\gamma}\mathrm{d}k k\Big[\,|\mathbf{k}+\mathbf{q}_i| - \lambda\Big]^2 \\ &\approx \frac{\hbar^2}{2m}\frac{1}{(2\pi)^2}\int_0^{2\pi}\mathrm{d}\gamma\int_0^{R_i \pm q_1\cos\gamma}\mathrm{d}k k\left[(k-\lambda)^2 + 2q_i\,(k-\lambda)\cos\gamma + q_i^2\left(1 - \frac{\lambda}{k}\sin^2\gamma\right)\right],\end{aligned} \tag{5.56}$$

where the upper (lower) sign corresponds to the outer (inner) Fermi circumference. In order to simplify the integral and to see the different contributions, we separate the integrand in Eq. (5.56) into two terms. The first integrand does not depend on the momentum

kick q_i and corresponds to a pure deformation. Obviously, the other two integrands corresponds to a displacement and a simultaneous deformation, since the dependence on q_i it is explicit. The deformation term $\mathcal{E}_i^{(D)}$, with $i = I, O$ corresponds to

$$\mathcal{E}_i^{(D)} = \frac{\hbar^2}{2m}\frac{1}{(2\pi)^2}\int_0^{2\pi} \mathrm{d}\gamma \int_0^{R_i \pm q_1 \cos\gamma} \mathrm{d}k\, k\,(k-\lambda)^2\,. \tag{5.57}$$

The energy density difference between the virtual Fermi sea of particles and the virtual Fermi sea of holes reads[5]

$$\mathcal{E}_O^{(D)} - \mathcal{E}_I^{(D)} = \frac{\hbar^2}{4\pi m}\lambda\left(\frac{2}{3}k_F^3 + k_F q_1^2\right), \tag{5.58}$$

where we used $R_i = \lambda \mp k_F$ for the inner and outer radius. The first term in the RHS of Eq. (5.58) corresponds to the energy density of the ground state, Eq. (5.40).

The second and third terms in the RHS of Eq. (5.56) correspond to a displacement happening simultaneously as a deformation of the Fermi circumference with opposite dipolar coefficients, we name this term as $\mathcal{E}_i^{(DD)}$, where $i = I, O$. The energy density difference between the outer and inner circumference is

$$\begin{aligned}
\mathcal{E}_O^{(DD)} - \mathcal{E}_I^{(DD)} =& \frac{\hbar^2}{8\pi^2 m}\int_0^{2\pi}\mathrm{d}\gamma\left(\int_0^{R_O+q_1\cos\gamma}\mathrm{d}k k\left[2q_O\,(k-\lambda)\cos\gamma + q_O^2\left(1-\frac{\lambda}{k}\sin^2\gamma\right)\right]\right.\\
&\left. - \int_0^{R_I-q_1\cos\gamma}\mathrm{d}k k\left[2q_I\,(k-\lambda)\cos\gamma + q_I^2\left(1-\frac{\lambda}{k}\sin^2\gamma\right)\right]\right)\\
=& \frac{\hbar^2}{16\pi m}\Big[\left(q_O^2 - q_I^2\right)\left(q_1^2 + 2k_F^2\right) + q_1\left(q_O + q_I\right)\left(q_1^2 + 4k_F^2\right)\\
&+ 4k_F\lambda q_1\left(q_O - q_I\right) + 2k_F\lambda\left(q_O^2 + q_I^2\right)\Big].
\end{aligned} \tag{5.59}$$

Combining Eq. (5.58) and Eq. (5.59) we recover the excess of energy density for a displaced deformation

$$\begin{aligned}
\Delta\mathcal{E}_{DD} = \frac{\hbar^2}{16\pi m}\Big[&4k_F\lambda q_1^2 + \left(q_O^2 - q_I^2\right)\left(q_1^2 + 2k_F^2\right) + q_1\left(q_O + q_I\right)\left(q_1^2 + 4k_F^2\right)\\
&+ 4k_F\lambda q_1\left(q_O - q_I\right) + 2k_F\lambda\left(q_O^2 + q_I^2\right)\Big].
\end{aligned} \tag{5.60}$$

Equation (5.60) has terms of quartic order in the momenta as $q_I^2 q_1^2$ or $q_O^2 q_1^2$. Since the dipolar coefficient q_1, the inner momentum kick q_I and the outer momentum kick q_O are of the same order and smaller than the Fermi wave vector k_F, it is possible to retain the

[5]Equation (5.58) was computed before in Eq. (5.46), but we rewrite it here as we use an explicit dependence on the Fermi vector k_F.

terms of order $\mathcal{O}\left(q_i^2\right)$, where $i = 1, I, O$, in Eq. (5.60) to get

$$\Delta\mathcal{E}_{DD} = \frac{\hbar^2}{8\pi m}\Big[k_F^2\left(q_O^2 - q_I^2\right) + k_F\lambda\left(q_O^2 + q_I^2\right) + 2k_F q_1\left[k_F\left(q_O + q_I\right) + \lambda\left(q_O - q_I\right) + \lambda q_1\right]\Big]. \tag{5.61}$$

Equation (5.61) gives the excess of energy density for a momentum kick that induces on the Fermi sea a displacement along with a deformation, but it does not preserve, in general, constant momentum density. Since we have three momenta, the momentum density, Eq (5.22), is

$$\mathbf{k}_0\rho = \mathbf{q}_O\rho_O - \mathbf{q}_I\rho_I + \mathbf{q}_1\rho_1, \tag{5.62}$$

where $\mathbf{q}_1\rho_1$ is included to take into account the region of the gas that is deformed. The total momenta in the deformed region S_1 is

$$\begin{aligned}\mathbf{Q}_1 &= \sum_{i=1}^{N_1} k_i\cos\gamma_i \\ &= \frac{S_1}{(2\pi)^2}\int_0^{2\pi}\mathrm{d}\gamma\int_{R_I - q_1\cos\gamma}^{R_O + q_1\cos\gamma}\mathrm{d}k k^2\cos\gamma,\end{aligned} \tag{5.63}$$

where N_1 is the number of fermions in the deformed region S_1. The total momenta $\hbar\mathbf{Q}_1$ and the momenta per particle $\hbar\mathbf{q}_1$ are related via $\hbar\mathbf{Q}_1 = N_1\hbar\mathbf{q}_1$. Hence the third term in the RHS of Eq. (5.62) is

$$\begin{aligned}q_1\rho_1 &= \frac{1}{4\pi}\left[q_1\left(R_O^2 + R_I^2\right) + \frac{q_1^3}{2}\right] \\ &= \frac{1+z^2}{2z}q_1\rho + \frac{q_1^3}{8\pi}.\end{aligned} \tag{5.64}$$

Therefore to first order in q_1 we have

$$q_1\rho_1 \approx \frac{1+z^2}{2z}q_1\rho. \tag{5.65}$$

Substituting Eq. (5.65) into the momentum density, Eq. (5.62), gives

$$k_0\rho = q_O\rho_O - q_I\rho_I + \frac{1+z^2}{2z}q_1\rho. \tag{5.66}$$

We obtain now q_I as a function of q_O and q_1

$$q_I = \frac{1}{\rho_I}\left[-k_0\rho + q_O\rho_O + \frac{1+z^2}{2z}q_1\rho\right]. \tag{5.67}$$

Substituting q_I into (5.61) allows us to write the excess of energy density as a function of the remaining momenta

$$\begin{aligned}\Delta\mathcal{E}_{DD} = \frac{\hbar^2}{8\pi m}\Bigg(& k_F q_O^2\left(\lambda + k_F\right) + \frac{k_F}{\rho_I^2}\left[-k_0\rho + q_O\rho_O + \frac{1+z^2}{2z}q_1\rho\right]^2\left(\lambda - k_F\right) \\ &+ 2k_F q_1\left[q_O\left(\lambda + k_F\right) - \frac{1}{\rho_I}\left[-k_0\rho + q_O\rho_O + \frac{1+z^2}{2z}q_1\rho\right]\left(\lambda - k_F\right) + \lambda q_1\right]\Bigg).\end{aligned} \tag{5.68}$$

The wave vector q_O that minimises (5.68) reads

$$q_O^{\min} = -q_1 + \frac{2z\left(1+z\right)}{1+3z^2}k_0, \tag{5.69}$$

that yields an expression for the minimum energy

$$\Delta\mathcal{E}_{DD}^{\min} = \frac{\hbar^2 k_0^2}{m}\frac{z^2}{1+3z^2}\rho. \tag{5.70}$$

The minimum energy density is infinitely degenerate in the dipolar coefficient q_1 and it is upper bounded by the excess of energy density for a Galilean boost of the Fermi sea, Eq. (5.43), for all z and for each z by the excess of energy density for a deformation of the Fermi sea with opposite dipolar coefficients, Eq. (5.54).

5.4 Non-Galilean transformations in a weakly interacting gas

We now study the response of a weakly interacting Rashba-coupled Fermi gas to a finite momentum kick. We consider a contact s-wave interaction in the negative helicity branch given by Eq. (4.9). We introduced the dimensionless parameter z, Eq. (5.23), for the non-interacting Rashba-coupled Fermi gas. We define another dimensionless parameter for the interacting theory [90] as

$$\xi = \frac{mg}{4\pi\hbar^2}. \tag{5.71}$$

Typically, for mean field theory to be valid, the interaction energy to first order in perturbation theory, Eq. (4.62), must be smaller than the Fermi energy, Eq. (2.63). Therefore we

have

$$\frac{g\rho}{4} < \frac{\hbar^2 k_F^2}{2m} \implies \xi < \frac{z}{2}, \tag{5.72}$$

where $k_F = \pi\rho/\lambda$ has been used.

In Sec. 4.4 we obtained the first correction to the energy in perturbation theory, Eq. (4.60), in three dimensions. In two dimensions, the Hartree shift reads

$$\mathcal{E}^{HS} = \frac{g\rho^2}{4} - \frac{g}{4}\int_{\mathrm{FS}} \frac{\mathrm{d}\mathbf{k}}{(2\pi)^2}\int_{\mathrm{FS}} \frac{\mathrm{d}\mathbf{q}}{(2\pi)^2}\cos\left(\gamma_k - \gamma_q\right). \tag{5.73}$$

In Eq. (5.73) the first term is independent of the shape of the Fermi sea, thence it is not affected by displacements nor deformations. On the other hand, the second term vanishes in a spherically symmetric ground state, but deformations of the Fermi sea reduce the interaction energy for repulsive interactions ($g > 0$).

We perform a momentum kick per particle $\hbar\mathbf{k}_0$ to a weakly interacting Rashba-coupled Fermi gas and we allow the Fermi circumferences to displace and deform with opposite dipolar coefficients, since we showed in Sec. 5.3 that opposite dipolar coefficients yield a lower energy density. We proceed as in the previous section: first we determine the resulting interacting Fermi sea due to the deformation and displacement. Then we compute the excess of energy density, given by the integral in Eq. (5.73). Secondly, we calculate the relation between the inner momentum q_I, the outer momentum q_O and the dipolar coefficient q_1 in order for the momentum density $\rho\mathbf{k}_0$ to remain constant. Finally we obtain the outer momentum q_O that minimises the excess of energy.

The parametrisation of the displacement and the deformation is slightly more complicated than any previous case, since the displacement of the Fermi sea cannot be described by performing a Galilean boost in the single-particle energy $\epsilon_-(\mathbf{k})$. Therefore, we introduce the displacement and the deformation into the integration limits of Eq. (5.73). We first show how to parametrise a displacement and afterwards we include deformations. Initially, the Fermi circumferences are defined in momentum space as

$$k_x^{(i)} = k^{(i)}\cos\gamma_k, \tag{5.74}$$

$$k_y^{(i)} = k^{(i)}\sin\gamma_k, \tag{5.75}$$

where $i = I, O$ and the corresponding radii are $R_i(\gamma_k) = \sqrt{\left(k_x^{(i)}\right)^2 + \left(k_y^{(i)}\right)^2}$. After

performing a displacement in the x direction, the Fermi circumferences change to

$$\tilde{k}_x^{(i)} = k^{(i)} \cos\gamma_k + q_i, \tag{5.76}$$

$$\tilde{k}_y^{(i)} = k^{(i)} \sin\gamma_k. \tag{5.77}$$

Hence, the displaced radius $\tilde{R}_i$ is defined as

$$\tilde{R}_i\left(\gamma_k\right) = \sqrt{R_i^2 + q_i^2 + 2R_i q_i \cos\gamma_k}. \tag{5.78}$$

The radius defined in Eq. (5.78) considers only displacements. Deformations with opposite dipolar coefficients are considered by substituting R_i by $R_{O(I)} \to R_{O(I)} \pm q_1 \cos\gamma$ in Eq. (5.78), where the positive (negative) sign corresponds to the outer (inner) Fermi circumference

$$\tilde{R}_i\left(\gamma_k\right) = \sqrt{\left(R_i \pm q_1 \cos\gamma_k\right)^2 + q_i^2 + 2q_i\left(R_i \pm q_1 \cos\gamma_k\right)\cos\gamma_k}. \tag{5.79}$$

The resulting interacting Fermi sea due to a displacement and opposite dipolar coefficients deformation corresponds to the region defined by

$$\begin{aligned}\mathrm{FS} : [0, 2\pi) \times \Bigg[& \sqrt{\left(R_I - q_1 \cos\gamma_k\right)^2 + q_I^2 + 2q_I\left(R_I - q_1 \cos\gamma_k\right)\cos\gamma_k}, \\ & \sqrt{\left(R_O + q_1 \cos\gamma_k\right)^2 + q_O^2 + 2q_O\left(R_O + q_1 \cos\gamma_k\right)\cos\gamma_k}\Bigg],\end{aligned} \tag{5.80}$$

which is depicted in Fig. 5.2.

Instead of substituting the Fermi sea, Eq. (5.80), into the expression for the Hartree shift, Eq. (5.73), let us use the symmetry of the Fermi sea to simplify it. One of the integrals in Eq. (5.80) can be evaluated as follows

$$\begin{aligned}\int_{\mathrm{FS}} \frac{\mathrm{d}\mathbf{k}}{(2\pi)^2} \cos\left(\gamma_k - \gamma_q\right) &= \frac{1}{(2\pi)^2} \int_0^{2\pi} \mathrm{d}\gamma_k \int_{\tilde{R}_I(\gamma_k)}^{\tilde{R}_O(\gamma_k)} \mathrm{d}k\, k \cos\left(\gamma_k - \gamma_q\right) \\ &= \frac{1}{2(2\pi)^2} \int_0^{2\pi} \mathrm{d}\gamma_k \cos\left(\gamma_k - \gamma_q\right) \left[\tilde{R}_O^2\left(\gamma_k\right) - \tilde{R}_I^2\left(\gamma_k\right)\right].\end{aligned} \tag{5.81}$$

By means of the trigonometric identity $\cos\left(\gamma_k - \gamma_q\right) = \cos\gamma_k \cos\gamma_q - \sin\gamma_k \sin\gamma_q$ we express Eq. (5.81) as

$$\frac{1}{2(2\pi)^2} \int_0^{2\pi} \mathrm{d}\gamma_k \Big[\cos\gamma_k \cos\gamma_q - \sin\gamma_k \sin\gamma_q\Big] \left[\tilde{R}_O^2\left(\gamma_k\right) - \tilde{R}_I^2\left(\gamma_k\right)\right]. \tag{5.82}$$

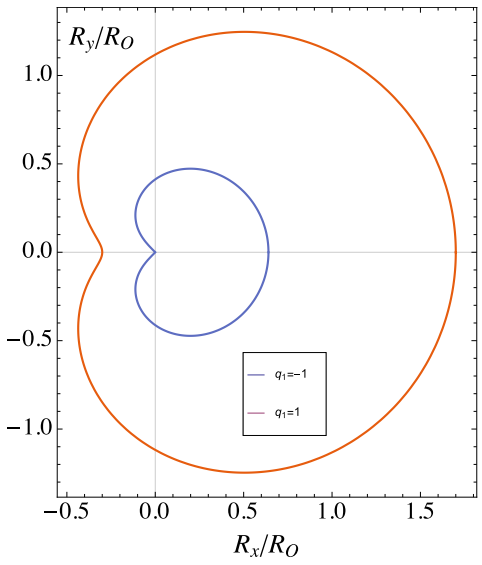

Figure 5.2: Deformed Fermi sea by a general non-Galilean transformation with different dipolar coefficients according to Eq. (5.80), with $q_1/R_O = 0.2$, $q_I/R_O = 0.1$, $q_O/R_O = 0.5$ and $R_I/R_O = 0.4$.

The inner and outer radii given by Eq. (5.79) are symmetric functions of the angle γ_k in the interval $[0, 2\pi)$. Therefore, the integrals in Eq. (5.82) that involve $\sin\gamma_k$ vanish. We define the integral in the Hartree shift, Eq. (5.73), as

$$\begin{aligned}\mathcal{I} &= -\frac{g}{4}\int_{\mathrm{FS}}\frac{\mathbf{dk}}{(2\pi)^2}\int_{\mathrm{FS}}\frac{\mathbf{dq}}{(2\pi)^2}\cos\left(\gamma_k-\gamma_q\right)\\ &= -\frac{g}{4}\left[\int_{\mathrm{FS}}\frac{\mathbf{dk}}{(2\pi)^2}\cos\gamma_k\right]^2.\end{aligned} \tag{5.83}$$

Performing the integral in Eq. (5.83) within the Fermi sea, Eq. (5.80), gives

$$\mathcal{I} = -\frac{g\rho}{64\pi z}\left[q_O\left(1+z\right)-q_I\left(1-z\right)+2q_1\right]^2, \tag{5.84}$$

which allows us to write the Hartree shift, Eq. (5.73) as

$$\mathcal{E}^{HS} = \frac{g\rho}{4}\left(1-\frac{1}{16\pi z}\left[q_O\left(1+z\right)-q_I\left(1-z\right)+2q_1\right]^2\right). \tag{5.85}$$

The excess of energy density for an interacting Rashba-coupled Fermi gas whose Fermi sea is deformed and displaced comes from combining the noninteracting excess of energy

density $\Delta\mathcal{E}_{DD}$, Eq. (5.61), and the Hartree shift $\mathcal{E}^{HS}$, given by Eq. (5.85),

$$\Delta\mathcal{E}_{\text{Int}} = \frac{\hbar^2\rho}{8m}\Bigg[\frac{1}{z}\left(q_O^2 - q_I^2\right) + \left(q_O^2 + q_I^2\right) + 2q_1\left(\frac{1}{z}\left(q_O + q_I\right) + \left(q_O - q_I\right) + q_1\right) + \frac{g\rho}{4}\left(1 - \frac{1}{16\pi z}\left[q_O\left(1+z\right) - q_I\left(1-z\right) + 2q_1\right]^2\right)\Bigg]. \tag{5.86}$$

Since we impose a constant momentum density, $\rho\mathbf{k}_0$, the three momenta q_I, q_O and q_1 are related by Eq. (5.66). Clearing q_I in favour of q_1 and q_O gives Eq. (5.67). Substituting $q_I = q_I\left(q_1, q_O\right)$, Eq. (5.67), into Eq. (5.86) yields the excess of energy density as a function of q_1 and q_O

$$\begin{aligned}\Delta\mathcal{E}_{\text{Int}} =& \frac{\hbar^2\rho}{128m\pi\left(1-z\right)^3} \\ &\Bigg[32\pi\Big(-8k_0 z + \left(q_1+q_O\right)\left(1+z\right)\left[4k_0\left(1+z\right) - \left(q_1+q_O\right)\left(3+z^2\right)\right]\Big) \\ &+ g\rho\left(1-z\right)\Big(4\pi\left(1-z\right)^2 - z\left[-2k_0 + \left(q_1+q_O\right)\left(1+z\right)\right]^2\Big)\Bigg].\end{aligned} \tag{5.87}$$

We look now for the momentum q_O that minimises the excess of energy density given by Eq. (5.87), by solving $\partial\left(\Delta\mathcal{E}_{\text{Int}}\right)/\partial q_O|_{q_O^{\min}} = 0$, which yields

$$q_O^{\min} = \frac{2k_0 z\left(-2 + 2\xi\left[1-z\right]\right) + q_1\left(2 - z - 2z\left[z+\xi\right]\right)}{2\left(-1 + 2z^2 + z\xi\left[1-z^2\right]\right)}. \tag{5.88}$$

Substituting the minimum outer momentum $q_O^{\min}$, Eq. (5.88), into the excess of energy density, Eq. (5.87), we obtain the minimum excess of energy density for an interacting Rashba-coupled Fermi gas

$$\Delta\mathcal{E}_T^{\min} = G\left(\xi, z\right)\frac{\hbar^2 k_0^2}{m}\rho, \tag{5.89}$$

where the function $G\left(\xi, z\right)$ is given by

$$G\left(\xi, z\right) = \frac{z\left(z-\xi\right)}{z\xi\left(z^2-1\right) + 1 + 3z^2}. \tag{5.90}$$

Since $G\left(\xi, z\right)$ is independent of the choice of the dipolar coefficient q_1, the minimum excess of energy density is infinitely degenerate at small q_1 even in the presence of interactions.

In Fig. 5.3 we summarise the excess of energy density hierarchy for the different cases considered.

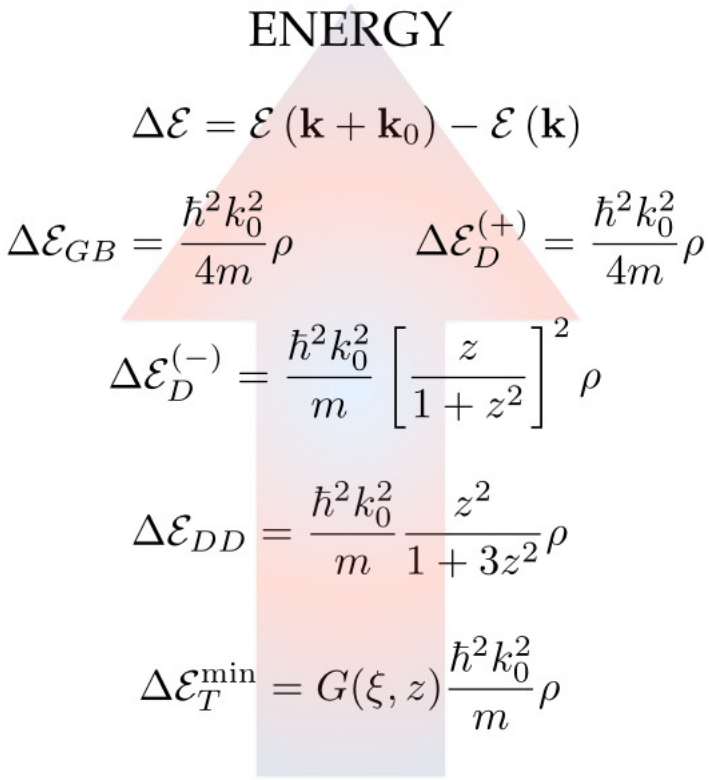

Figure 5.3: This figure represents the excess of energy density hierarchy for the different cases considered. Applying a Galilean boost to the system or performing a deformation with equal dipolar coefficients yields the maximum excess of energy density, given by $\Delta\mathcal{E}_{GB}$ and $\Delta\mathcal{E}_D^{(+)}$, which is independent of the dimensionless parameter $z = \pi\rho/\lambda^2$. The excess of energy density is reduced when a deformation with opposite dipolar coefficients is applied to the Rashba-coupled Fermi gas, $\Delta\mathcal{E}_D^{(-)}$. The most general transformation of the Fermi surface, joint displacement and opposite dipolar coefficients deformation, gives the minimum excess of energy density $\Delta\mathcal{E}_{DD}$ for the noninteracting case. In the noninteracting case, the upper bound is reached when the system is saturated ($z = 1$). We attain the minimum excess of energy density for an interacting Rashba-coupled Fermi gas that is displaced and deformed with opposite dipolar coefficients $\Delta\mathcal{E}_T^{\min}$. It is important to notice that every case is infinitely degenerate in the dipolar coefficients.

5.4.1 Phase transition to a finite momentum ground state

As we infer from Eq. (5.89), the systems' ground state of the Rashba-coupled Fermi gas will change from the noninteracting Fermi sea to a Fermi sea with an infinitesimally small momentum at a critical value $\xi(z) = \xi_c$, where $G(\xi, z) = 0$. This happens for

$$\xi_c(z) = z, \tag{5.91}$$

which is in good agreement with self consistent Hartree-Fock methods used in systems with strong-coupling limit [91, 92] where they showed that the Fermi surfaces can be deformed. However, with their choice of the self-consistent Zeeman field, the degeneracy of the ground state or the absence thereof was not investigated. We are considering the system's noninteracting energy to order $\mathcal{O}\left(k_0^2\right)$, since we used the small momentum expansion given by Eq. (5.28) to obtain $\Delta\mathcal{E}_{DD}^{\min}$, Eq. (5.70). On the other hand, the interacting energy is indeed not approximate but proportional to k_0^2 in the cases $q_I = q_O = 0$ with $q_1 \neq 0$ and $q_1 = 0$ with $q_I, q_O \neq 0$. This comes from the fact that we used the excess of energy for a deformed and displaced noninteracting Fermi sea, Eq. (5.68), to obtain the ground state energy in the Hartree shift, Eq (5.73). Hence, for a momentum kick that only yields a displacement ($q_1 = 0$) or a deformation $q_I = q_O = 0$ of the Fermi sea, the interacting energy is proportional to k_0^2. The critical point $\xi_c = z$ lies slightly away from the validity of mean-field theory. This also happens in ferromagnetic [93] transitions in repulsive Fermi gases [94–96]. This problem is solved going beyond first order perturbation theory, which gives rise to apparent first order phase transitions [96–98]. Non-perturbative methods also overcome this problem, although they predict second order phase transitions [99, 100] which are in good agreement with Monte Carlo simulations [101, 102].

The low-momentum theory of the Rashba-coupled Fermi gas predicts only whether the system evolves towards a finite-momentum ground state in a continuous manner. This is to say that the theory can describe, correctly, only derivatives in the energy at zero momenta. The first derivative of the excess of energy density, Eq. (5.89), with respect to k_0 vanishes when $k_0 = 0$, while its second derivative with respect to k_0 reads

$$\frac{\mathrm{d}^2}{\mathrm{d}k_0^2}\Delta\mathcal{E}_T^{\min} = \frac{2\hbar^2\rho}{m}\mathcal{G}(\xi, z)\Big|_{k_0=0}. \tag{5.92}$$

Combined with (5.90) the expression above is positive for interactions smaller than the

critical point $\xi_c = z$. If interactions are larger than the critical point the second derivative of the energy becomes negative and the system acquires a nonzero overall momentum.[6] The change of sign in $\mathcal{G}(\xi, z)$ denotes the transition from a minimum to a maximum at $k_0 = 0$, which implies that for repulsions stronger than the critical value ξ_c the system's ground state has nonzero momentum. To calculate the actual momentum of the ground state for $\xi > \xi_c$ we need more terms in k_0.

5.5 Experimental considerations

In the previous section we considered the momentum acquired by the gas to be in a particular direction. In an experiment, however, no direction is in principle preferred. Obviously, after the critical point is reached, the ground state is highly degenerate, since the same momentum in any direction yields the same energy. The many-body wave function is therefore an arbitrary superposition of states with momenta pointing at different directions. For instance, we may expect to observe an equal superposition of these states, up to arbitrary phases, which yields a circularly symmetric momentum distribution. Even if a finite momentum is acquired in a particular direction, this will be different in each experimental realisation, and the averaged momentum distribution after many realisations will be spherically symmetric. Momentum distributions are especially relevant to cold atom experiments where these can be obtained via time-of-flight measurements [5], in combination with spin-injection spectroscopy [13] and resolved-momentum radio-frequency spectroscopy [12].

We can easily map out, starting from a Fermi sea at finite momentum in a particular direction, the integrated, circularly symmetric momentum distribution. The momentum distribution is denoted by $n(\mathbf{k})$, and is defined such that

$$\rho = \int \frac{\mathrm{d}\mathbf{k}}{(2\pi)^3} n(\mathbf{k}) . \tag{5.93}$$

From Eq. (5.93) it is possible to define the integrated, angle-independent momentum distribution $\tilde{n}(\mathbf{k})$ as

$$\tilde{n}(\mathbf{k}) = \int_0^{2\pi} \frac{\mathrm{d}\phi}{2\pi} n(\mathbf{k}) . \tag{5.94}$$

Geometrically, $n(k)$ is the arc length of occupied states on a circumference of radius k

[6] Strictly speaking this happens when the pole $\xi_\infty = \left(1 + 3z^2\right)/z\left(1 - z^2\right) \gg \xi_c$, which is far beyond the limit of validity of mean-field theory.

in momentum space. Closed circumferences map into unit length (fully occupied states) while open arcs give shorter lengths (smaller average occupations). The circularly symmetric momentum distribution arising from the superposition of the different states is obtained as a surface of revolution by rotating the Fermi sea at finite momentum in a particular direction with respect to the origin in momentum space. Clearly, the resulting momentum distribution coincides with $n\,(k)$.

In Fig. (5.4) we show the integrated momentum distribution for a particular case of an interacting Fermi sea at nonzero total momentum compared to the noninteracting momentum distribution. There, we observe a shortening of the unit occupation plateau, together with a smoothing of the momentum distribution at the edges of the Fermi sea, with an obvious change in concavity, which can be a relevant experimental signature for finite-momentum states. In cold-atom experiments, where an external trap is always present, the Fermi sea and the homogeneous momentum distribution can be observed by selectively probing fermions around the centre of the trap [103, 104]. An alternative way to observe these effects consists of adding to the system a small symmetry-breaking term, i.e., a small momentum kick in a chosen direction, in order to observe the deformations *per se*. In Ref. [105] authors reported splitting a BEC with the use of standing-wave light-pulse sequences. This technique was used in Ref. [106] to reverse the movement of two ^{87}Rb BEC clouds. Authors used a 6.2μW pulse applied during 150μs onto both BEC clouds to make them collide, in order to recover the originally split BEC cloud. Additionally, two BEC with synthetic contact s-wave interaction were collided using standing-wave light-pulse sequences [107]. Typically, for ^{40}Kb Rashba spin-orbit gases the Fermi vector is given by $k_F = 1.35 k_r = 1.15 \times 10^{-27}\mathrm{m}^{-1}$, see Ref. [12], where $E_r = 2\pi\hbar \times 8.34$ kHz is

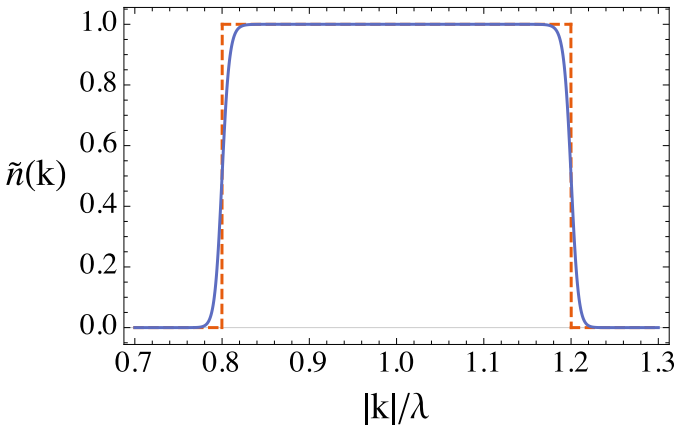

Figure 5.4: Integrated momentum distribution (blue solid line) at critical interaction strength $\xi = z$, with $k_0/\lambda = 5 \times 10^{-2}$ and $z = 1/5$, compared to the noninteracting momentum distribution (red-dashed line).

the recoil energy and k_r the recoil momentum. In order to displace and deform the Fermi surfaces for dilute gases ($z \ll 1$), a standing-light wave-pulse which infers a momentum kick per particle $k_0 \ll k_F$ onto the Rashba-coupled Fermi gas should be applied.

5.6 Conclusions

In this Chapter, we have studied the response of a dilute two-dimensional Fermi gas with Rashba spin-orbit coupling to a small overall constant velocity kick. We have found that the moving Fermi sea deforms in a nontrivial manner due to the non-Galilean nature of the system and is highly degenerate. We have then considered repulsive interactions at the Hartree-Fock level and found that the ground state of the system acquires a finite momentum. The Fermi sea becomes deformed beyond a critical interaction strength in a continuous fashion, which we identified as a possible experimental signature. These results open the path towards the observation of finite-momentum ground states, constitute the starting point for more elaborate treatments of interactions, and can be generalised to higher dimensions and more general types of spin-orbit coupling.

Chapter 6

Generality of time-local master equations

In Nature, quantum systems are never truly isolated; the dynamics of a quantum system depends, to lesser or greater extent, on its interactions with its surroundings [30, 108–112]. For an isolated system, the evolution is unitary and it is determined by the system Hamiltonian. On the other hand, the interaction with the environment yields a non-unitary time evolution of the reduced density matrix of the system. The dynamic of the reduced density matrix of the system is governed by a Master Equation where the environment enters as parameters. Given the complete Hamiltonian of the system and environment it is possible to obtain a Master Equation tracing out the environment, however different system-environment Hamiltonians yield the same Master Equation [113].

We begin this Chapter by introducing classical Markov processes. We continue by extending the definition to Markovian and non-Markovian quantum evolution. We will explain the fully quantised light-matter interaction model by Jaynes and Cummings [114]. Based on this model, we will construct a Jaynes-Cummings Hamiltonian that changes from an on-resonance evolution to an off-resonance evolution. We will show that the decay rate and the Master Equation do not change during the time evolution.

6.1 Classical Markov processes

In this section we define the basic mathematical concepts to introduce and describe classical Markov processes [30]. Let us begin by defining a stochastic process. A one-parameter stochastic process is a family of random variables $Y(t) = y$, where $y \in \mathbb{R}$ and t is the parameter (usually time). The evolution of a stochastic process is determined by a family of

joint probability distributions

$$p\left(y_n, t_n; y_{n-1}, t_{n-1}; \ldots; y_0, t_0\right) \tag{6.1}$$

that describe all the possible realisation of the random variable Y from $Y\left(t_0\right) = y_0$ to $Y\left(t_n\right) = y_n$. A stochastic process is called stationary if all joint probability densities are invariant under time translations

$$p\left(y, t + \Delta t; \ldots; y_0, t_0 + \Delta t\right) = p\left(y, t; \ldots; y_0, t_0\right). \tag{6.2}$$

We define a classical Markov process as a memoryless stochastic process. This means that the conditional probability of the random variable Y to take the value y_n at t_n, provided that $Y\left(t_{n-1}\right) = y_{n-1}$, only depends on the value y_{n-1} of the random variable Y at t_{n-1}

$$p\left(y_n, t_n | y_{n-1}, t_{n-1}; \ldots; y_0, t_0\right) = p\left(y_n, t_n | y_{n-1}, t_{n-1}\right). \tag{6.3}$$

The propagator of a stochastic process is defined as the conditional probability for the random variable Y to take the value y at t provided that at time $t' < t$ the random variable Y took the value y'

$$T\left(y, t | y', t'\right) \equiv p\left(y, t | y', t'\right), \tag{6.4}$$

with the following properties

$$\int \mathrm{d}y'\, T\left(y, t | y', t'\right) = 1, \tag{6.5}$$

$$\lim_{t \to t'} T\left(y, t | y', t'\right) = \delta\left(y - y'\right). \tag{6.6}$$

The above equations have a simple interpretation. Equation (6.5) represents the fact that the random variable $Y\left(t\right)$ will evolve to any available state (ergodic property), while Eq. (6.6) shows that the random variable $Y\left(t\right)$ will not change if time does not change. It is possible to express the probability of an event in terms of the propagator as

$$p\left(y, t\right) = \int \mathrm{d}y'\, T\left(y, t | y', t'\right) p\left(y', t'\right). \tag{6.7}$$

The memoryless condition for a Markov process is given by the Chapman-Kolmogorov equation

$$T\left(y,t|y',t'\right)=\int \mathrm{d}y''\,T\left(y,t|y'',t''\right)T\left(y'',t''|y',t'\right). \tag{6.8}$$

Equation (6.8) represents the conditional transition probability of the random variable at $Y\left(t'\right)=y'$ to reach $Y\left(t\right)=y$ via all the possible intermediate states y'' at a fixed intermediate time t''. The Chapman-Kolmogorov equation can be written as a differential equation

$$\frac{\partial}{\partial t}T\left(y,t|y',t'\right)=A\left(t\right)T\left(y,t|y',t'\right), \tag{6.9}$$

where $A\left(t\right)$ is the time-dependent operator that generates the infinitesimal time translations. Integrating Eq. (6.9) yields the propagator for a time inhomogeneous Markov process

$$T\left(y,t|y',t'\right)=\mathcal{T}_{\leftarrow}\left[e^{\int_{t'}^{t}\mathrm{d}\tau A(\tau)}\right]\delta\left(y-y'\right), \tag{6.10}$$

where $\mathcal{T}_{\leftarrow}$ is the time-order operator. For time-independent generators A, the propagator is called *homogeneous* in time, as it only depends on time differences. In this case, integrating the Chapman-Kolmogorov equation yields

$$T\left(y,t|y',t'\right)=e^{A(t-t')}\delta\left(y-y'\right). \tag{6.11}$$

Since the time interval $t-t'\geq 0$, Eq. (6.11) defines the semigroup structure for a homogeneous Markov process.

6.2 Open quantum systems

There are processes in Nature which are inherently quantum but only appear when the quantum system interacts with its surroundings, such as decoherence [115, 116]. Controlling decoherence has become important since long decoherence times are needed to efficiently perform quantum computing [117]. Several approaches have been proposed to reduce decoherence in quantum computation [118] by means of the Zeno effect [119]. In Ref. [120] remarkable coherence times for superconducting qubits were reported. Other examples where the environment plays an important role are biological processes such

as photosynthesis [121, 122], or improving energy transfer efficiency [123].

In a closed quantum system, the time evolution of the density operator ρ of the state $|\psi\rangle$ is constructed from the time-dependent Schrödinger equation $\mathcal{H}|\psi\rangle = i\hbar\partial_t|\psi\rangle$, where $\mathcal{H}$ is the Hamiltonian of the system, to yield

$$\frac{\mathrm{d}}{\mathrm{d}t}\rho(t) = -\frac{i}{\hbar}[\mathcal{H}, \rho(t)]. \tag{6.12}$$

The solution of Eq. (6.12) is given in terms of the unitary transformation

$$U(t) = \exp(-i\mathcal{H}t/\hbar), \tag{6.13}$$

that gives rise to a unitary time evolution

$$\rho(t) = U(t)\,\rho(0)\,U^{\dagger}(t). \tag{6.14}$$

On the other hand, an open quantum system is a quantum system S coupled to its environment E. The composite system is described by a tensor product Hilbert space between the Hilbert space of the system $\mathbb{H}_S$ and the Hilbert space of the environment $\mathbb{H}_E$, this is

$$\mathbb{H} = \mathbb{H}_S \otimes \mathbb{H}_E. \tag{6.15}$$

The Hamiltonian of the composite system is

$$\mathcal{H}_T = \mathcal{H}_S + \mathcal{H}_E + \mathcal{H}_I, \tag{6.16}$$

where $\mathcal{H}_S$, $\mathcal{H}_E$ and $\mathcal{H}_I$ represent the Hamiltonian for the system, environment and the interaction between the system and environment, respectively. It is possible to have a unitary evolution for the joint system-environment density matrix $\rho(t)$

$$\frac{\mathrm{d}}{\mathrm{d}t}\rho(t) = -\frac{i}{\hbar}[\mathcal{H}_S + \mathcal{H}_E + \mathcal{H}_I, \rho(t)]. \tag{6.17}$$

Unfortunately, due to the number of degrees of freedom of the environment, it is a quite formidable problem to solve the differential equation for the composite system. Therefore, tracing out the environment in Eq. (6.17) gives the equation of motion for the re-

duced density matrix of the system

$$\frac{\mathrm{d}}{\mathrm{d}t}\rho_S(t) = -\frac{i}{\hbar}\mathrm{Tr}_E\left([\mathcal{H}_S + \mathcal{H}_E + \mathcal{H}_I, \rho(t)]\right), \tag{6.18}$$

where $\rho_S(t) = \mathrm{Tr}_E[\rho(t)]$ and the environment enters the description as parameters instead of variables. In the following sections we will analyse how the environment affects the time evolution of the reduced density matrix of the system, which is no longer described by a unitary time evolution.

6.2.1 Markovian and non-Markovian time evolution in quantum systems

The time evolution of a quantum system can be seen as a linear map from the initial state $\rho(0)$ to the final state $\rho(t)$. Physically valid time evolutions are represented by completely positive trace-preserving (CPTP) maps [30, 124]. Let us first introduce the concepts of positive map, completely positive map and trace preserving map. Let $\mathcal{B}(\mathbb{H})$ be the algebra of bounded operators of the Hilbert space $\mathbb{H}$. A one-parameter map $\phi : \mathcal{B}(\mathbb{H}) \to \mathcal{B}(\mathbb{H})$ is said to be positive if $\phi_t\left(\rho^\dagger\rho\right) \geq 0$ for all $\rho \in \mathcal{B}(\mathbb{H})$. A one-parameter linear map $\phi_t : \mathcal{B}(\mathbb{H}) \to \mathcal{B}(\mathbb{H}')$ is said to be completely positive if $\phi_t \otimes \mathbb{1}_n$ is positive for any $n \in \mathbb{N}$, this means that not only the map ϕ_t acting on $\rho \in \mathcal{B}(\mathbb{H})$ is positive but also $\rho_t \otimes \mathbb{1}_n$ acting on an arbitrary finite extension of the Hilbert space. Finally, a one-parameter linear map is said to be trace-preserving if $\mathrm{Tr}[\rho] = \mathrm{Tr}[\phi_t(\rho)]$, for all $\rho \in \mathcal{B}(\mathbb{H})$. It is important to mention that every CPTP map ϕ_t admits a Kraus decomposition [125, 126]

$$\phi_t[\rho(0)] = \sum_{k=1}^{n} A_k(t)\,\rho(0)\,A_k^\dagger(t), \tag{6.19}$$

where $n \leq \dim^2\mathbb{H}$, and $A_k(t)$ are the time-dependent Kraus operators that satisfy

$$\sum_{k=1}^{n} A_k^\dagger(t)\,A_k(t) = \mathbb{1}. \tag{6.20}$$

A CPTP map ϕ_t is called divisible if

$$\phi_{t,0} = \phi_{t,s}\phi_{s,0}, \tag{6.21}$$

where $\phi_{t,s}$ is a CPTP map for all $t \geq s \geq 0$.

We can now say that a quantum system undergoes a Markovian time evolution [127] if the time evolution is governed by a family of CPTP maps ϕ_t that obey the composi-

tion law given by Eq. (6.21). This condition is the quantum analogue for the classical Chapman-Kolmogorov equation (6.8).

For a homogeneous in time quantum Markov process, the CPTP map [30] is given by

$$\phi_{t,t'} = e^{\mathcal{L}(t-t')}, \tag{6.22}$$

where $\mathcal{L}$ is time independent generator of the homogeneous in time quantum Markov process. The CPTP map defined by Eq. (6.22) has a semigroup structure similar to that of a homogeneous in time classical propagator in Eq. (6.11). Given the time independent generator $\mathcal{L}$ of a homogeneous-in-time quantum Markov process, the Master Equation for the reduced density matrix is

$$\frac{\mathrm{d}}{\mathrm{d}t}\rho_S(t) = \mathcal{L}\rho_S(t) = -\frac{i}{\hbar}\left[\mathcal{H}, \rho_S(t)\right] + \sum_k \gamma_k \left[V_k \rho_S(t) V_k^\dagger - \frac{1}{2}\left\{V_k^\dagger V_k, \rho_S(t)\right\}\right], \tag{6.23}$$

where $\gamma_k \geq 0 \,\forall\, k$ are the decay rates of the system and V_k are the time independent operators that define the decoherence channels. This is the Lindblad-Gorini-Kossakowski-Sudarshan theorem [31, 32]. A quantum system coupled to an environment does not always produce memory-less dynamics. Under certain situations, the Markov approximation is not valid. Since the time evolution of a quantum Markov process is defined by a family of divisible CPTP maps, the time evolution of a quantum non-Markovian process is described by a family of CPTP maps which all of them do not need to be divisible [127], hence Eq. (6.21) does not hold for all $t \geq s \geq 0$.

Recently, there have been different proposals to characterise the non-Markovianity of a quantum system that undergoes a non-Markovian time evolution. The RHP-measure by Rivas, Huelga and Plenio defines the non-Markovianity of a process based on the divisibility of the CPTP map [128], while the BLP-measure by Breuer, Laine and Piilo quantifies non-Markovianity using the time evolution of the trace distance between two different initial states [129, 130]. Although any Master Equation describing a homogeneous-in-time quantum Markov process can be written in Lindblad-like form, given by Eq. (6.23), also non-Markovian processes can be expressed in Lindblad-like form with time-dependent decay rates $\gamma_k(t)$ and decoherence channels $V_k(t)$ [33].

6.2.2 Quantum Markovian Master Equation

In this section we derive a quantum Master Equation for a Markov process [131]. In the Schrödinger picture, the time evolution for the composite system-environment density

matrix $\rho(t)$ is given by

$$\frac{\mathrm{d}}{\mathrm{d}t}\rho(t) = -\frac{i}{\hbar}\left[\mathcal{H}_S + \mathcal{H}_E + \mathcal{H}_I, \rho(t)\right], \tag{6.24}$$

where $\mathcal{H}_S$ is the system Hamiltonian, $\mathcal{H}_E$ is the environment Hamiltonian and $\mathcal{H}_I$ the interaction Hamiltonian between system and environment. Since we are interested in the effects of the interaction Hamiltonian $\mathcal{H}_I$ onto the dynamics of the composite system-environment density matrix $\rho(t)$, we move to the interaction picture by the transformation

$$\mathcal{H}_I = e^{-i\mathcal{H}_0 t/\hbar}\,\widetilde{\mathcal{H}}_I(t)\,e^{i\mathcal{H}_0 t/\hbar}, \tag{6.25}$$

$$\rho(t) = e^{-i\mathcal{H}_0 t/\hbar}\,\tilde{\rho}(t)\,e^{i\mathcal{H}_0 t/\hbar}, \tag{6.26}$$

where the noninteracting Hamiltonian is $\mathcal{H}_0 = \mathcal{H}_S + \mathcal{H}_E$, and $\widetilde{\mathcal{H}}_I$ and $\tilde{\rho}(t)$ represent the interaction Hamiltonian and the system-environment density matrix in the interaction picture. Differentiating Eq. (6.26) with respect to time yields

$$\begin{aligned}\frac{\mathrm{d}}{\mathrm{d}t}\rho(t) &= \frac{\mathrm{d}}{\mathrm{d}t}\left(e^{-i\mathcal{H}_0 t/\hbar}\,\tilde{\rho}(t)\,e^{i\mathcal{H}_0 t/\hbar}\right)\\ &= e^{-i\mathcal{H}_0 t/\hbar}\left(-i\frac{\mathcal{H}_0}{\hbar}\tilde{\rho}(t) + \dot{\tilde{\rho}}(t) + i\tilde{\rho}(t)\frac{\mathcal{H}_0}{\hbar}\right)e^{i\mathcal{H}_0 t/\hbar}\\ &= e^{-i\mathcal{H}_0 t/\hbar}\left(-\frac{i}{\hbar}\left[\mathcal{H}_0, \tilde{\rho}(t)\right] + \dot{\tilde{\rho}}(t)\right)e^{i\mathcal{H}_0 t/\hbar}.\end{aligned} \tag{6.27}$$

Substituting $\widetilde{\mathcal{H}}_I(t)$ and $\tilde{\rho}(t)$, from the inverse transformation of Eqs. (6.25) and (6.26), into the RHS of Eq. (6.24) yields

$$-\frac{i}{\hbar}\left[\mathcal{H}_0 + \mathcal{H}_I(t), \rho(t)\right] = -\frac{i}{\hbar}e^{-i\mathcal{H}_0 t/\hbar}\left[\mathcal{H}_0 + \widetilde{\mathcal{H}}_I(t), \tilde{\rho}(t)\right]e^{i\mathcal{H}_0 t/\hbar}. \tag{6.28}$$

Finally, Eqs. (6.27) and (6.28) give the time evolution for joint density matrix in the interaction picture as

$$\frac{\mathrm{d}}{\mathrm{d}t}\tilde{\rho}(t) = -\frac{i}{\hbar}\left[\widetilde{\mathcal{H}}_I(t), \tilde{\rho}(t)\right]. \tag{6.29}$$

Formally, Eq. (6.29) can be integrated to give

$$\tilde{\rho}(t) - \tilde{\rho}(0) = -\frac{i}{\hbar}\int_0^t \mathrm{d}t'\left[\widetilde{\mathcal{H}}_I(t'), \tilde{\rho}(t')\right]. \tag{6.30}$$

We substitute the formal solution of the joint density matrix (6.30) into the RHS of Eq. (6.29) to obtain

$$\frac{\mathrm{d}}{\mathrm{d}t}\tilde{\rho}\left(t\right)=-\frac{i}{\hbar}\left[\widetilde{\mathcal{H}}_{I}\left(t\right),\tilde{\rho}(0)\right]+\left(\frac{i}{\hbar}\right)^{2}\int_{0}^{t}\mathrm{d}t'\left[\widetilde{\mathcal{H}}_{I}\left(t\right),\left[\widetilde{\mathcal{H}}_{I}\left(t'\right),\tilde{\rho}\left(t'\right)\right]\right]. \tag{6.31}$$

We consider that initially the environment (a zero-temperature reservoir or a thermal reservoir) and the system are independent

$$\tilde{\rho}(0)=\tilde{\rho}_{S}(0)\otimes\rho_{E}, \tag{6.32}$$

and since the system and the environment are weak coupled, the time evolution of the composite system-environment density matrix remains factorised

$$\tilde{\rho}\left(t\right)\approx\tilde{\rho}_{S}\left(t\right)\otimes\rho_{E}. \tag{6.33}$$

Equation (6.33) is called the Born approximation as it allows a perturbative solution, Eq. (6.31), in the coupling constant as the one for the T-matrix (see Eq. (3.29) in Sec. 3.1). A differential equation for the reduced density matrix of the system, $\tilde{\rho}_{S}\left(t\right)$, is obtained by tracing out the environment in Eq. (6.31)

$$\frac{\mathrm{d}}{\mathrm{d}t}\tilde{\rho}_{S}\left(t\right)=-\frac{i}{\hbar}\mathrm{Tr}_{E}\left(\left[\widetilde{\mathcal{H}}_{I}\left(t\right),\tilde{\rho}\left(0\right)\right]\right)+\left(\frac{i}{\hbar}\right)^{2}\int_{0}^{t}\mathrm{d}t'\mathrm{Tr}_{E}\left(\left[\widetilde{\mathcal{H}}_{I}\left(t\right),\left[\widetilde{\mathcal{H}}_{I}\left(t'\right),\tilde{\rho}\left(t'\right)\right]\right]\right). \tag{6.34}$$

Let us consider that the operators representing the interaction have zero mean value in the initial state of the environment, hence the first term of the RHS in Eq. (6.34) can be simplified as follows

$$\mathrm{Tr}_{E}\left(\left[\widetilde{\mathcal{H}}_{I}\left(t\right),\tilde{\rho}_{S}(0)\otimes\rho_{E}\right]\right)=0. \tag{6.35}$$

Equation (6.34) reads now

$$\frac{\mathrm{d}}{\mathrm{d}t}\tilde{\rho}_{S}\left(t\right)=-\frac{1}{\hbar^{2}}\int_{0}^{t}\mathrm{d}t'\mathrm{Tr}_{E}\left(\left[\widetilde{\mathcal{H}}_{I}\left(t\right),\left[\widetilde{\mathcal{H}}_{I}\left(t'\right),\tilde{\rho}_{S}\left(t'\right)\otimes\rho_{E}\right]\right]\right). \tag{6.36}$$

Equation (6.36) has a explicit dependence on the initial time $t' = 0$ in the second Hamiltonian $\mathcal{H}_I(t')$. Therefore we define $\tau = t - t'$ and we express the above equation as

$$\frac{\mathrm{d}}{\mathrm{d}t}\tilde{\rho}_S(t) = -\frac{1}{\hbar^2}\int_0^t \mathrm{d}\tau \mathrm{Tr}_E\left(\left[\widetilde{\mathcal{H}}_I(t), \left[\widetilde{\mathcal{H}}_I(t-\tau), \tilde{\rho}_S(t-\tau)\otimes\rho_E\right]\right]\right). \tag{6.37}$$

Correlation times for the environment operators are typically much shorter than the typical time scales for the reduced density matrix. Therefore, the reduced density matrix for the system does not change at all in this time scale. Hence, it is possible to substitute $\tilde{\rho}_S(t-\tau) \to \tilde{\rho}_S(t)$ in the RHS of Eq. (6.37). As a consequence, the upper limit of the integral in Eq. (6.37) can go to infinity. This is the Markov approximation. Hence, the quantum Markov Master Equation reads

$$\frac{\mathrm{d}}{\mathrm{d}t}\tilde{\rho}_S(t) = -\frac{1}{\hbar^2}\int_0^\infty \mathrm{d}\tau \mathrm{Tr}_E\left(\left[\widetilde{\mathcal{H}}_I(t), \left[\widetilde{\mathcal{H}}_I(t-\tau), \tilde{\rho}_S(t)\otimes\rho_E\right]\right]\right). \tag{6.38}$$

Tracing out the environment in Eq. (6.38) yields a time-independent Lindblad-like form Master Equation, given by Eq. (6.23) [31, 32].

6.3 Light-matter interaction

In 1963 E. T. Jaynes and F. W. Cummings introduced a model to describe light-matter interaction in a completely quantised way [114]. Named after them, the Jaynes-Cummings model describes the interaction between a two-level atom and a light mode of the fully quantised electromagnetic field. In this description, $|e\rangle$ and $|g\rangle$ represent the excited and ground state of the two-level atom, respectively. The operators a and $a^\dagger$ are the annihilation and creation operator of a mode of the electromagnetic field and they obey the canonical commutation relation $\left[a, a^\dagger\right] = 1$.

The complete Hamiltonian of the system consists of three parts: the free evolution for the field, the free evolution for the atom and the interaction between the atom and the field [132, 133]. The Hamiltonian that describes the free evolution of the atom is given by

$$\mathcal{H}_A = \frac{1}{2}\hbar\omega_0\sigma_z, \tag{6.39}$$

where $\hbar\omega_0$ is the energetic distance between the two atomic levels $|g\rangle$ and $|e\rangle$, and σ_z is one of the Pauli matrices (2.8). Expressed in terms of $|g\rangle$ and $|e\rangle$, the Pauli matrix $\sigma_z = |e\rangle\langle e| - |g\rangle\langle g|$ represents the atomic inversion operator.

The free evolution of a single-mode of the electromagnetic field is described by the

harmonic oscillator Hamiltonian

$$\mathcal{H}_F = \hbar\omega \left(a^\dagger a + \frac{1}{2} \right), \tag{6.40}$$

where ω is the frequency of the mode.

The two-level atom and the electromagnetic field interact via a dipole interaction

$$\mathcal{H}_I = -\mathbf{d} \cdot \mathbf{E}, \tag{6.41}$$

where $\mathbf{E}$ is the electromagnetic field operator and $\mathbf{d}$ is the dipole moment of the atom. By parity, the only transitions allowed are between adjacent levels: from $|e\rangle$ to $|g\rangle$ and from $|g\rangle$ to $|e\rangle$. Therefore, $\mathbf{d}$ is expressed in terms of the atomic transition operators $\sigma_- = |g\rangle\langle e|$ and $\sigma_+ = |e\rangle\langle g|$ as

$$\mathbf{d} = d\sigma_+ + d^*\sigma_-, \tag{6.42}$$

where d is the dipolar coefficient, which we will consider real for simplicity. We define the interaction Hamiltonian as

$$\mathcal{H}_I = -i\hbar\Omega \left(\sigma_- + \sigma_+ \right) \left(a - a^\dagger \right), \tag{6.43}$$

where Ω is the coupling strength between the atom and the field.

With all these ingredients, the fully quantised light-matter Hamiltonian reads

$$\mathcal{H}_T = \hbar\omega \left(a^\dagger a + \frac{1}{2} \right) + \frac{1}{2}\hbar\omega_0\sigma_z - i\hbar\Omega \left(\sigma_- + \sigma_+ \right) \left(a - a^\dagger \right). \tag{6.44}$$

6.3.1 The rotating wave approximation and Jaynes-Cummings Hamiltonian

The fully quantised light-matter Hamiltonian (6.44) can be simplified by eliminating fast-rotating and non-conserving energy terms. Expanding the interaction Hamiltonian (6.43) yields four terms $\sigma_- a^\dagger$, $\sigma_- a$, $\sigma_+ a^\dagger$ and $\sigma_+ a$. Their time evolution in the interaction picture is given by

$$\sigma_\pm (t) = \sigma_\pm (0)\, e^{\pm i\omega_0 t},\ a(t) = a(0)\, e^{-i\omega t}. \tag{6.45}$$

Therefore, close to resonance ($\omega \approx \omega_0$) the terms $\sigma_+ a^\dagger \sim e^{i(\omega_0+\omega)t}$ and $\sigma_- a \sim e^{-i(\omega_0+\omega)t}$ rotate faster than $\sigma_+ a \sim e^{i(\omega_0-\omega)t}$ and $\sigma_- a^\dagger \sim e^{-i(\omega_0-\omega)t}$, hence it is possible to discard

them. These two terms also correspond to processes where energy is not conserved, as the creation of a photon of the electromagnetic field and the excitation of the two-level system ($\sigma_+ a^\dagger$), or the opposite process ($\sigma_- a$), where a photon is annihilated while the two-level system remains in the ground state. Discarding the fast rotating terms in the Hamiltonian (6.44) is called the rotating wave approximation (RWA) and yields the Jaynes-Cummings Hamiltonian [114], which in the Schrödinger picture is expressed as

$$\mathcal{H}_{JC} = \hbar\omega\left(a^\dagger a + \frac{1}{2}\right) + \frac{1}{2}\hbar\omega_0\sigma_z - i\hbar\Omega\left(\sigma_+ a - \sigma_- a^\dagger\right). \tag{6.46}$$

Let us fist calculate the eigenstates of the Jaynes-Cummings Hamiltonian (6.46). In the subspace spanned by $\{|n\rangle, |n+1\rangle\}$, Eq. (6.46) is written in matrix form as

$$\mathcal{H}_{JC} = \hbar\begin{pmatrix} \omega n + \frac{1}{2}\omega_0 & -i\Omega\sqrt{n+1} \\ i\Omega\sqrt{n+1} & \omega(n+1) - \frac{1}{2}\omega_0 \end{pmatrix}, \tag{6.47}$$

where n is the eigenvalue of the electromagnetic field number operator $a^\dagger a$ acting on the state $|n\rangle$ and the zero-point energy of the electromagnetic field $\hbar\omega/2$ has been dropped. The corresponding eigenvalues of the Jaynes-Cummings Hamiltonian (6.47) are given by

$$E_\pm = E_n \pm \frac{\hbar}{2}\sqrt{\Delta^2 + 4\Omega^2(n+1)} \tag{6.48}$$

where $E_n = \hbar\omega(n + 1/2)$ is the energy of a mode of the electromagnetic field, $\Delta = \omega_0 - \omega$ is the detuning of the system and we introduce $\lambda = \sqrt{\Delta^2 + 4\Omega^2(n+1)}$ for simplicity. The dressed states $\{|n,+\rangle, |n,-\rangle\}$ are the eigenstates of the Jaynes-Cummings Hamiltonian (6.47), they can be written in terms of the bare states $\{|e\rangle\otimes|n\rangle, |g\rangle\otimes|n+1\rangle\}$ as

$$|n,+\rangle = i\cos\frac{\theta}{2}|e\rangle\otimes|n\rangle + \sin\frac{\theta}{2}|g\rangle\otimes|n+1\rangle, \tag{6.49}$$

$$|n,-\rangle = \sin\frac{\theta}{2}|e\rangle\otimes|n\rangle + i\cos\frac{\theta}{2}|g\rangle\otimes|n+1\rangle, \tag{6.50}$$

where

$$\cos\frac{\theta}{2} = \frac{2\Omega\sqrt{n+1}}{\sqrt{4\Omega^2(n+1) + (\Delta-\lambda)^2}}, \tag{6.51}$$

$$\sin\frac{\theta}{2} = \frac{\Delta-\lambda}{\sqrt{4\Omega^2(n+1) + (\Delta-\lambda)^2}}. \tag{6.52}$$

The time evolution of the state is given by the time-dependent Schrödinger equation

$$\mathcal{H}_{JC}\left|\Psi\left(t\right)\right\rangle = i\hbar\frac{\partial}{\partial t}\left|\Psi\left(t\right)\right\rangle, \tag{6.53}$$

where the time-dependent state of the system is expressed in the bare state basis as

$$\left|\Psi\left(t\right)\right\rangle = c_e\left(t\right)\left|e\right\rangle\otimes\left|n\right\rangle + c_g\left(t\right)\left|g\right\rangle\otimes\left|n+1\right\rangle, \tag{6.54}$$

where $c_e\left(t\right)$ and $c_g\left(t\right)$ are the time-dependent coefficients that determine the time evolution. Substituting Eq. (6.54) into the time-dependent Schrödinger equation (6.53) yields a system of first order differential equation for the time-dependent coefficients $c_e\left(t\right)$ and $c_g\left(t\right)$

$$-i\begin{pmatrix} \omega n+\frac{1}{2}\omega_0 & -i\Omega\sqrt{n+1} \\ i\Omega\sqrt{n+1} & \omega\left(n+1\right)-\frac{1}{2}\omega_0 \end{pmatrix}\begin{pmatrix} c_e\left(t\right) \\ c_g\left(t\right) \end{pmatrix} = \begin{pmatrix} \dot{c}_e\left(t\right) \\ \dot{c}_g\left(t\right) \end{pmatrix}, \tag{6.55}$$

If we use for instance the initial conditions $c_g\left(0\right)=0$ and $c_e\left(0\right)=1$, i.e., initially the system is in the excited state, the system evolves as

$$\begin{aligned}\left|\Psi\left(t\right)\right\rangle = e^{-iE_nt/\hbar}\left(e^{-i\lambda t/2}\cos^2\frac{\theta}{2}+e^{i\lambda t/2}\sin^2\frac{\theta}{2}\right)\left|e\right\rangle\otimes\left|n\right\rangle \\ -e^{-iE_nt/\hbar}\sin\theta\sin\left(\frac{\lambda t}{2}\right)\left|g\right\rangle\otimes\left|n+1\right\rangle.\end{aligned} \tag{6.56}$$

Let us calculate now the expectation value of the inversion operator σ_z in the time-dependent state defined by Eq. (6.56). Hence, we obtain

$$\begin{aligned}\left\langle\sigma_z\right\rangle_{\left|\Psi(t)\right\rangle} &= \left\langle\Psi\left(t\right)|e\right\rangle\left\langle e|\Psi\left(t\right)\right\rangle - \left\langle\Psi\left(t\right)|g\right\rangle\left\langle g|\Psi\left(t\right)\right\rangle \\ &= 1-2\sin^2\theta\sin^2\left(\frac{\lambda t}{2}\right).\end{aligned} \tag{6.57}$$

Setting the detuning Δ to zero, gives $\lambda=2\Omega\sqrt{n+1}$ and $\sin\theta=1$, therefore Eq. (6.57) yields

$$\left\langle\sigma_z\right\rangle_{\left|\Psi(t)\right\rangle} = \cos\left(2\Omega\sqrt{n+1}t\right), \tag{6.58}$$

which allows us to define the Rabi frequency as $\omega_R=2\Omega\sqrt{n+1}$, see Ref. [132, 133]. This frequency defines the transition of population between the ground state $\left|g\right\rangle$ and the excited state $\left|e\right\rangle$. It was introduced by Rabi in his semiclassical approach in 1937 [134].

6.4 Master Equation for a two-level system

In this section we show how different time evolutions of a two-level system yield the same Master Equation for the reduced density matrix of the system. The Kraus decomposition for the reduced density matrix of the two-level system is

$$\rho_S(t) = \sum_{k=1}^{2} A_k(t)\,\rho_S(0)\,A_k^\dagger(t)\,, \tag{6.59}$$

where the Kraus operators are defined as

$$A_1(t) = |g\rangle\langle g| + f(t)\,|e\rangle\langle e|, \tag{6.60}$$

$$A_2(t) = \sqrt{1-|f(t)|^2}|g\rangle\langle e|, \tag{6.61}$$

and $f(t)$ is a continuous real-valued function, bounded by $0 \leq |f(t)| \leq 1$, see Ref. [135]. The Kraus operators fulfil

$$\begin{aligned}\sum_{k=1}^{2} A_k^\dagger(t)\,A_k(t) &= A_1^\dagger(t)\,A_1(t) + A_2^\dagger(t)\,A_2(t)\\ &= |g\rangle\langle g| + |f(t)|^2\,|e\rangle\langle e| + \left(1-|f(t)|^2\right)|e\rangle\langle e|\\ &= |g\rangle\langle g| + |e\rangle\langle e|\\ &= \mathbb{1}.\end{aligned} \tag{6.62}$$

The time evolution of the reduced density matrix (6.59) is

$$\begin{aligned}\rho_S(t) = |f(t)|^2\,\rho_{ee}(0)\,|e\rangle\langle e| + \left[\rho_{gg}(0) + \left(1-|f(t)|^2\right)\rho_{ee}(0)\right]|g\rangle\langle g|\\ + f(t)\,\rho_{eg}(0)\,|e\rangle\langle g| + f^*(t)\,\rho_{ge}(0)\,|g\rangle\langle e|.\end{aligned} \tag{6.63}$$

If the system is initially in the excited state $\rho(0) = |e\rangle\langle e|$, then Eq. (6.63) reads

$$\rho_S(t) = |f(t)|^2\,|e\rangle\langle e| + \left(1-|f(t)|^2\right)|g\rangle\langle g|. \tag{6.64}$$

Accordingly to Ref.[135], the time evolution (6.64) corresponds to a time-local Lindblad-like Master Equation given by

$$\dot{\rho}_S(t) = -\frac{\dot{f}(t)}{f(t)}\left(2\sigma_-\rho(t)\,\sigma_+ - \sigma_+\sigma_-\rho(t) - \rho(t)\,\sigma_+\sigma_-\right). \tag{6.65}$$

Inspection of Eq. (6.65) allows us to define a time dependent decay rate for the transition between the excited level $|e\rangle$ and the ground level $|g\rangle$ as

$$\gamma(t) = -\frac{2\dot{f}(t)}{f(t)}. \tag{6.66}$$

Analysing the function $f(t)$ it is possible to determine certain aspects of the Master Equation (6.65). The decay rate is positive, and therefore it corresponds to a Markovian process if $f(t)$ is positive (negative) and monotonically decreasing (increasing). On the other hand, the process described by the Master Equation (6.65) has negative decay rate, hence it is non-Markovian [33] if $f(t)$ is positive (negative) and monotonically increasing (decreasing).

The existence and uniqueness theorem, (see Appendix B), sets the conditions to determine if the solution of a differential equation is unique. The differential equation (6.65) is not invertible when $f(t) = 0$, independently of the initial conditions, therefore it admits multiple solutions in any subset of $\mathbb{R}$ where $f(t) = 0$. Setting $f(t) = 0$ in Eq. (6.64) yields

$$\rho_S(t)|_{f(t)=0} = \rho_{ee}(0)\,|g\rangle\langle g|. \tag{6.67}$$

Hence Eq. (6.65) has one and only one solution in a time interval $[t_1, t_2]$ if the system does not reach the ground state in that interval.

Let us now show how different time evolutions of the reduced density matrix $\rho(t)$ yield the same Master Equation (6.65). The first case we consider corresponds to a choice of $f(t) = \cos(\omega t)$ and $\rho(0) = |e\rangle\langle e|$ as initial condition. Substituting $f(t) = \cos(\omega t)$ into Eq. (6.64) yields the time evolution of the reduced density matrix, given by

$$\rho_S(t) = \cos^2(\omega t)\,|e\rangle\langle e| + \sin^2(\omega t)\,|g\rangle\langle g|. \tag{6.68}$$

Substituting $f(t) = \cos(\omega t)$ in the time-local Master Equation (6.65) yields

$$\dot{\rho}_S(t) = 2\omega\tan(\omega t)\left(\sigma_+\rho(t)\,\sigma_- - \frac{1}{2}\{\rho(t), \sigma_+\sigma_-\}\right), \tag{6.69}$$

where $\gamma(t) = 2\omega\tan(\omega t)$ is the time-dependent decay rate. The decay rate is negative when $\omega t \in \pi(-1/2 + n, n)$ and it diverges when the evolution becomes non-invertible at $\omega t = \pi(n + 1/2)$, where $n \in \mathbb{Z}$.

The second time evolution we consider starts with the same choice of $f(t)$ (system

on-resonance) and initial conditions as before. When the system reaches the ground state $|g\rangle$, the Hamiltonian is rapidly switched to off-resonance ($\Delta \neq 0$). This change happens at $\omega t = \pi\,(n + 1/2)$. Changing from an on-resonance evolution to an off-resonance evolution implies that the function $f\,(t) = \cos(\omega t)$ changes to $f\,(t) = A\cos(\omega t)$, where $0 < A < 1$. From this point onwards the time evolution of the reduced density matrix (6.64) is

$$\rho_S\,(t) = A^2\cos^2(\omega t)\,|e\rangle\langle e| + \left[1 - A^2\cos^2(\omega t)\right]|g\rangle\langle g|. \tag{6.70}$$

Substituting now $f\,(t) = A\cos(\omega t)$ into the time-local Master Equation (6.65) yields the same Master Equation as $f\,(t) = \cos(\omega t)$, Eq. (6.69).

6.5 Hamiltonian and time evolution

The Jaynes-Cummings Hamiltonian (6.46) gives the perfect example to explicitly construct two different Hamiltonians, therefore two different time evolutions, that correspond to the same time-local Master Equation. In order to simplify the calculations, we will restrict to the subspace spanned by $\{|e\rangle \otimes |0\rangle\,, |g\rangle \otimes |1\rangle\}$. Hence Eq. (6.55) reduces to

$$-i\begin{pmatrix} \frac{\Delta}{2} & -i\Omega \\ i\Omega & -\frac{\Delta}{2} \end{pmatrix}\begin{pmatrix} c_e\,(t) \\ c_g\,(t) \end{pmatrix} = \begin{pmatrix} \dot{c}_e\,(t) \\ \dot{c}_g\,(t) \end{pmatrix}, \tag{6.71}$$

where zero-point energy $\hbar\omega/2$ has been dropped. We introduce τ as the scale of the problem to use dimensionless units, $\tilde{t} = t/\tau$, $\tilde{\omega}_0 = \tau\omega_0$, $\tilde{\omega} = \tau\omega$, $\tilde{\Omega} = \tau\Omega$ and $\tilde{\Delta} = \tau\Delta$. The eigenvalues of the time dependent Schrödinger equation (6.55) are $\tilde{\omega}_R = \pm\frac{1}{2}\sqrt{\tilde{\Delta}^2 + 4\tilde{\Omega}^2}$ as the scaled Rabi frequency. By varying $\tilde{\Delta}$ and $\tilde{\Omega}$ but keeping $\tilde{\omega}_R$ constant, we can construct two different Hamiltonian that give the same Master Equation, Eq. (6.69).

The first case to be considered corresponds to a Jaynes-Cummings Hamiltonian on-resonance ($\tilde{\Delta} = 0$), see Fig. 6.1(a). From Eq. (6.56) we get to

$$|\Psi\,(t)\rangle = \cos\left(\tilde{\omega}_R\tilde{t}\right)|e\rangle \otimes |0\rangle - \sin\left(\tilde{\omega}_R\tilde{t}\right)|g\rangle \otimes |1\rangle\,. \tag{6.72}$$

From Eq. (6.51) and Eq. (6.52) it is easy to see that $\Delta = 0$ implies $\sin\theta = 1$ and $\sin(\theta/2) = \cos(\theta/2) = 1/\sqrt{2}$. The reduced density matrix for the system reads then

$$\rho_S\left(\tilde{t}\right) = \cos^2\left(\tilde{\omega}_R\tilde{t}\right)|e\rangle\langle e| + \sin^2\left(\tilde{\omega}_R\tilde{t}\right)|g\rangle\langle g|. \tag{6.73}$$

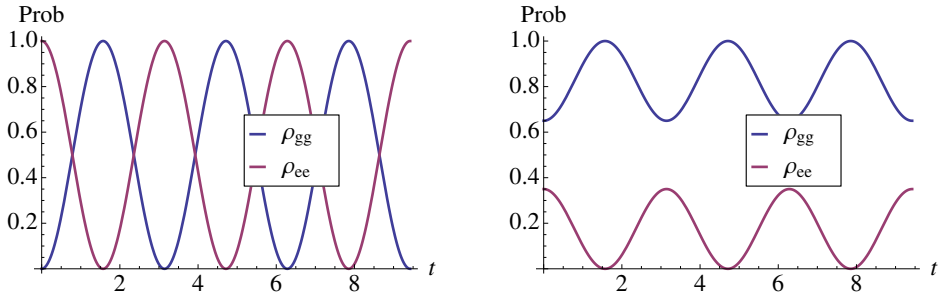

(a) On-resonance oscillations ($\Delta = 0$). (b) Off-resonance oscillations ($\Delta \neq 0$)

Figure 6.1: On-resonance and off-resonance oscillations for the diagonal elements of the density matrix in the Jaynes-Cummings model.

The second case we considered consists of a Jaynes-Cummings Hamiltonian with a time dependent coupling $\tilde{\Omega}(t)$ and a time dependent detuning $\tilde{\Delta}(t)$ provided that the Rabi frequency is kept constant, hence $\tilde{\omega}_R = \frac{1}{2}\sqrt{\tilde{\Delta}^2(t) + 4\tilde{\Omega}^2(t)}$. The system will evolve from an on-resonance evolution ($\tilde{\Delta}(t) = 0$) with $\tilde{\Omega}(t) = \tilde{\Omega}$ to an off-resonance ($\tilde{\Delta}(t) \neq 0$), where the coupling is $\tilde{\Omega}(t) = \tilde{\Omega}'$. The change from on-resonance to off-resonance evolution is performed when the two-level atom is in the ground state and the cavity in the first excited level $|g\rangle \otimes |1\rangle$. From Eq. (6.73) we see that this happens when $\tilde{\omega}_R \tilde{t}_i = (n + 1/2)\pi$, where $n \in \mathbb{N}$. Solving Eq. (6.71) with initial conditions $c_e(\tilde{t}_i) = 0$ and $c_g(\tilde{t}_i) = 1$ allows us to construct the time evolution of the reduced density matrix as

$$\rho_S(\tilde{t}) = \left|\frac{\tilde{\Omega}'}{\tilde{\omega}_R}\right|^2 \cos^2(\tilde{\omega}_R \tilde{t})\,|e\rangle\langle e| + \left[1 - \left|\frac{\tilde{\Omega}'}{\tilde{\omega}_R}\right|^2 \cos^2(\tilde{\omega}_R \tilde{t})\right]|g\rangle\langle g| \tag{6.74}$$

If the change is instantaneous and occurs at the right time, i.e., when the time evolution is non-invertible, then the Master Equation for Eqs. (6.73) and (6.74), is the same, Eq. (6.69).

6.5.1 Evolution with time-dependent coupling

The system evolves from on-resonance to off-resonance by a simultaneous change in the detuning $\tilde{\Delta}$ and the coupling $\tilde{\Omega}$ that keeps the Rabi frequency $\tilde{\omega}_R$ constant. We introduce a time-dependent coupling $\Omega(t)$ that changes smoothly from a maximum value Ω_{max} to a minimum value Ω_{min} as

$$\Omega(t) = \frac{\Omega_{\text{max}} - \Omega_{\text{min}}}{2}\left[1 - \tanh\left(k\left[t - t_i\right]\right)\right] + \Omega_{\text{min}}, \tag{6.75}$$

where $k = \tilde{k}/\tau$ controls the rate of change - slope of the function - and t_i is the point at which $\Omega(t)$ takes it average value $(\Omega_{\text{max}} + \Omega_{\text{min}})/2$, Fig. 6.2. The detuning changes

as $\tilde{\Delta}(t) = \sqrt{2\tilde{\omega}_R^2 - 4\tilde{\Omega}^2(t)}$ with $\tilde{\omega}_R$ constant. Changing the coupling strength might be feasible in cavity QED [136] by changing the position of an atom in a laser cavity or by changing the laser field strength. In circuit QED, it is possible to realise tunable resonators [137, 138].

We solve Eq. (6.71) for $c_g(t)$ and $c_e(t)$ with initial conditions $c_g(0) = 0$ and $c_e(0) = 1$. The solution for $\tilde{k} = 1.6$, depicted in Fig. 6.3, shows how the time-dependent coupling (6.75) changes from $\tilde{\Omega} = 0.3$ to $\tilde{\Omega} = 0.2$ when the system is in the ground state, $\tilde{t}_i$ is chosen to have $c_g(\tilde{t}_i) = 0$. If the time-dependent coupling $\tilde{\Omega}(t)$ does not change fast enough, the system evolves off-resonance but it does not reach the ground state anymore, Fig. 6.4. Fourier analysis of the time-dependent coefficient $c_e(t)$ (see Fig. 6.5) confirms that the Rabi frequency remains constant during the time evolution.

6.5.2 How rapidly should the coupling change?

The impulse approximation [139] states that if a Hamiltonian changes smoothly from $\mathcal{H}(t_0) = \mathcal{H}_0$ at t_0 to $\mathcal{H}(t_1) = \mathcal{H}_1$ at t_1, then the probability that the system remains in the previous state $|\psi_0\rangle$ from $\mathcal{H}_0$ is

$$\xi = \frac{T^2}{\hbar^2}\left(\langle\psi_0|\,\overline{\mathcal{H}}^2\,|\psi_0\rangle - \langle\psi_0|\,\overline{\mathcal{H}}\,|\psi_0\rangle^2\right), \tag{6.76}$$

where $T = t_1 - t_0$ and

$$\overline{\mathcal{H}} = \frac{1}{T}\int_{t_0}^{t_1} \mathrm{d}t\mathcal{H}(t) \tag{6.77}$$

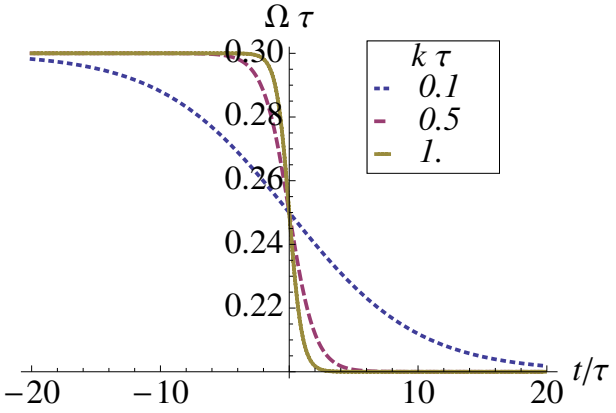

Figure 6.2: Scaled coupling strengths $\tilde{\Omega} = \tau\Omega$ for different rates of change $\tilde{k} = \tau k$, varying according to Eq. (6.75) with $\tilde{t}_i = t_i/\tau = 0$, $\tilde{\Omega}_{\text{max}} = 0.3$ and $\tilde{\Omega}_{\text{min}} = 0.2$.

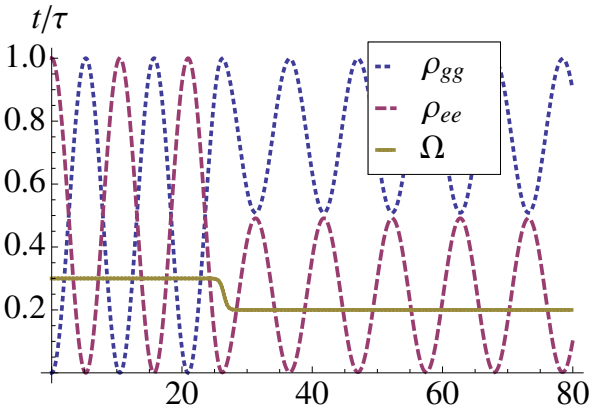

Figure 6.3: Time evolution of the reduced density matrix elements of the atom for changing detuning $\tilde{\Delta}(t)$ and time-dependent coupling $\tilde{\Omega}(t)$ with $\tilde{\Omega}_{\text{max}} = 0.3$ and $\tilde{\Omega}_{\text{min}} = 0.2$. The Rabi frequency $\tilde{\omega}_R = 0.3$ is kept constant. The dotted line (blue) shows $\rho_{gg}(\tilde{t})$ and the dashed line (red) $\rho_{ee}(\tilde{t})$. The parameter controlling the rate of change of the coupling $\tilde{\Omega}(t)$ is given by $\widetilde{k} = 1.6$. The solid line (gold) shows how the coupling is changing.

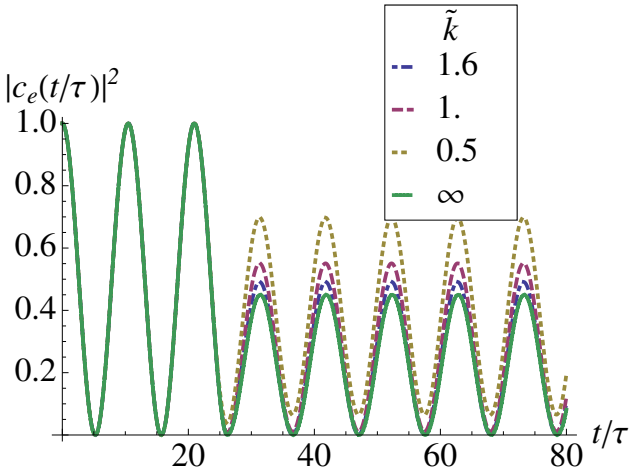

Figure 6.4: Time evolution of $\rho_{ee}(t)$ for different values of $\widetilde{k}$. The dotted curve (gold) corresponds to $\widetilde{k} = 0.5$, in which case the system never reaches the ground state. As will be seen later, this affects the decay rate. The dashed curve (red) corresponds to $\widetilde{k} = 1.0$ and the dot-dashed (blue) one to $\widetilde{k} = 1.6$. The solid line (green) corresponds to $\widetilde{k} \to \infty$, that is, an instant change.

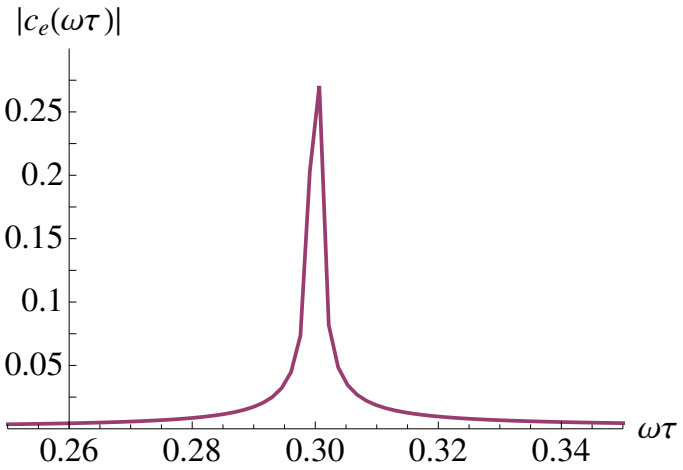

Figure 6.5: Fourier analysis of $c_e(\tilde{t})$ with $\tilde{k} = 1.6$, $\tilde{\Omega}_{\text{max}} = 0.3$ and $\tilde{\Omega}_{\text{min}} = 0.2$. When $k \to \infty$, $c_e(t)$ and $c_g(t)$ are piecewise defined functions, with $c_e(t) = \cos(\omega_R t)$ if $t < t_i$ and $c_e(t) = A\cos(\omega_R t)$ if $t > t_i$, with $0 < A < 1$, and $c_g(t) = \sqrt{1 - |c_e(t)|^2}$ (up to a phase sign). Fourier analysis of $c_e(t)$ when $k \to \infty$ gives a delta-function peak at $\tilde{\omega}_R = \tau\omega_R = 0.3$, together with a term proportional to $1/\tau(\omega - \omega_R)$.

is the averaged value of the Hamiltonian in T. We impose $\xi \ll 1$ in order to make sure that the system evolves from $|\psi_0\rangle$ to $|\psi_1\rangle$. The initial and final Hamiltonian correspond to $\mathcal{H}_0 = \mathcal{H}(\Omega_{\text{max}})$ and $\mathcal{H}_1 = \mathcal{H}(\Omega_{\text{min}})$ respectively.[1] We write the initial state of the system as

$$|\Psi(t_0)\rangle = c_e(t_0)|e\rangle \otimes |n\rangle + c_g(t_0)|g\rangle \otimes |n+1\rangle . \tag{6.78}$$

The time averaged Hamiltonian (6.71) reads

$$\overline{\mathcal{H}} = \hbar \begin{pmatrix} \frac{\overline{\Delta}}{2} & -i\overline{\Omega} \\ i\overline{\Omega} & -\frac{\overline{\Delta}}{2} \end{pmatrix}, \tag{6.79}$$

then also is straightforward to obtain

$$\overline{\mathcal{H}}^2 = \hbar^2 \begin{pmatrix} \frac{\overline{\Delta}^2}{4} + \overline{\Omega}^2 & 0 \\ 0 & \frac{\overline{\Delta}^2}{4} + \overline{\Omega}^2 \end{pmatrix}. \tag{6.80}$$

[1] During this section of the Chapter, the tilde that represents dimensionless variables will be omitted as expressions will get overloaded with notation.

The expectation value of the Hamiltonian (6.79) is

$$\begin{aligned}
\langle \Psi(t)| \overline{\mathcal{H}} |\Psi(t)\rangle &= \hbar \langle \Psi(t)| \begin{pmatrix} \frac{\overline{\Delta}}{2} & -i\overline{\Omega} \\ i\overline{\Omega} & -\frac{\overline{\Delta}}{2} \end{pmatrix} |\Psi(t)\rangle \\
&= \hbar \left(c_e^*(t), c_g^*(t)\right) \begin{pmatrix} \frac{\overline{\Delta}}{2} & -i\overline{\Omega} \\ i\overline{\Omega} & -\frac{\overline{\Delta}}{2} \end{pmatrix} \begin{pmatrix} c_e(t) \\ c_g(t) \end{pmatrix} \\
&= \hbar \frac{\overline{\Delta}}{2} \left(|c_e(t)|^2 - |c_g(t)|^2 \right) + i\hbar\overline{\Omega} \left[c_g^*(t) c_e(t) - c_e(t) c_g^*(t) \right] \\
&= \hbar \frac{\overline{\Delta}}{2} \left(|c_e(t)|^2 - |c_g(t)|^2 \right) - 2\hbar\overline{\Omega} \mathrm{Im} \left[c_g^*(t) c_e(t) \right]. \qquad (6.81)
\end{aligned}$$

The expectation value of Eq. (6.80) reads

$$\begin{aligned}
\langle \Psi(t)| \overline{\mathcal{H}}^2 |\Psi(t)\rangle &= \hbar^2 \langle \Psi(t)| \begin{pmatrix} \frac{\overline{\Delta}^2}{4} + \overline{\Omega}^2 & 0 \\ 0 & \frac{\overline{\Delta}^2}{4} + \overline{\Omega}^2 \end{pmatrix} |\Psi(t)\rangle \\
&= \hbar^2 \left(c_e^*(t), c_g^*(t)\right) \begin{pmatrix} \frac{\overline{\Delta}^2}{4} + \overline{\Omega}^2 & 0 \\ 0 & \frac{\overline{\Delta}^2}{4} + \overline{\Omega}^2 \end{pmatrix} \begin{pmatrix} c_e(t) \\ c_g(t) \end{pmatrix} \\
&= \hbar^2 \left(\frac{\overline{\Delta}^2}{4} + \overline{\Omega}^2 \right) \left(|c_e(t)|^2 + |c_g(t)|^2 \right) \\
&= \hbar^2 \left(\frac{\overline{\Delta}^2}{4} + \overline{\Omega}^2 \right), \qquad (6.82)
\end{aligned}$$

since $|c_e(t)|^2 + |c_g(t)|^2 = 1$, due to normalisation condition. The probability that after a time t the system is still in the initial state is

$$\xi = T^2 \left(\frac{\overline{\Delta}^2}{4} + \overline{\Omega}^2 - \left(\frac{\overline{\Delta}}{2} \left(|c_e(t)|^2 - |c_g(t)|^2 \right) - 2\overline{\Omega} \mathrm{Im} \left[c_g^*(t) c_e(t) \right] \right)^2 \right). \qquad (6.83)$$

The last term of the RHS of Eq. (6.83) vanishes as both coefficients are real since the system is on-resonance initially. Therefore Eq. (6.83) can be reduced to

$$\begin{aligned}
\xi &= T^2 \left(\frac{\overline{\Delta}^2}{4} + \overline{\Omega}^2 \frac{\overline{\Delta}}{2} \left(1 - 2|c_g(t)|^2 \right)^2 \right) \\
&= T^2 \left(\overline{\Omega}^2 + \overline{\Delta}^2 |c_g(t)|^2 \left(1 - |c_g(t)|^2 \right) \right) \\
&= T^2 \left(\overline{\Omega}^2 + \overline{\Delta}^2 |c_g(t)|^2 |c_e(t)|^2 \right). \qquad (6.84)
\end{aligned}$$

Imposing $\xi \ll 1$ to Eq. (6.84) is

$$T^2\left(\overline{\Omega}^2+\overline{\Delta}^2\left|c_g\left(t\right)\right|^2\left|c_e\left(t\right)\right|^2\right)\ll 1. \tag{6.85}$$

If we consider the time averaged detuning to be real $\left(\overline{\Delta}\in \text{Re}\right)$ then the following inequality holds

$$T^2\overline{\Omega}^2 \ll T^2\left(\overline{\Omega}^2+\overline{\Delta}^2\left|c_g\left(t\right)\right|^2\left|c_e\left(t\right)\right|^2\right). \tag{6.86}$$

Finally, the above inequality yields

$$T^2\overline{\Omega}^2 \ll 1. \tag{6.87}$$

The time averaged coupling is

$$\begin{aligned}\overline{\Omega} &= \frac{1}{T}\int_{t_0}^{t_1}\mathrm{d}t\Omega\left(t\right)\\ &= \frac{1}{T}\int_{t_0}^{t_1}\mathrm{d}t\left(\frac{\Omega_{\text{max}}-\Omega_{\text{min}}}{2}\left[1-\tanh\left(k\left[t-t_i\right]\right)\right]+\Omega_{\text{min}}\right)\\ &= \frac{\Omega_{\text{max}}+\Omega_{\text{min}}}{2}-\frac{\Omega_{\text{max}}-\Omega_{\text{min}}}{2kT}\ln\left(\frac{\cosh\left[k\left(t_1-t_i\right)\right]}{\cosh\left[k\left(t_0-t_i\right)\right]}\right).\end{aligned} \tag{6.88}$$

Working in a symmetric time interval ($-t_0 = t_1$) simplifies the last expression, so the average value of the coupling reads

$$\overline{\Omega} = \frac{\Omega_{\text{max}}+\Omega_{\text{min}}}{2} \tag{6.89}$$

Condition in Eq. (6.87) reads now

$$\frac{T^2\left(\Omega_{\text{max}}+\Omega_{\text{min}}\right)^2}{4} \ll 1, \tag{6.90}$$

which leads to

$$\frac{T\left(\Omega_{\text{max}}+\Omega_{\text{min}}\right)}{2} \ll 1, \tag{6.91}$$

Achieving this limits experimentally can be challenging and difficult as it involves controlling simultaneously the coupling and the detuning.

6.5.3 Decay rate in the time-local master equation

In this section we will compute the decay rate (6.66). Since the time evolution of the reduced density matrix element is $\rho_{ee}(t) = |f(t)|^2 \rho_{ee}(0)$, where $f(t)$ is real, then

$$\dot{f}(t) = \frac{1}{2f(t)} \frac{\dot{\rho}_{ee}(t)}{\rho_{ee}(0)}. \tag{6.92}$$

Substituting Eq. (6.92) into Eq. (6.66) we obtain a time dependent decay rate

$$\gamma(t) = -\frac{1}{f^2(t)} \frac{\dot{\rho}_{ee}(t)}{\rho_{ee}(0)}. \tag{6.93}$$

Figure 6.6 shows how the decay rate approaches the ideal case of an instantaneous change $\gamma(t) = 2\omega_R \tan(\omega_R t)$, as $\tilde{k}$ grows. The decay rate does not give enough information to distinguish two different time evolutions if the coupling changes fast enough at the right time. The decay rate becomes negative in certain time intervals which correspond to "recoherence" of the system and hence, to non-Markovian time evolution [33].

6.5.4 Master Equation for a two-level system with time-dependent coupling

In this section we will sketch the microscopical derivation of the Master Equation for a two-level atom interacting with a cavity via a time-dependent coupling $\Omega(t)$, given by Eq. (6.96). Let us start by defining the noninteracting Hamiltonian as

$$\mathcal{H}_0 = \hbar\omega \left(a^\dagger a + \frac{1}{2} \right) + \frac{\hbar\omega_0}{2} \sigma_z. \tag{6.94}$$

We now write the time-dependent interaction Hamiltonian in the Schrödinger picture as $\mathcal{H}_I(t) \equiv \Omega(t) \mathcal{H}_I$. This is done to explicitly point out the importance of the time-dependent coupling in the analysis. The interaction Hamiltonian then reads

$$\Omega(t) \mathcal{H}_I = -i\hbar\Omega(t) \left(a\sigma_+ - a^\dagger \sigma_- \right). \tag{6.95}$$

Following the steps in Sec. 6.2.2, we get to a Master Equation for the reduced density matrix of the system, similar to Eq. (6.37), given by

$$\frac{\mathrm{d}}{\mathrm{d}t} \tilde{\rho}_S(t) = -\frac{\Omega(t)}{\hbar^2} \int_0^t \mathrm{d}\tau \Omega(t-\tau) \operatorname{Tr}_E \left(\left[\widetilde{\mathcal{H}}_I(t), \left[\widetilde{\mathcal{H}}_I(t-\tau), \tilde{\rho}_S(t-\tau) \otimes \rho_E \right] \right] \right). \tag{6.96}$$

In order to reach to Eq. (6.96) only the Born approximation, Eq. (6.33), was used. Hence, solving Eq. (6.96), a non-Markovian integro-differential equation, might give evidence of

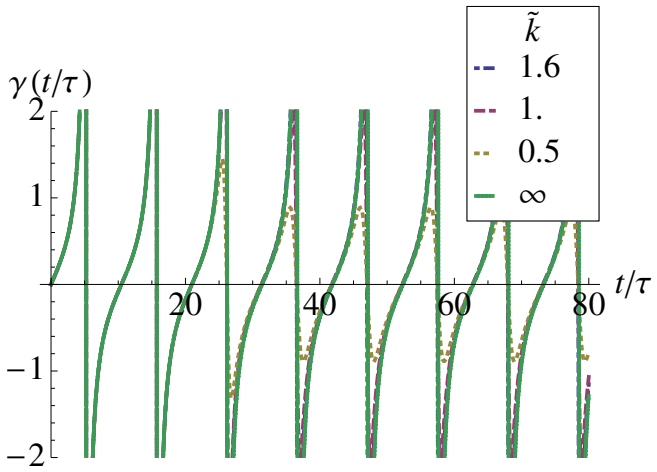

Figure 6.6: Decay rate for different values of $\tilde{k}$. The dotted curve (gold) corresponds to $\tilde{k} = 0.5$, the dashed curve (red) corresponds to $\tilde{k} = 1.0$ and the dot-dashed line (blue) to $\tilde{k} = 1.6$. The solid line (green) corresponds to $\tilde{k} \to \infty$.

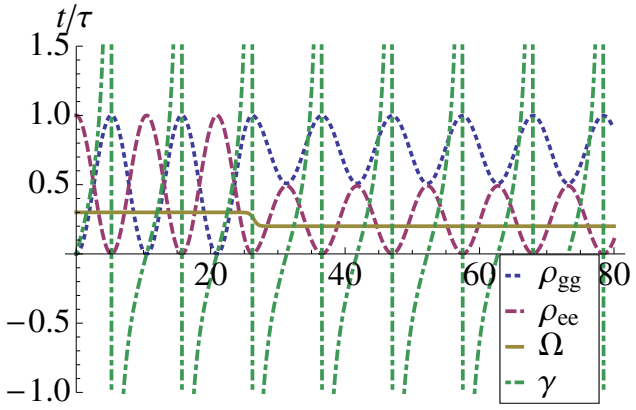

Figure 6.7: This figure shows the numerically obtained decay rate, the time evolution of the reduced density matrix elements and the change in the coupling for our example with the Jaynes-Cummings model. The dotted line (blue) and dashed line (red) correspond to $\rho_{gg}(t)$ and $\rho_{ee}(t)$ respectively. The dot-dashed line (green) represents the tangent-like decay rate and the solid line (gold) the time-dependent coupling with $\tilde{\Omega}_{\text{max}} = 0.3$, $\tilde{\Omega}_{\text{min}} = 0.2$ and $\tilde{k} = 1.6$.

the system changing from an on-resonance evolution to an off-resonance evolution.

6.6 Conclusions

In this Chapter we have investigated time-local Master Equations through an example involving a two-level system. We constructed two different system-environment Hamiltonians, corresponding to two different time evolutions for the system, which nevertheless both give the same time-local Master Equation. This explicitly shows that the time-local Master Equation on its own is not enough to solve for the time evolution, if the time evolution is not invertible.

The example is nevertheless somewhat artificial since it involves rapid changes in one of the system-environment Hamiltonians at a specific instant in time. If any Hamiltonian is guaranteed to be "physically well-behaved", for example, that it is continuous and does not change too fast (or more precisely, that its matrix elements are Lipshitz-continuous), one may conjecture that the corresponding time-local Master Equation does determine the time evolution, at least in principle, even when the time evolution is not invertible. This would in other words mean that two "physically well-behaved" system-environment Hamiltonians, corresponding to different time evolutions for a quantum system when its environment is traced out, cannot both lead to the same Master Equation for the system. Equivalently, this would mean that if a Master Equation does not have a unique solution, then at least one of the solutions corresponds to an "ill-behaved" system-environment Hamiltonian involving rapid changes.

Now, as our example shows, even a "well-behaved" Hamiltonian, such as the one in the Jaynes-Cummings model on resonance, may result in divergencies in the decay rate in the corresponding Master Equation. The usual theorems related to the existence and uniqueness of solutions of differential equations are of little help in proving our conjecture. The Picard-Lindelöf theorem, for example, just tells us that the solution of such a Master Equation, with diverging decay rates, is not unique. If the decay rates in a Lindblad-like Master Equation do not diverge, then its solution would be unique – but this simply corresponds to the case where the time evolution is always invertible. When the time evolution is not invertible, then decay rates will inevitably diverge at these times, and as already stated, this can and does happen even for very well-behaved system-environment Hamiltonians.

If the time evolution is not invertible, then even if our conjecture holds true, and if the Hamiltonian is well-behaved enough for the time evolution to be uniquely defined by the

time-local in a formal sense, one would still need to take care when numerically solving a time-local Master Equation. This is because the diverging decay rates may lead to instabilities in numerical calculations. Nonetheless, our results would generally support the view that time local Master Equations are applicable to a wider class of problems than one might expect on first inspection.

Chapter 7

Conclusions

This thesis focuses on two different topics, the first one a spin-orbit-coupled condensed matter system, while the second one considered a problem from open quantum systems. Let us summarise here the most important achievements presented in this thesis.

We have strongly emphasised the importance of Rashba-coupled spin-orbit systems on the development of future technologies and applications, such as quantum computation or superconductivity. In Chapter 2 we reviewed the origin of spin as a relativistic quantum mechanical effect and we described the most important properties of noninteracting Rashba-coupled Fermi gases.

In Chapter 3 we gave a short review of scattering theory and renormalisation. Scattering theory allows us to explain interactions between particles using a different but equivalent approach — Green's functions and the T-matrix — than the Schrödinger or Heisenberg equation approach. Effective theories that include contact interactions yield infinities that do not appear in experiments. We briefly explained how to treat such infinities and we gave an example of the UV divergences that appear in the T-matrix when describing interactions.

A method to describe a single-channel UV divergent-free Rashba-coupled Fermi gas is proposed in Chapter 4. We showed that this theory has predictive power, since the logarithmic UV divergence that appears in the T-matrix is renormalised into the particle-particle interaction constant. As a consequence, we also found that the corrections to the energy in second order perturbation theory are finite.

In Chapter 5 we used the lack of Galilean invariance in a Rashba-coupled Fermi gas, to show how the Fermi surface deforms when a momentum kick is applied onto the system. Using the single-branch theory for an interacting Rashba-coupled Fermi gas, introduced in the previous Chapter, we saw that the momentum kick induces a phase

transition to a finite momentum ground-state. We also discussed experimental signatures to detect this effect. Additionally, it would be interesting to study the lifetime of excitations when a momentum kick per particle $\mathbf{k}_0$ is applied to an excited state of the Rashba-coupled Fermi gas. These results could be compared with the lifetime of quasiparticles subject to Pomeranchuk instabilities.

In the second part we change tack, and study the dynamics of open quantum systems described by master equations of the reduced density matrix of the system. In Chapter 6 we considered two different systems described by two different Jaynes-Cummings Hamiltonians coupled to a bath that yield a same non-Markovian master equation. We analyse the validity of the master equation approach when the coupling between the two-level system and the bath changes suddenly. If the coupling changes fast enough at the right time, when the Master Equation is not invertible, then it is not possible to distinguish between on-resonance and off-resonance evolution in the Master Equation, Eq. (6.69). On the other hand, numerically solving the Master Equation obtained from microscopic principles for a Jaynes-Cummings model with time-dependent coupling, see Sec. 6.5.4,might yield signatures to distinguish between the on-resonance and off-resonance evolution.

Appendix A

Deltas, Fourier transformations and Wick's theorem

In this Appendix we introduce some concepts and intermediate calculations of Chapter 4.

A.1 Dirac & Kronecker delta functions

We define the Kronecker delta for the discretised momentum coordinate as

$$\delta_{\mathbf{k},\mathbf{q}} = \frac{1}{V}\int_{[0,L)^3} \mathbf{dr}\, e^{i\mathbf{r}(\mathbf{k}-\mathbf{q})}, \tag{A.1}$$

where $V = L^3$ is the volume of the system. We also introduce the Dirac delta

$$\delta\left(\mathbf{r}-\mathbf{r}'\right) = \int_{\mathbb{R}^3} \frac{\mathbf{dk}}{(2\pi)^3} e^{i\mathbf{k}(\mathbf{r}-\mathbf{r}')}, \tag{A.2}$$

$$\delta\left(\mathbf{k}-\mathbf{k}'\right) = \int_{\mathbb{R}^3} \frac{\mathbf{dr}}{(2\pi)^3} e^{i\mathbf{r}(\mathbf{k}-\mathbf{k}')}. \tag{A.3}$$

It is possible to connect the Kronecker delta with the Dirac delta. We start from

$$\sum_{\mathbf{q}} \delta_{\mathbf{k},\mathbf{q}} = 1. \tag{A.4}$$

We transform the sum to an integral, therefore we have

$$\frac{V}{(2\pi)^3}\int \mathbf{dq}\, \delta_{\mathbf{k},\mathbf{q}} = 1. \tag{A.5}$$

In order to write $\delta_{\mathbf{k},\mathbf{q}}$ as a Dirac delta we have to cancel the factors in (A.5). Hence

$$\delta_{\mathbf{k},\mathbf{q}} \to \frac{(2\pi)^3}{V}\delta\left(\mathbf{k}-\mathbf{q}\right) \tag{A.6}$$

gives the same result as (A.4).

A.2 Fourier transform of operators

We now show the Fourier transform of the creation and annihilation operators (for any kind of spin system). The position representation of the creation $c^{\dagger}_{\mathbf{k},\sigma}$ and annihilation $c_{\mathbf{k},\sigma}$ operator are

$$\Phi^{\dagger}_{\sigma}\left(\mathbf{r}\right) = \frac{1}{\sqrt{V}}\sum_{\mathbf{k}} e^{-i\mathbf{k}\cdot\mathbf{r}} c^{\dagger}_{\mathbf{k},\sigma}, \tag{A.7}$$

$$\Phi_{\sigma}\left(\mathbf{r}\right) = \frac{1}{\sqrt{V}}\sum_{\mathbf{k}} e^{i\mathbf{k}\cdot\mathbf{r}} c_{\mathbf{k},\sigma}. \tag{A.8}$$

To define the inverse transformation we multiply (A.7) by $e^{i\mathbf{q}\cdot\mathbf{r}}$

$$e^{i\mathbf{q}\cdot\mathbf{r}}\,\Phi^{\dagger}_{\sigma}\left(\mathbf{r}\right) = \frac{1}{\sqrt{V}}\sum_{\mathbf{k}} e^{i\mathbf{q}\cdot\mathbf{r}} e^{-i\mathbf{k}\cdot\mathbf{r}} c^{\dagger}_{\mathbf{k},\sigma}, \tag{A.9}$$

we integrate over position in the expression above to get

$$\begin{aligned}\int \mathrm{d}\mathbf{r}\, e^{i\mathbf{q}\cdot\mathbf{r}}\,\Phi^{\dagger}_{\sigma}\left(\mathbf{r}\right) &= \frac{1}{\sqrt{V}}\sum_{\mathbf{k}}\int \mathrm{d}\mathbf{r}\, e^{i\mathbf{q}\cdot\mathbf{r}} e^{-i\mathbf{k}\cdot\mathbf{r}} c^{\dagger}_{\mathbf{k},\sigma} \\ &= \sqrt{V}\sum_{\mathbf{k}}\delta_{\mathbf{q},\mathbf{k}} c^{\dagger}_{\mathbf{k},\sigma}.\end{aligned} \tag{A.10}$$

Where we have made use of Eq. (A.1). We obtain finally

$$c^{\dagger}_{\mathbf{k},\sigma} = \frac{1}{\sqrt{V}}\int \mathrm{d}\mathbf{r}\, e^{i\mathbf{k}\cdot\mathbf{r}}\Phi^{\dagger}_{\sigma}\left(\mathbf{r}\right), \tag{A.11}$$

$$c_{\mathbf{k},\sigma} = \frac{1}{\sqrt{V}}\int \mathrm{d}\mathbf{r}\, e^{-i\mathbf{k}\cdot\mathbf{r}}\Phi_{\sigma}\left(\mathbf{r}\right). \tag{A.12}$$

A.3 Anticommutation relations

The anticommutation relations for fermionic operators are given by

$$\left\{c_{\mathbf{q},\sigma'}, c^{\dagger}_{\mathbf{k},\sigma}\right\} = \delta_{\mathbf{q},\mathbf{k}}\delta_{\sigma,\sigma'},\ \left\{c_{\mathbf{q},\sigma'}, c_{\mathbf{k},\sigma}\right\} = \left\{c^{\dagger}_{\mathbf{q},\sigma'}, c^{\dagger}_{\mathbf{k},\sigma}\right\} = 0. \tag{A.13}$$

We Fourier transform (A.13) using (A.7) and (A.8)

$$\begin{aligned}\left\{\Phi_{\sigma}\left(\mathbf{r}\right),\Phi_{\sigma'}^{\dagger}\left(\mathbf{r}'\right)\right\} &= \frac{1}{V}\sum_{\mathbf{k},\mathbf{q}} e^{-i\mathbf{r}\cdot\mathbf{k}}e^{i\mathbf{r}'\cdot\mathbf{q}}\left\{c_{\mathbf{k},\sigma},c_{\mathbf{q},\sigma'}^{\dagger}\right\}\\ &= \frac{1}{V}\sum_{\mathbf{k},\mathbf{q}} e^{-i\mathbf{r}\cdot\mathbf{k}}e^{i\mathbf{r}'\cdot\mathbf{q}}\delta_{\mathbf{k},\mathbf{q}}\delta_{\sigma,\sigma'}\\ &= \frac{1}{V}\sum_{\mathbf{k}} e^{i\mathbf{k}(\mathbf{r}'-\mathbf{r})}\delta_{\sigma,\sigma'},\end{aligned} \tag{A.14}$$

writing the sum as an integral and using (A.2) we get to

$$\left\{\Phi_{\sigma}\left(\mathbf{r}\right),\Phi_{\sigma'}^{\dagger}\left(\mathbf{r}'\right)\right\} = \delta\left(\mathbf{r}-\mathbf{r}'\right)\delta_{\sigma,\sigma'}. \tag{A.15}$$

A.4 Properties of the Δ function

In this section we give some details about the negative-helicity fermion-fermion interaction introduced in Chapter 4. The interaction reads

$$\mathcal{V} = \frac{g_*}{2V}\sum_{\mathbf{k}_1+\mathbf{k}_2=\mathbf{k}_3+\mathbf{k}_4}\Delta\left(\gamma_1,\gamma_2,\gamma_3,\gamma_4\right)d_{\mathbf{k}_4}^{\dagger}d_{\mathbf{k}_3}^{\dagger}d_{\mathbf{k}_2}d_{\mathbf{k}_1}, \tag{A.16}$$

where the angular dependence of Δ are

$$\Delta\left(\gamma_1,\gamma_2,\gamma_3,\gamma_4\right) = -\frac{1}{8}\left(e^{i\gamma_1}-e^{i\gamma_2}\right)\left(e^{-i\gamma_3}-e^{-i\gamma_4}\right). \tag{A.17}$$

The Δ function is antisymmetric under the permutation of the first and second argument or the third and fourth

$$\begin{aligned}\Delta\left(\gamma_1,\gamma_2,\gamma_3,\gamma_4\right) &= -\Delta\left(\gamma_1,\gamma_2,\gamma_4,\gamma_3\right)\\ &= \Delta\left(\gamma_2,\gamma_1,\gamma_4,\gamma_3\right)\\ &= -\Delta\left(\gamma_2,\gamma_1,\gamma_3,\gamma_4\right).\end{aligned} \tag{A.18}$$

The complex conjugate of Δ is equivalent to interchange the two first arguments with the last two

$$\begin{aligned}\left[\Delta\left(\gamma_1,\gamma_2,\gamma_3,\gamma_4\right)\right]^* &= -\frac{1}{8}\left(e^{-i\gamma_1}-e^{-i\gamma_2}\right)\left(e^{i\gamma_3}-e^{i\gamma_4}\right)\\ &= \Delta\left(\gamma_3,\gamma_4,\gamma_1,\gamma_2\right).\end{aligned} \tag{A.19}$$

If the incident and outgoing angles are the same, Δ reduces to

$$\begin{aligned}\Delta(\gamma_1,\gamma_2,\gamma_1,\gamma_2) &= -\frac{1}{8}\left(e^{i\gamma_1}-e^{i\gamma_2}\right)\left(e^{-i\gamma_1}-e^{-i\gamma_2}\right)\\ &= -\frac{1}{8}\left(2-e^{i\gamma_1-i\gamma_2}-e^{-i\gamma_1+i\gamma_2}\right)\\ &= -\frac{1}{4}\left[1-\cos(\gamma_2-\gamma_1)\right].\end{aligned} \tag{A.20}$$

Second order processes involve two different Δ functions with intermediate states which simplifies as follows

$$\begin{aligned}\Delta(\gamma_1,\gamma_2,\gamma_5,\gamma_6)\,\Delta(\gamma_5,\gamma_6,\gamma_3,\gamma_4) &= \frac{1}{64}\left(e^{i\gamma_1}-e^{i\gamma_2}\right)\left(e^{-i\gamma_5}-e^{-i\gamma_6}\right)\\ &\times\left(e^{i\gamma_5}-e^{i\gamma_6}\right)\left(e^{-i\gamma_3}-e^{-i\gamma_4}\right)\\ &= -\frac{1}{4}\left[1-\cos(\gamma_6-\gamma_5)\right]\Delta(\gamma_1,\gamma_2,\gamma_3,\gamma_4)\\ &= \Delta(\gamma_1,\gamma_2,\gamma_3,\gamma_4)\,\Delta(\gamma_5,\gamma_6,\gamma_5,\gamma_6)\end{aligned} \tag{A.21}$$

A.5 Wick's Theorem

Wick's theorem is one of the most powerful techniques to compute expectation values which involve multiple operators. We do not show any proof of the theorem, as it can be found in the original paper [140] or in any Quantum Field Theory textbook [47]. Before stating Wick's theorem we need to introduce the time ordering, the normal order and the contraction of two operators.

Given a product of time-dependent operators, time-ordering the product consists on rearranging the product in such a way that the operators which act at latest times are placed to the left. For the case of a product of two time-dependent operators $c^\dagger_{\mathbf{k}}(t)$ and $c_{\mathbf{k}}(t')$ we have

$$\mathcal{T}\left(c^\dagger_{\mathbf{k}}(t)\,c_{\mathbf{q}}(t')\right) = \begin{cases} c^\dagger_{\mathbf{k}}(t)\,c_{\mathbf{q}}(t') & \text{if } t'<t\\ c_{\mathbf{q}}(t')\,c^\dagger_{\mathbf{k}}(t) & \text{if } t<t'.\end{cases} \tag{A.22}$$

Normal Ordering works as follows. Given a product of n operators, the normal order places the creation operators with respect to vacuum to the left and the annihilation operators to the right. In the case of four operators we have

$$\mathcal{N}\left(c_{\mathbf{k}}c^\dagger_{\mathbf{q}}c^\dagger_{\mathbf{u}}c_{\mathbf{r}}\right) = c^\dagger_{\mathbf{q}}c^\dagger_{\mathbf{u}}c_{\mathbf{k}}c_{\mathbf{r}}. \tag{A.23}$$

Finally the contraction of two operators is a complex number represented by its commutator

$$\overset{\sqcap}{a}\overset{\sqcap}{b} = [a, b]\,. \tag{A.24}$$

We are now ready to state Wick's theorem. The time-ordered product of operators is equal to the normal product plus all the possible combinations of contractions. Therefore, the time-ordered product of n operators A reads

$$\begin{aligned}\mathcal{T}\left(A_n A_{n-1}\cdots A_1\right) = \mathcal{N}\left(A_n A_{n-1}\cdots A_1\right) &+ \sum_{\text{Single contractions}} (-1)^p \mathcal{N}\left(A_n A_{n-1}\cdots A_1\right) \\ &+ \sum_{\text{Double contractions}} (-1)^p \mathcal{N}\left(A_n A_{n-1}\cdots A_1\right) \\ &+ \sum_{\text{Triple contractions}} (-1)^p \mathcal{N}\left(A_n A_{n-1}\cdots A_1\right) + \cdots\,,\end{aligned} \tag{A.25}$$

where p represents the number of permutations needed to normal order the product in the case of fermions. For bosons the permutations do not involve any sign, hence we replace $(-1)^p$ by 1. As an example, we make explicit the calculation of the time-ordered product of four operators A, B, C, D

$$\begin{aligned}\mathcal{T}\left(ABCD\right) = \mathcal{N}\left(ABCD\right) &+ (-1)^p \mathcal{N}\left(\overset{\sqcap}{A}BCD\right) + (-1)^p \mathcal{N}\left(\overbrace{ABCD}\right) + \\ &(-1)^p \mathcal{N}\left(\overbrace{ABC}D\right) + (-1)^p \mathcal{N}\left(A\overset{\sqcap}{B}CD\right) + (-1)^p \mathcal{N}\left(A\overbrace{BCD}\right) + \\ &(-1)^p \mathcal{N}\left(AB\overset{\sqcap}{C}D\right) + (-1)^p \mathcal{N}\left(\overset{\sqcap}{A}\overset{\sqcap}{B}CD\right) + \\ &(-1)^p \mathcal{N}\left(\overbrace{\overset{\sqcap}{A}BC}D\right) + (-1)^p \mathcal{N}\left(\overbrace{\overset{\sqcap}{A}BCD}\right)\,.\end{aligned} \tag{A.26}$$

Wick's theorem is specially useful to compute expectation values of products of field operators on the vacuum as all the terms in (A.26) which include non-contracted operators or either contractions of the same type of operators (creation-creation or annihilation-annihilation) vanish. In Chapter 4 we encounter expectation values of 4 and 8 creation and annihilation operators. Now we analyse with detail the expectation value of 4 cre-

ation and annihilation operators. Therefore the time-order product of $c^\dagger_{\mathbf{q}} c^\dagger_{\mathbf{k}} c_{\mathbf{k}'} c_{\mathbf{q}'}$ reads

$$\begin{aligned}\langle 0|\,\mathcal{T}\left(c^\dagger_{\mathbf{q}} c^\dagger_{\mathbf{k}} c_{\mathbf{k}'} c_{\mathbf{q}'}\right)|0\rangle = {} & \langle 0|\,\mathcal{N}\left(c^\dagger_{\mathbf{q}} c^\dagger_{\mathbf{k}} c_{\mathbf{k}'} c_{\mathbf{q}'}\right)|0\rangle + \langle 0|\,\mathcal{N}\left(\overbrace{c^\dagger_{\mathbf{q}} c^\dagger_{\mathbf{k}}} c_{\mathbf{k}'} c_{\mathbf{q}'}\right)|0\rangle \\ & + \langle 0|\,\mathcal{N}\left(\overbrace{c^\dagger_{\mathbf{q}} c^\dagger_{\mathbf{k}} c_{\mathbf{k}'}} c_{\mathbf{q}'}\right)|0\rangle + \langle 0|\,\mathcal{N}\left(\overbrace{c^\dagger_{\mathbf{q}} c^\dagger_{\mathbf{k}} c_{\mathbf{k}'} c_{\mathbf{q}'}}\right)|0\rangle \\ & + \langle 0|\,\mathcal{N}\left(c^\dagger_{\mathbf{q}} \overbrace{c^\dagger_{\mathbf{k}} c_{\mathbf{k}'}} c_{\mathbf{q}'}\right)|0\rangle + \langle 0|\,\mathcal{N}\left(c^\dagger_{\mathbf{q}} \overbrace{c^\dagger_{\mathbf{k}} c_{\mathbf{k}'} c_{\mathbf{q}'}}\right)|0\rangle \\ & + \langle 0|\,\mathcal{N}\left(c^\dagger_{\mathbf{q}} c^\dagger_{\mathbf{k}} \overbrace{c_{\mathbf{k}'} c_{\mathbf{q}'}}\right)|0\rangle + \langle 0|\,\mathcal{N}\left(\overbrace{c^\dagger_{\mathbf{q}} c^\dagger_{\mathbf{k}}} \overbrace{c_{\mathbf{k}'} c_{\mathbf{q}'}}\right)|0\rangle \\ & + \langle 0|\,\mathcal{N}\left(\overbrace{c^\dagger_{\mathbf{q}} \overbrace{c^\dagger_{\mathbf{k}} c_{\mathbf{k}'}} c_{\mathbf{q}'}}\right)|0\rangle + \langle 0|\,\mathcal{N}\left(\overbrace{c^\dagger_{\mathbf{q}} \overbrace{c^\dagger_{\mathbf{k}} c_{\mathbf{k}'} c_{\mathbf{q}'}}}\right)|0\rangle . \end{aligned} \tag{A.27}$$

All the terms in (A.27) that have non-contracted operators vanish as $c_{\mathbf{k}'}|0\rangle = 0$ and $\langle 0|\,c^\dagger_{\mathbf{k}} = 0$. The term $\langle 0|\,\mathcal{N}\left(\overbrace{c^\dagger_{\mathbf{q}} c^\dagger_{\mathbf{k}}} \overbrace{c_{\mathbf{k}'} c_{\mathbf{q}'}}\right)|0\rangle$ also vanishes as $\left[c^\dagger_{\mathbf{q}}, c^\dagger_{\mathbf{k}}\right] = \left[c_{\mathbf{k}'}, c_{\mathbf{q}'}\right] = 0$. Hence (A.27) reduces to

$$\langle 0|\,\mathcal{T}\left(c^\dagger_{\mathbf{q}} c^\dagger_{\mathbf{k}} c_{\mathbf{k}'} c_{\mathbf{q}'}\right)|0\rangle = -\left[c^\dagger_{\mathbf{q}}, c_{\mathbf{k}'}\right]\left[c^\dagger_{\mathbf{k}}, c_{\mathbf{q}'}\right] + \left[c^\dagger_{\mathbf{q}}, c_{\mathbf{q}'}\right]\left[c^\dagger_{\mathbf{k}}, c_{\mathbf{k}'}\right]. \tag{A.28}$$

Finally we get to

$$\langle 0|\,\mathcal{T}\left(c^\dagger_{\mathbf{q}} c^\dagger_{\mathbf{k}} c_{\mathbf{k}'} c_{\mathbf{q}'}\right)|0\rangle = -\delta_{\mathbf{q},\mathbf{k}'}\delta_{\mathbf{k},\mathbf{q}'} + \delta_{\mathbf{q},\mathbf{q}'}\delta_{\mathbf{k},\mathbf{k}'}. \tag{A.29}$$

In Chapter 4 we also compute the expectation value on the Fermi sea. Wick's theorem is applied in the same way, with the vacuum of particles replaced by the Fermi sea (the noninteracting vacuum).

Appendix B

Existence and uniqueness theorem

The Picard-Lindelöf-Lipschitz-Cauchy theorem or existence and uniqueness theorem defines the conditions for a differential equation to have a valid solution [141]. Let us assume the initial condition problem

$$y'(t) = f(t, y(t)), \tag{B.1}$$

$$y(t_0) = y_0, \tag{B.2}$$

if $f(t, y(t))$ and $\partial_y f(t, y(t))$ are continuous in a subset $[t_0, t_0 + h] \times [y_0 - r, y_0 + r]$, then there is one and only one solution to Eq. (B.1) with the initial condition (B.2) defined in the interval $[t_0, t_0 + d]$ where $d \leq h$.

References

[1] S. Chu, J. Bjorkholm, A. Ashkin, and A. Cable. Experimental Observation of Optically Trapped Atoms. *Physical Review Letters* **57**(3), 314–317 (1986).

[2] A. J. McCulloch, D. V. Sheludko, S. D. Saliba, S. C. Bell, M. Junker, K. A. Nugent, and R. E. Scholten. Arbitrarily shaped high-coherence electron bunches from cold atoms. *Nat Phys* **7**(10), 785–788 (2011).

[3] J. F. Sherson, C. Weitenberg, M. Endres, M. Cheneau, I. Bloch, and S. Kuhr. Single-atom-resolved fluorescence imaging of an atomic Mott insulator. *Nature* **467**(7311), 68–72 (2010).

[4] M. Lewenstein, A. Sanpera, and V. Ahufinger. *Ultracold Atoms in Optical Lattices. Simulating Quantum Many-Body Systems*. Oxford University Press, 2012.

[5] I. Bloch, J. Dalibard, and W. Zwerger. Many-body physics with ultracold gases. *Reviews of Modern Physics* **80**(3), 885–964 (2008).

[6] M. H. Anderson, J. R. Ensher, M. R. Matthews, C. E. Wieman, and E. A. Cornell. Observation of Bose-Einstein Condensation in a Dilute Atomic Vapor. *Science* **269**(5221), 198–201 (1995).

[7] K. Davis, M. Mewes, M. Andrews, N. van Druten, D. Durfee, D. Kurn, and W. Ketterle. Bose-Einstein Condensation in a Gas of Sodium Atoms. *Physical Review Letters* **75**(22), 3969–3973 (1995).

[8] T. Bourdel, L. Khaykovich, J. Cubizolles, J. Zhang, F. Chevy, M. Teichmann, L. Tarruell, S. Kokkelmans, and C. Salomon. Experimental Study of the BEC-BCS Crossover Region in Lithium 6. *Physical Review Letters* **93**(5), 050401 (2004).

[9] P. A. M. Dirac. The Quantum Theory of the Electron. *Proceedings of the Royal Society of London A: Mathematical, Physical and Engineering Sciences* **117**(778), 610–624 (1928).

[10] Y. A. Bychkov and E. I. Rashba. Oscillatory effects and the magnetic susceptibility of carriers in inversion layers. *Journal of Physics C: Solid State Physics* **17**(33), 6039 (1984).

[11] G. Dresselhaus, A. Kip, and C. Kittel. Spin-Orbit Interaction and the Effective Masses of Holes in Germanium. *Physical Review* **95**(2), 568–569 (1954).

[12] P. Wang, Z.-Q. Yu, Z. Fu, J. Miao, L. Huang, S. Chai, H. Zhai, and J. Zhang. Spin-Orbit Coupled Degenerate Fermi Gases. *Physical Review Letters* **109**(9), 095301 (2012).

[13] L. Cheuk, A. Sommer, Z. Hadzibabic, T. Yefsah, W. Bakr, and M. Zwierlein. Spin-Injection Spectroscopy of a Spin-Orbit Coupled Fermi Gas. *Physical Review Letters* **109**(9), 095302 (2012).

[14] D. Jaksch, C. Bruder, J. I. Cirac, C. W. Gardiner, and P. Zoller. Cold Bosonic Atoms in Optical Lattices. *Physical Review Letters* **81**(15), 3108–3111 (1998).

[15] D. Jaksch and P. Zoller. Creation of effective magnetic fields in optical lattices: the Hofstadter butterfly for cold neutral atoms. *New Journal of Physics* **5**(1), 56 (2003).

[16] G. Juzeliūnas and P. Öhberg. Slow Light in Degenerate Fermi Gases. *Physical Review Letters* **93**(3), 033602 (2004).

[17] J. Ruseckas, G. Juzeliūnas, P. Öhberg, and M. Fleischhauer. Non-Abelian Gauge Potentials for Ultracold Atoms with Degenerate Dark States. *Physical Review Letters* **95**(1), 010404 (2005).

[18] J. Dalibard, F. Gerbier, G. Juzeliūnas, and P. Öhberg. Colloquium: Artificial gauge potentials for neutral atoms. *Reviews of Modern Physics* **83**(4), 1523–1543 (2011).

[19] N. Goldman, G. Juzeliūnas, P. Öhberg, and I. B. Spielman. Light-induced gauge fields for ultracold atoms. *Reports on Progress in Physics* **77**(12), 126401 (2014).

[20] Y.-J. Lin, R. L. Compton, K. Jimenez-Garcia, W. D. Phillips, J. V. Porto, and I. B. Spielman. A synthetic electric force acting on neutral atoms. *Nat Phys* **7**(7), 531–534 (2011).

[21] Y. J. Lin, R. L. Compton, K. Jimenez-Garcia, J. V. Porto, and I. B. Spielman. Synthetic magnetic fields for ultracold neutral atoms. *Nature* **462**(7273), 628–632 (2009).

[22] V. Galitski and I. B. Spielman. Spin-orbit coupling in quantum gases. *Nature* **494**(7435), 49–54 (2013).

[23] J. Sau, R. Sensarma, S. Powell, I. Spielman, and S. Das Sarma. Chiral Rashba spin textures in ultracold Fermi gases. *Physical Review B* **83**(14), 140510 (2011).

[24] R. Barnett, G. Boyd, and V. Galitski. SU(3) Spin-Orbit Coupling in Systems of Ultracold Atoms. *Physical Review Letters* **109**(23), 235308 (2012).

[25] Y. J. Lin, K. Jimenez-Garcia, and I. B. Spielman. Spin-orbit-coupled Bose-Einstein condensates. *Nature* **471**(7336), 83–86 (2011).

[26] J. R. Taylor. *Scattering Theory. The Quantum Theory of nonrelativistic Collisions*. Dover Publications, 2006.

[27] T. Ozawa and G. Baym. Renormalization of interactions of ultracold atoms in simulated Rashba gauge fields. *Physical Review A* **84**(4), 043622 (2011).

[28] D. Maldonado-Mundo, P. Öhberg, and M. Valiente. Single-branch theory of ultracold Fermi gases with artificial Rashba spin–orbit coupling. *Journal of Physics B: Atomic, Molecular and Optical Physics* **46**(13), 134002 (2013).

[29] D. Maldonado-Mundo, L. He, P. Öhberg, and M. Valiente. Non-Galilean response of Rashba-coupled Fermi gases. *Physical Review A* **88**(5), 053609 (2013).

[30] H.-P. Breuer and F. Petruccione. *The Theory of Open Quantum Systems*. Oxford University Press, Oxford, 2006.

[31] G. Lindblad. On the generators of quantum dynamical semigroups. *Commun. Math. Phys.* **48**(2), 119–130 (1976).

[32] V. Gorini, A. Kossakowski, and E. C. G. Sudarshan. Completely positive dynamical semigroups of Nlevel systems. *Journal of Mathematical Physics* **17**(5), 821–825 (1976).

[33] M. J. W. Hall, J. D. Cresser, L. Li, and E. Andersson. Canonical form of master equations and characterization of non-Markovianity. *Physical Review A* **89**(4), 042120 (2014).

[34] G. Baym. *Lectures on Quantum Mechanics*. Westview Press, 1974.

[35] A. Galindo and P. Pascual. *Quantum Mechanics*, volume I. Springer-Verlag, 1990.

[36] B. Thaller. *The Dirac Equation*. Springer-Verlag, 1992.

[37] R. Winkler. *Spin-Orbit Coupling Effects in Two-Dimensional Electron and Hole Systems*, volume 191 of *Springer Tracts in Modern Physics*. Springer-Verlag Berlin Heidelberg, 2003.

[38] D. L. Campbell, G. Juzeliūnas, and I. B. Spielman. Realistic Rashba and Dresselhaus spin-orbit coupling for neutral atoms. *Physical Review A* **84**(2), 025602 (2011).

[39] G. Juzeliūnas, J. Ruseckas, and J. Dalibard. Generalized Rashba-Dresselhaus spin-orbit coupling for cold atoms. *Physical Review A* **81**(5), 053403 (2010).

[40] J. Vyasanakere and V. Shenoy. Bound states of two spin-$\frac{1}{2}$ fermions in a synthetic non-Abelian gauge field. *Physical Review B* **83**(9), 094515 (2011).

[41] Z. Fu, L. Huang, Z. Meng, P. Wang, L. Zhang, S. Zhang, H. Zhai, P. Zhang, and J. Zhang. Production of Feshbach molecules induced by spin-orbit coupling in Fermi gases. *Nat Phys* **10**(2), 110–115 (2014).

[42] L. He and X.-G. Huang. BCS-BEC Crossover in 2D Fermi Gases with Rashba Spin-Orbit CouplingCoupling. *Physical Review Letters* **108**(14), 145302 (2012).

[43] L. He and X.-G. Huang. Superfluidity and collective modes in Rashba spin–orbit coupled Fermi gases. *Annals of Physics* **337**(0), 163–207 (2013).

[44] J. D. Jackson. *Classical Electrodynamics*. Wiley, 3rd edition, 1998.

[45] L. Meier, G. Salis, I. Shorubalko, E. Gini, S. Schon, and K. Ensslin. Measurement of Rashba and Dresselhaus spin-orbit magnetic fields. *Nat Phys* **3**(9), 650–654 (2007).

[46] F. Halzen and A. D. Martin. *Quarks Leptons: An Introductory Course in Modern Particle Physics*. John Wiley Sons, 1984.

[47] M. E. Peskin and D. V. Schroeder. *An Introduction to Quantum Field Theory*. Westview Press Inc, 1995.

[48] N. Read and D. Green. Paired states of fermions in two dimensions with breaking of parity and time-reversal symmetries and the fractional quantum Hall effect. *Physical Review B* **61**(15), 10267–10297 (2000).

[49] M. Gong, G. Chen, S. Jia, and C. Zhang. Searching for Majorana Fermions in 2D Spin-Orbit Coupled Fermi Superfluids at Finite Temperature. *Physical Review Letters* **109**(10), 105302 (2012).

[50] J. Sau, R. Lutchyn, S. Tewari, and S. Das Sarma. Generic New Platform for Topological Quantum Computation Using Semiconductor Heterostructures. *Physical Review Letters* **104**(4), 040502 (2010).

[51] J. Alicea. Majorana fermions in a tunable semiconductor device. *Physical Review B* **81**(12), 125318 (2010).

[52] A. N. Wenz, G. Zürn, S. Murmann, I. Brouzos, T. Lompe, and S. Jochim. From Few to Many: Observing the Formation of a Fermi Sea One Atom at a Time. *Science* **342**(6157), 457–460 (2013).

[53] M. Köhl, H. Moritz, T. Stöferle, K. Günter, and T. Esslinger. Fermionic Atoms in a Three Dimensional Optical Lattice: Observing Fermi Surfaces, Dynamics, and Interactions. *Physical Review Letters* **94**(8), 080403 (2005).

[54] E. Cappelluti, C. Grimaldi, and F. Marsiglio. Topological Change of the Fermi Surface in Low-Density Rashba Gases: Application to Superconductivity. *Physical Review Letters* **98**(16), 167002 (2007).

[55] X.-J. Liu, L. Jiang, H. Pu, and H. Hu. Probing Majorana fermions in spin-orbit-coupled atomic Fermi gases. *Physical Review A* **85**(2), 021603 (2012).

[56] R.-L. Chu, G.-B. Liu, W. Yao, X. Xu, D. Xiao, and C. Zhang. Spin-orbit-coupled quantum wires and Majorana fermions on zigzag edges of monolayer transition-metal dichalcogenides. *Physical Review B* **89**(15), 155317 (2014).

[57] J. J. Sakurai. *Modern Quantum Mechanics (Revised Edition)*. Addison-Wesley, 1st edition, 1993.

[58] A. L. Fetter and J. D. Walecka. *Quantum Theory of Many-Particle Systems*. Dover Publications, 2003.

[59] H. Bruus and K. Flensberg. *Many-Body Quantum Theory in Condensed Matter Physics. An Introduction*. Oxford Graduate Texts. Oxford University Press, 2004.

[60] Z. Zheng, H. Pu, X. Zou, and G. Guo. Thermodynamic properties of Rashba spin-orbit-coupled Fermi gas. *Physical Review A* **90**(6), 063623 (2014).

[61] B. Lippmann and J. Schwinger. Variational Principles for Scattering Processes. *Physical Review* **79**(3), 469–480 (1950).

[62] J. M. Howie. *Complex Analysis*. Springer, 2004.

[63] G. 't Hooft. Renormalization without infinities. *International Journal of Modern Physics A* **20**(06), 1336–1345 (2005).

[64] J. Cardy. *Scaling and Renormalization in Statistical Physics*. Cambridge University Press, 1996.

[65] J. C. Collins. *Renormalization. An introduction to renormalization, the renormalization group, and the operator-product expansion*. Cambridge University Press, 1984.

[66] W. D. McComb. *Renormalization Methods: A Guide For Beginners*. OUP Oxford, 1st edition, 2007.

[67] S. Tan. Energetics of a strongly correlated Fermi gas. *Annals of Physics* **323**(12), 2952–2970 (2008).

[68] M. Valiente. Tan's distributions and Fermi-Huang pseudopotential in momentum space. *Physical Review A* **85**(1), 014701 (2012).

[69] B. Delamotte. A hint of renormalization. *American Journal of Physics* **72**(2), 170–184 (2004).

[70] T. Lee, K. Huang, and C. Yang. Eigenvalues and Eigenfunctions of a Bose System of Hard Spheres and Its Low-Temperature Properties. *Physical Review* **106**(6), 1135–1145 (1957).

[71] K. Yang and S. Sachdev. Quantum Criticality of a Fermi Gas with a Spherical Dispersion Minimum. *Physical Review Letters* **96**(18), 187001 (2006).

[72] S. Gopalakrishnan, A. Lamacraft, and P. Goldbart. Universal phase structure of dilute Bose gases with Rashba spin-orbit coupling. *Physical Review A* **84**(6), 061604 (2011).

[73] N. Moiseyev. *Non-Hermitian Quantum Mechanics*. Cambridge University Press, 1st edition, 2011.

[74] G. Baym and C. Pethick. *Landau Fermi-Liquid Theory. Concepts and Applications*. Wiley-VCH Verlag GmbH, 2004.

[75] N. Doiron-Leyraud, I. R. Walker, L. Taillefer, M. J. Steiner, S. R. Julian, and G. G. Lonzarich. Fermi-liquid breakdown in the paramagnetic phase of a pure metal. *Nature* **425**(6958), 595–599 (2003).

[76] D. Bergeron, D. Chowdhury, M. Punk, S. Sachdev, and A. M. S. Tremblay. Breakdown of Fermi liquid behavior at the $(\pi, \pi) = 2k_F$ spin-density wave quantum-critical point: The case of electron-doped cuprates. *Physical Review B* **86**(15), 155123 (2012).

[77] R. W. Hill, C. Proust, L. Taillefer, P. Fournier, and R. L. Greene. Breakdown of Fermi-liquid theory in a copper-oxide superconductor. *Nature* **414**(6865), 711–715 (2001).

[78] M. Ossadnik, C. Honerkamp, T. Rice, and M. Sigrist. Breakdown of Landau Theory in Overdoped Cuprates near the Onset of Superconductivity. *Physical Review Letters* **101**(25), 256405 (2008).

[79] C. Honerkamp, M. Salmhofer, N. Furukawa, and T. Rice. Breakdown of the Landau-Fermi liquid in two dimensions due to umklapp scattering. *Physical Review B* **63**(3), 035109 (2001).

[80] I. Pomeranchuk. *Sov. Phys. JETP* **8**, 361 (1958).

[81] W. Metzner, D. Rohe, and S. Andergassen. Soft Fermi Surfaces and Breakdown of Fermi-Liquid Behavior. *Physical Review Letters* **91**(6), 066402 (2003).

[82] A. Messiah. *Quantum Mechanics*. Dover Publications, 1999.

[83] K. Zhou and Z. Zhang. Opposite Effect of Spin-Orbit Coupling on Condensation and Superfluidity. *Physical Review Letters* **108**(2), 025301 (2012).

[84] L. He and X.-G. Huang. BCS-BEC crossover in three-dimensional Fermi gases with spherical spin-orbit coupling. *Physical Review B* **86**(1), 014511 (2012).

[85] P. Ring and P. Schuck. *The Nuclear Many-Body Problem*. Springer, 2004.

[86] H. Yamase, V. Oganesyan, and W. Metzner. Mean-field theory for symmetry-breaking Fermi surface deformations on a square lattice. *Physical Review B* **72**(3), 035114 (2005).

[87] A. Neumayr and W. Metzner. Renormalized perturbation theory for Fermi systems: Fermi surface deformation and superconductivity in the two-dimensional Hubbard model. *Physical Review B* **67**(3), 035112 (2003).

[88] K. Aikawa, S. Baier, A. Frisch, M. Mark, C. Ravensbergen, and F. Ferlaino. Observation of Fermi surface deformation in a dipolar quantum gas. *Science* **345**(6203), 1484–1487 (2014).

[89] J. Quintanilla, M. Haque, and A. Schofield. Symmetry-breaking Fermi surface deformations from central interactions in two dimensions. *Physical Review B* **78**(3), 035131 (2008).

[90] D. Petrov, M. Holzmann, and G. Shlyapnikov. Bose-Einstein Condensation in Quasi-2D Trapped Gases. *Physical Review Letters* **84**(12), 2551–2555 (2000).

[91] E. Berg, M. S. Rudner, and S. A. Kivelson. Electronic liquid crystalline phases in a spin-orbit coupled two-dimensional electron gas. *Physical Review B* **85**(3), 035116 (2012).

[92] T. Sedrakyan, A. Kamenev, and L. Glazman. Composite fermion state of spin-orbit-coupled bosons. *Physical Review A* **86**(6), 063639 (2012).

[93] E. C. Stoner. Atomic moments in ferromagnetic metals and alloys with non-ferromagnetic elements. *The London, Edinburgh, and Dublin Philosophical Magazine and Journal of Science* **15**(101), 1018–1034 (1933).

[94] K. Huang. *Statistical Mechanics*. Wiley, New York, 1987.

[95] S. Kanno. Criterion for the Ferromagnetism of Hard Sphere Fermi Liquid. II. *Progress of Theoretical Physics* **44**(3), 813–815 (1970).

[96] R. Duine and A. MacDonald. Itinerant Ferromagnetism in an Ultracold Atom Fermi Gas. *Physical Review Letters* **95**(23), 230403 (2005).

[97] G. Conduit, A. Green, and B. Simons. Inhomogeneous Phase Formation on the Border of Itinerant Ferromagnetism. *Physical Review Letters* **103**(20), 207201 (2009).

[98] G. Conduit and B. Simons. Itinerant ferromagnetism in an atomic Fermi gas: Influence of population imbalance. *Physical Review A* **79**(5), 053606 (2009).

[99] L. He and X.-G. Huang. Nonperturbative effects on the ferromagnetic transition in repulsive Fermi gases. *Physical Review A* **85**(4), 043624 (2012).

[100] H. Heiselberg. Itinerant ferromagnetism in ultracold Fermi gases. *Physical Review A* **83**(5), 053635 (2011).

[101] S. Pilati, G. Bertaina, S. Giorgini, and M. Troyer. Itinerant Ferromagnetism of a Repulsive Atomic Fermi Gas: A Quantum Monte Carlo Study. *Physical Review Letters* **105**(3), 030405 (2010).

[102] S.-Y. Chang, M. Randeria, and N. Trivedi. Ferromagnetism in the upper branch of the Feshbach resonance and the hard-sphere Fermi gas. *Proceedings of the National Academy of Sciences* **108**(1), 51–54 (2011).

[103] T. Drake, Y. Sagi, R. Paudel, J. Stewart, J. Gaebler, and D. Jin. Direct observation of the Fermi surface in an ultracold atomic gas. *Physical Review A* **86**(3), 031601 (2012).

[104] Y. Sagi, T. Drake, R. Paudel, and D. Jin. Measurement of the Homogeneous Contact of a Unitary Fermi Gas. *Physical Review Letters* **109**(22), 220402 (2012).

[105] S. Wu, Y.-J. Wang, Q. Diot, and M. Prentiss. Splitting matter waves using an optimized standing-wave light-pulse sequence. *Physical Review A* **71**(4), 043602 (2005).

[106] Y.-J. Wang, D. Z. Anderson, V. M. Bright, E. A. Cornell, Q. Diot, T. Kishimoto, M. Prentiss, R. A. Saravanan, S. R. Segal, and S. Wu. Atom Michelson Interferometer on a Chip Using a Bose-Einstein Condensate. *Physical Review Letters* **94**(9), 090405 (2005).

[107] R. A. Williams, L. J. LeBlanc, K. Jiménez-García, M. C. Beeler, A. R. Perry, W. D. Phillips, and I. B. Spielman. Synthetic Partial Waves in Ultracold Atomic Collisions. *Science* **335**(6066), 314–317 (2012).

[108] U. Weiss. *Quantum Dissipative Systems*. World Scientific Publishing Company, 4th edition, 2012.

[109] S. Attal, A. Joye, and C.-A. Pillet, editors. *Open Quantum Systems. The Markovian approach*, volume 2. Springer, 1st edition, 2003.

[110] H. J. Carmichael. *Statistical Methods in Quantum Optics 1. Master Equations and Fokker-Planck Equations*, volume 1. Springer, 2 edition, 2002.

[111] Á. Rivas and S. F. Huelga. *Open Quantum Systems. An Introduction*. Springer Briefs in Physics. Springer Berlin Heidelberg, 2012.

[112] H.-P. Breuer. Foundations and measures of quantum non-Markovianity. *Journal of Physics B: Atomic, Molecular and Optical Physics* **45**(15), 154001 (2012).

[113] D. Maldonado-Mundo, P. Öhberg, B. Lovett, and E. Andersson. Investigating the generality of time-local master equations. *Physical Review A* **86**(4), 042107 (2012).

[114] E. T. Jaynes and F. W. Cummings. Comparison of quantum and semiclassical radiation theories with application to the beam maser. *Proceedings of the IEEE* **51**(1), 89–109 (1963).

[115] W. Zurek. Decoherence, einselection, and the quantum origins of the classical. *Reviews of Modern Physics* **75**(3), 715–775 (2003).

[116] M. Schlosshauer. Decoherence, the measurement problem, and interpretations of quantum mechanics. *Reviews of Modern Physics* **76**(4), 1267–1305 (2005).

[117] M. A. Nielsen and I. L. Chuang. *Quantum Computation and Quantum Information*. Cambridge Series on Information and the Natural Sciences. Cambridge University Press, 2000.

[118] P. Shor. Scheme for reducing decoherence in quantum computer memory. *Physical Review A* **52**(4), R2493–R2496 (1995).

[119] A. Beige, D. Braun, B. Tregenna, and P. Knight. Quantum Computing Using Dissipation to Remain in a Decoherence-Free Subspace. *Physical Review Letters* **85**(8), 1762–1765 (2000).

[120] H. Paik, D. Schuster, L. Bishop, G. Kirchmair, G. Catelani, A. Sears, B. Johnson, M. Reagor, L. Frunzio, L. Glazman, S. Girvin, M. Devoret, and R. Schoelkopf. Observation of High Coherence in Josephson Junction Qubits Measured in a Three-Dimensional Circuit QED Architecture. *Physical Review Letters* **107**(24), 240501 (2011).

[121] A. Ishizaki and G. R. Fleming. Theoretical examination of quantum coherence in a photosynthetic system at physiological temperature. *Proceedings of the National Academy of Sciences* **106**(41), 17255–17260 (2009).

[122] G. Panitchayangkoon, D. Hayes, K. A. Fransted, J. R. Caram, E. Harel, J. Wen, R. E. Blankenship, and G. S. Engel. Long-lived quantum coherence in photosynthetic complexes at physiological temperature. *Proceedings of the National Academy of Sciences* **107**(29), 12766–12770 (2010).

[123] M. Mohseni, P. Rebentrost, S. Lloyd, and A. Aspuru-Guzik. Environment-assisted quantum walks in photosynthetic energy transfer. *The Journal of Chemical Physics* **129**(17), 174106 (2008).

[124] D. Bruß and G. Leuchs, editors. *Lectures on Quantum Information*. Wiley-vch, Weinheim, 2006.

[125] K. Kraus, A. Böhm, J. D. Dollard, and W. H. Wootters, editors. *States, Effects and Operations. Fundamental Notions of Quantum Theory*, volume 190 of *Lecture Notes in Physics*. Springer Berlin Heidelberg, 1983.

[126] M.-D. Choi. Completely positive linear maps on complex matrices. *Linear Algebra and its Applications* **10**(3), 285–290 (1975).

[127] Á. Rivas, S. F. Huelga, and M. B. Plenio. Quantum non-Markovianity: characterization, quantification and detection. *Reports on Progress in Physics* **77**(9), 094001 (2014).

[128] Á. Rivas, S. Huelga, and M. Plenio. Entanglement and Non-Markovianity of Quantum Evolutions. *Physical Review Letters* **105**(5), 050403 (2010).

[129] H.-P. Breuer, E.-M. Laine, and J. Piilo. Measure for the Degree of Non-Markovian Behavior of Quantum Processes in Open Systems. *Physical Review Letters* **103**(21), 210401 (2009).

[130] B.-H. Liu, L. Li, Y.-F. Huang, C.-F. Li, G.-C. Guo, E.-M. Laine, H.-P. Breuer, and J. Piilo. Experimental control of the transition from Markovian to non-Markovian dynamics of open quantum systems. *Nat Phys* **7**(12), 931–934 (2011).

[131] C. W. Gardiner and P. Zoller. *Quantum Noise*. Springer-Verlag, Berlin, 3rd edition, 2004.

[132] C. C. Gerry and P. L. Knight. *Introductory Quantum Optics*. Cambridge University Press, 2005.

[133] S. M. Barnett and P. M. Radmore. *Methods in Theoretical Quantum Optics*. Oxford University Press, 3rd edition, 1997.

[134] I. Rabi. Space Quantization in a Gyrating Magnetic Field. *Physical Review* **51**(8), 652–654 (1937).

[135] E. Andersson, J. D. Cresser, and M. J. W. Hall. Finding the Kraus decomposition from a master equation and vice versa. *Journal of Modern Optics* **54**(12), 1695–1716 (2007).

[136] M. Brune, F. Schmidt-Kaler, A. Maali, J. Dreyer, E. Hagley, J. Raimond, and S. Haroche. Quantum Rabi Oscillation: A Direct Test of Field Quantization in a Cavity. *Physical Review Letters* **76**(11), 1800–1803 (1996).

[137] A. Palacios-Laloy, F. Nguyen, F. Mallet, P. Bertet, D. Vion, and D. Esteve. Tunable Resonators for Quantum Circuits. *Journal of Low Temperature Physics* **151**(3-4), 1034–1042 (2008).

[138] T. Yamamoto, K. Inomata, M. Watanabe, K. Matsuba, T. Miyazaki, W. D. Oliver, Y. Nakamura, and J. S. Tsai. Flux-driven Josephson parametric amplifier. *Applied Physics Letters* **93**(4) (2008).

[139] V. K. Thankappan. *Quantum Mechanics*. New Age International Pvt Ltd Publishers, New Delhi, 2nd edition, May 1996.

[140] G. Wick. The Evaluation of the Collision Matrix. *Physical Review* **80**(2), 268–272 (1950).

[141] W. Boyce and R. DiPrima. *Elementary Differential Equations, 10th Edition*. Wiley Global Education, 2012.